6. SITE 661[1]

Shipboard Scientific Party[2]

HOLE 661A

Date occupied: 17 March 1986, 1915 UTC

Date departed: 20 March 1986, 1915 UTC

Time on hole: 72 hr

Position: 9°26.81'N, 19°23.166'W

Water depth (sea level; corrected m, echo-sounding): 4005.8

Water depth (rig floor; corrected m, echo-sounding): 4016.3

Bottom felt (rig floor; m, drill pipe): 4023.2

Distance between rig floor and sea level (m): 10.5

Total depth (rig floor, m): 4319.3

Penetration (m): 296.1

Number of cores (including cores with no recovery): 32

Total length of cored section (m): 296.1

Total core recovered (m): 235.1

Core recovery (%): 79.3

Oldest sediment cored:
Depth sub-bottom (m): 296.1
Nature: bluish gray clay
Age: ?middle-?Late Cretaceous
Measured velocity (km/s): approx. 1.65

HOLE 661B

Date occupied: 20 March 1986, 1915 UTC

Date departed: 21 March 1986, 1145 UTC

Time on hole: 16.5 hr

Position: 9°26.81'N, 19°23.166'W

Water depth (sea level; corrected m, echo-sounding): 4005.8

Water depth (rig floor; corrected m, echo-sounding): 4016.3

Bottom felt (rig floor; m, drill pipe): 4023.6

Distance between rig floor and sea level (m): 10.5

Total depth (rig floor, m): 4105.3

Penetration (m): 81.7

Number of cores (including cores with no recovery): 9

Total length of cored section (m): 81.7

Total core recovered (m): 81.41

Core recovery (%): 99.6

Oldest sediment cored:
Depth sub-bottom (m): 81.7
Nature: brownish clay cycles
Age: late Miocene, approx. 8 Ma
Measured velocity (km/s): approx. 1.54

Principal results: Site 661 (9°26.81'N; 19°23.166'W) lies at 4012.7 m water depth on a plateau east of the Kane Gap, the major deep-water passage through the Sierra Leone Rise between the southern and the northern eastern Atlantic. Site 661 is the shallower end-member of a two-site ODP transect (Sites 660 and 661) investigating bottom-current action and deep-water stagnation, the Cenozoic history of north equatorial surface ocean circulation, and the late Neogene advection of dust recording the history of African aridity. The upper part of the seismic record at this site is almost transparent, with few faint reflectors. Below are a layered and another transparent seismic unit on top of a thick layered unit draping middle Cretaceous basement (see "Seismic Stratigraphy" section, this chapter).

In Holes 661A and 661B we recovered a total of 24 advanced-piston-corer (APC) and 17 extended-core-barrel (XCB) cores to total depths of 296.1 and 81.7 meters below the seafloor (mbsf), respectively. Both holes were cored continuously (Table 1). Core recovery averaged 79.3% in Hole 661A, and 99.6% in Hole 661B.

The entire section cored (0–296.1 m) comprises three lithologic units of Late Cretaceous to Holocene age (Fig. 1). Unit I and the major part of Subunit IIIA have good biostratigraphic control. Unit II is nonfossiliferous except for its uppermost part. Subunit IIIB is completely fossil-barren. Magnetostratigraphic determinations are reliable for the last 3.2 m.y. Continuous magnetic susceptibility and *P*-wave-velocity curves enabled us to establish a complete composite-depth section of both holes down to about 85 mbsf, which leads to an accumulated downhole increase of penetration depth of 3 to 4 mbsf.

Unit I (0–72.55 mbsf) is uppermost Miocene to Holocene cyclic light gray foraminifer-nannofossil ooze to gray, muddy nannofossil ooze or clay and is divided into two subunits. Subunit IA is Pleistocene (last 1.4 m.y.), high-amplitude carbonate cycles distinguished from those of the underlying subunit by uniformly lower carbonate content (see "Geochemistry" section, this chapter) and higher pro-

---

[1] Ruddiman, W., Sarnthein, M., Baldauf, J., et al., 1988. *Proc., Init. Repts. (Pt. A), ODP*, 108.

[2] William Ruddiman (Co-Chief Scientist), Lamont-Doherty Geological Observatory, Palisades, NY 10964; Michael Sarnthein (Co-Chief Scientist), Geologisch-Paläontologisches Institut, Universität Kiel, Olshausenstrasse 40, D-2300 Kiel, Federal Republic of Germany; Jack Baldauf, ODP Staff Scientist, Ocean Drilling Program, Texas A&M University, College Station, TX 77843; Jan Backman, Department of Geology, University of Stockholm, S-106 91 Stockholm, Sweden; Jan Bloemendal, Graduate School of Oceanography, University of Rhode Island, Narragansett, RI 02882-1197; William Curry, Woods Hole Oceanographic Institution, Woods Hole, MA 02543; Paul Farrimond, School of Chemistry, University of Bristol, Cantocks Close, Bristol BS8 1TS, United Kingdom; Jean Claude Faugeres, Laboratoire de Géologie-Océanographie, Université de Bordeaux I, Avenue des Facultés Talence 33405, France; Thomas Janacek, Lamont-Doherty Geological Observatory, Palisades, NY 10964; Yuzo Katsura, Institute of Geosciences, University of Tsukuba, Ibaraki 305, Japan; Hélène Manivit, Laboratoire de Stratigraphie des Continents et Océans, (UA 319) Université Paris VI, 4 Place Jussieu, 75230 Paris Cedex, France; James Mazzullo, Department of Geology, Texas A&M University, College Station, TX 77843; Jürgen Mienert, Geologisch-Paläontologisches Institut, Universität Kiel, Olshausenstrasse 40, D-2300 Kiel, Federal Republic of Germany, and Woods Hole Oceanographic Institution, Woods Hole, MA 02543; Edward Pokras, Lamont-Doherty Geological Observatory, Palisades, NY 10964; Maureen Raymo, Lamont-Doherty Geological Observatory, Palisades, NY 10964; Peter Schultheiss, Institute of Oceanographic Sciences, Brook Road, Wormley, Godalming, Surrey GU8 5UG, United Kingdom; Rüdiger Stein, Geologisch-Paläontologisches Institut, Universität Giessen, Senckenbergstrasse 3, 6300 Giessen, Federal Republic of Germany; Lisa Tauxe, Scripps Institution of Oceanography, La Jolla, CA 92093; Jean-Pierre Valet, Centre des Faibles Radioactivités, CNRS, Avenue de la Terrasse, 91190 Gif-sur-Yvette, France; Philip Weaver, Institute of Oceanographic Sciences, Brook Road, Wormley, Godalming, Surrey GU8 5UG, United Kingdom; Hisato Yasuda, Department of Geology, Kochi University, Kochi 780, Japan.

Table 1. Coring summary, Site 661.

Core no. and type[a]	Date (March 1986)	Time (UTC)[b]	Depths (mbsf)	Length cored (m)	Length recovered (m)	Recovery (%)
Hole 661A						
1H	18	0320	0–1.6	1.6	1.6	101.0
2H	18	0410	1.6–11.1	9.5	9.4	98.9
3H	18	0456	11.1–20.6	9.5	9.0	95.1
4H	18	0550	20.6–30.1	9.5	9.8	102.0
5H	18	0635	30.1–39.6	9.5	9.0	94.7
6H	18	0722	39.6–49.1	9.5	9.4	98.5
7H	18	0805	49.1–58.6	9.5	9.3	97.9
8H	18	0845	58.6–68.1	9.5	9.3	97.5
9H	18	0930	68.1–77.6	9.5	9.3	98.0
10H	18	1010	77.6–87.1	9.5	8.7	91.0
11H	18	1055	87.1–96.6	9.5	9.4	99.0
12H	18	1141	96.6–106.1	9.5	9.0	94.7
13H	18	1235	106.1–115.6	9.5	8.9	94.1
14H	18	1325	115.6–125.1	9.5	9.4	99.2
15H	18	1413	125.1–134.6	9.5	8.6	90.8
16X	18	1635	134.6–144.1	9.5	9.2	96.4
17X	18	1915	144.1–153.6	9.5	1.9	19.8
18X	18	2033	153.6–163.1	9.5	2.8	29.5
19X	18	2215	163.1–172.6	9.5	9.4	99.0
20X	19	0035	172.6–182.1	9.5	9.7	102.0
21X	19	0315	182.1–191.6	9.5	3.5	36.6
22X	19	0625	191.6–201.1	9.5	2.3	24.2
23X	19	0823	201.1–210.6	9.5	5.6	59.3
24X	19	1010	210.6–220.1	9.5	9.1	96.1
25X	19	1158	220.1–229.6	9.5	8.3	87.5
26X	19	1351	229.6–239.1	9.5	8.5	89.6
27X	19	1604	239.1–248.6	9.5	3.1	32.2
28X	19	1818	248.6–258.1	9.5	8.5	89.1
29X	19	2039	258.1–267.6	9.5	5.9	62.5
30X	19	2233	267.6–277.1	9.5	3.2	34.1
31X	20	0028	277.1–286.6	9.5	5.7	60.2
32X	20	0225	286.6–296.1	9.5	8.1	84.9
Hole 661B						
1H	20	2047	0–5.7	5.7	5.7	100.0
2H	20	2200	5.7–15.2	9.5	9.8	103.0
3H	20	2257	15.2–24.7	9.5	9.3	97.6
4H	20	2356	24.7–34.2	9.5	9.6	101.0
5H	21	0050	34.2–43.7	9.5	9.7	102.0
6H	21	0151	43.7–53.2	9.5	9.0	94.8
7H	21	0235	53.2–62.7	9.5	9.5	100.0
8H	21	0345	62.7–72.2	9.5	9.7	102.0
9H	21	0440	72.2–81.7	9.5	9.1	95.5

[a] H = hydraulic piston; X = extended core barrel.
[b] UTC = Universal Time Coordinated.

portions of biogenic opal and organic carbon (up to 0.65%) that may imply increased ocean productivity. Subunit IB is small-amplitude sediment cycles with only minor amounts of clay, and decreasing carbonate below 60 mbsf (about 4.0 Ma). This stratigraphy closely matches that of neighboring Site 660 up to the precision of susceptibility-curve cycles, but with more carbonate and less organic carbon. The deposition rates varied from about 16 m/m.y. during the last 4.2 m.y. to 4 m/m.y. from 4.2 to 8.9 Ma. The marked change in $CaCO_3$ and sedimentation rate about 4.0 to 4.2 Ma matches changes of similar age at Sites 657, 659, and 660 and may indicate a major event of deep-water paleoceanography in the eastern Atlantic.

Unit II (72.55–90.8 mbsf) consists of lower upper Miocene and older olive brownish to brownish red silty clay cycles interbedded with rare nannofossil ooze near the top (down to 83 mbsf).

Unit III (90.8–296.1 mbsf) is composed of Upper Cretaceous and younger bluish-greenish zeolite clay and claystone. It is interbedded with Maestrichtian nannofossil ooze from 105.3 to 163.1 mbsf—i.e., within Subunit IIIA. Subunit IIIB is carbonate-free, fossil-barren clay and claystone from 163.1 to 296.1 mbsf.

The upper part of Unit III (92.5–93.75 mbsf) is marked by three distinctly weathered bedding planes with manganese nodules and clay (20 cm thick), or yellowish dolomite clay, which signify extended hiatuses, possibly contemporaneous with the thick radiolarian ooze and manganese zone at Site 660, dated near 43 Ma and younger. Based on the most conservative estimates of sedimentation rates, the Cretaceous/Tertiary boundary could occur 0.8 m (=0.13 m.y.), or less, above the nannofossil-ooze bed ending at 105.3 mbsf.

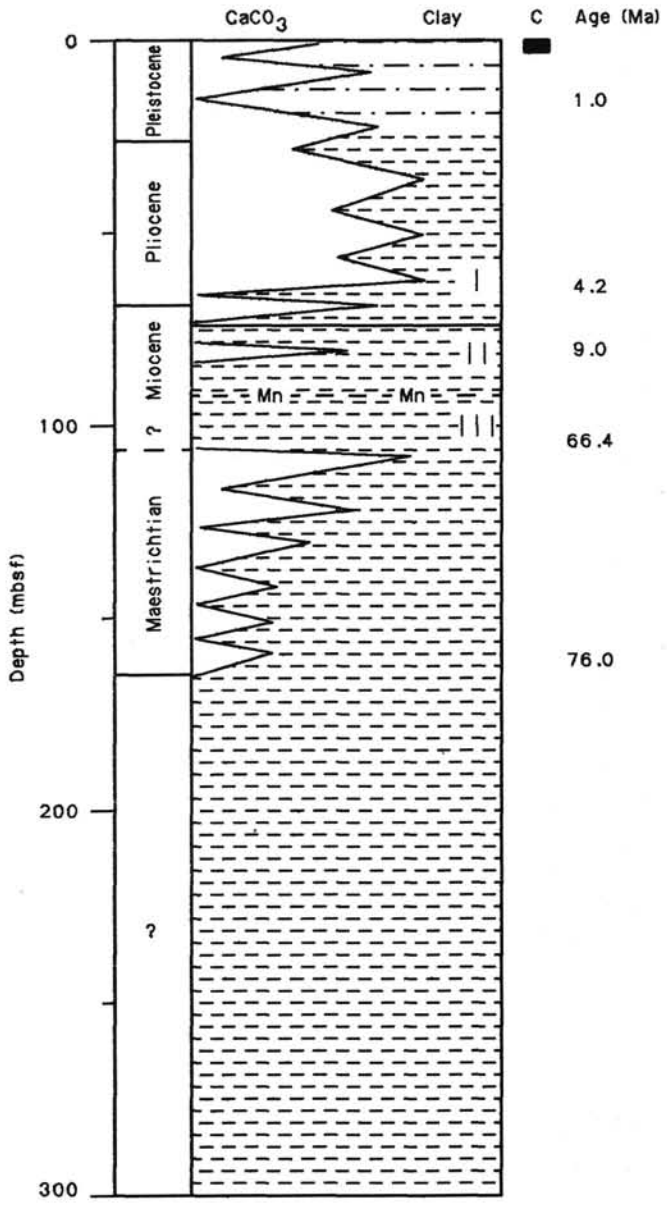

Figure 1. Lithostratigraphic and biostratigraphic summary of Site 661. Schematic $CaCO_3$ cycles show general range of $CaCO_3$ fluctuations markedly increasing upward. *I, II,* and *III* represent lithologic units. *C* = >0.5% organic carbon. *Mn* = manganese oxide zone.

Further work is required on shore to pin down this boundary more exactly.

BACKGROUND AND OBJECTIVES

Introduction

The scientific objectives at Site 661 (9°26.81′N, 19°23.166′W) are closely related to those of companion Site 660, which have already been explained in detail (see Site 660 chapter, this volume). Site 661 is the upper end-member of a transect across the eastern slope of the Kane Gap, the major deep-water passage through the barrier of the Sierra Leone Rise. The site position at 4012.7 m water depth, on top of a small, smooth plateau, lies about 600 m above the floor of the Kane Gap (Fig. 2) and below the upwelling of the northern equatorial divergence zone, the Guinea Dome, during the northern summer. Thereby, this site

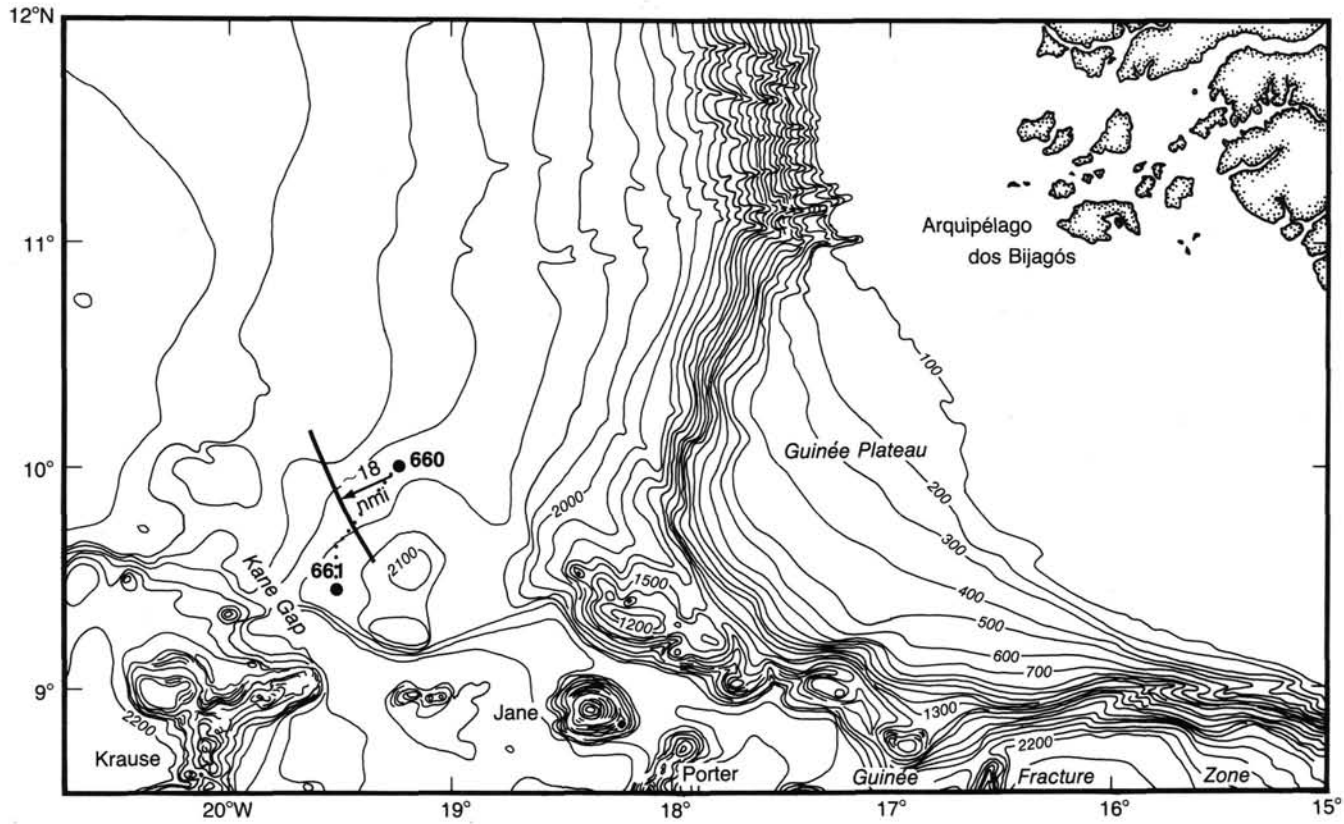

Figure 2. Bathymetry of the eastern equatorial Atlantic in the vicinity of Sites 660 and 661 (after Jones and Mgbatogu, 1982; depth in fathoms). Dotted line indicates seismic track of *JOIDES Resolution* (Fig. 3).

complements the sediment record of nearby Site 660, which lies at a water depth of 4327.8 m. The sediments at the shallower Site 661 are expected to be much less affected by deep-water current action and calcium carbonate dissolution. Site 661 was selected to provide a Cenozoic sediment record of the paleoceanographic and paleoclimatic features and had the following objectives:

1. To determine accumulation rates of organic carbon and various other sedimentary components in order to obtain a detailed record of oceanic productivity in the Northern Equatorial Divergence Zone for the late Neogene.
2. To reconstruct, by comparing the records of Sites 660 and 661, a bathymetric profile of sediment parameters (e.g., organic-carbon accumulation, carbonate dissolution and accumulation, and benthos stable isotopes) that record the history of deep-water circulation, hydrography, and chemistry, and especially to monitor the Neogene history of deep-water ventilation between the different basins of the Atlantic near the upper boundary of vertical glacial-to-interglacial lysocline fluctuations.
3. To study eolian-dust sediments that record the history of atmospheric paleocirculation during northern winter and of aridity in the North African Sahel zone, at a position close to the southern margin of North African dust outbreaks.
4. To compare the long-term time spectra of the fluctuations in atmospheric and oceanic surface circulation in order to separate the relative importance of high- and low-latitude insolation in the Milankovitch cycles and to decipher phase relationships between the various components.
5. To date and trace upslope various current events identified in cores and seismograms at Site 660 for the Cenozoic.
6. To trace the upslope distribution of Eocene radiolarian oozes and cherts observed at Site 660.

Geologic Setting

The position of Site 661 (Fig. 2) was selected on the basis of a detailed bathymetric map of the Kane Gap (Jones and Mgbatogu, 1982; Mienert, 1986), various 3.5-kHz lines, a 13.3-m-long *Meteor* core (16415) in the vicinity (Brassel et al., 1986), and the *JOIDES Resolution* seismic water-gun record during the approach to Site 661 (Fig. 3). The seismic profile is characterized by regularly layered reflectors with two more transparent horizons at 0.035–0.12 and 0.28–0.40 seconds below the seafloor (sbsf) and acoustic basement below 0.7-s two-way traveltime. Based on the stratigraphic section of DSDP Site 366 (approximately 420 km farther south on top of the Sierra Leone Rise), the age of an unknown lower part of the section at Site 661 was expected to be Cretaceous (Lancelot, Seibold, et al., 1978).

OPERATIONS

From Site 660, *JOIDES Resolution* steamed southwest to Site 661 (alternative target Site SLR 2). We continuously deployed the 80-in.^{3} water guns, the 3.5-kHz sub-bottom profiler, and the magnetometer in order to connect companion Sites 660 and 661 by a seismic record and to facilitate the selection and interpretation of the new Site 661 position. However, the quality of the water-gun record was not as good as those collected earlier on this leg, because the ship had to speed up in order to reach the Site 661 (target site SLR 2) survey area during a Global Positioning System (GPS) time window.

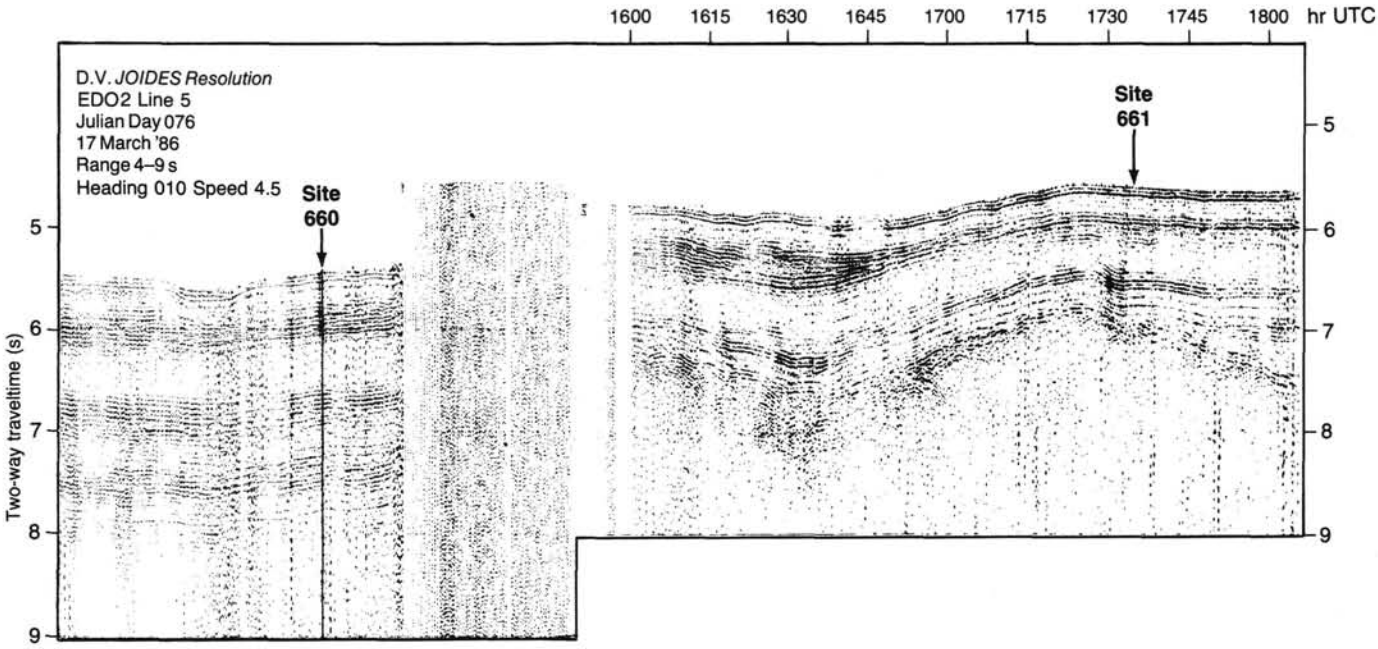

Figure 3. *JOIDES Resolution* water-gun seismic-reflection record near Site 661.

We entered the Site 661 survey area at 1600 UTC on 17 March 1986. (All times are expressed as UTC, Universal Time Coordinated, formerly expressed as GMT, Greenwich Mean Time.) At Point 1 (Fig. 2 and Table 2), the *JOIDES Resolution* slowed down from an average of 12 to 5.5 kt in order to achieve a high-quality seismic record of the north-south profile to Point 2. At 1800 hr the ship turned 180° and approached the presumptive site position at Point 2 at 1737 hr on the seismic profile (Fig. 3), where we dropped the beacon at 1845 hr and began to pull in the survey gear.

At 1915 hr we stopped over the beacon and began tripping the drill pipe. The first 1.6-m APC core was on deck at 0320 hr on 18 March. The mud line for Hole 661A was established by drill pipe at 4012.7 m water depth. APC coring continued with excellent recovery (96.6%; Table 1) for 15 cores. We changed to XCB coring at 1635 hr and cored in Hole 661A until Core 108-661A-32X was on deck from 296.1 mbsf at 0225 hr on 20 March. By this time, core recovery was strongly reduced and consisted of fossil-barren clay from the Cretaceous. Penetrating this lithology was near the technical limits of XCB drilling.

From 0230 to 1730 hr, time was allotted for two runs of borehole logging with dual-induction and sonic-gamma-ray tools. The first run was successful until a bridge was encountered in the hole below 160 mbsf. The second run was unsuccessful because of poor hole conditions, including narrowing of the hole to 4 in. as measured by calipers. After filling Hole 661A with mud, we tripped out the drill pipe and by 1915 hr had offset the hole by 15 m.

The first of nine APC cores from Hole 661B was on deck at 2047 hr on 20 March, and the last, from 81.7 mbsf, at 0440 hr on 21 March. We began tripping out of the hole at 0900 hr, brought the drill string on deck, and headed south to Site 662 (target Site EQ 7) at 1200 hr on 21 March.

Table 2. Positions of site-survey turning points.

Point no.	Position
1	9°36′N; 19°26′W
2	9°24.2′N; 9°22.6′W

LITHOSTRATIGRAPHY AND SEDIMENTOLOGY

Introduction

Three major lithologic units are recognized at Site 661 (Fig. 4). Unit I is composed of interbedded nannofossil and muddy nannofossil ooze with lesser amounts of nannofossil clay and silty clay, and is Pliocene to Pleistocene in age. Unit II is composed of interbedded silty clay and nannofossil ooze, and is Miocene and possibly older. Unit III is composed of clay and claystone, with lesser amounts of nannofossil ooze and nannofossil clay, and is Late Cretaceous and possibly younger.

Each lithologic unit is described in detail in the following sections.

Unit I

Cores 108-661A-1H to -661A-9H-3, 145 cm; depth, 0–72.55 mbsf; thickness, 72.55 m; age, latest Miocene to Pleistocene.
Cores 108-661B-1H to -661B-9H; depth, 0–81.7 mbsf; thickness, 81.7 m; age, latest Miocene to Pleistocene.

Unit I is composed of interbedded nannofossil ooze, muddy nannofossil ooze, and rare nannofossil clay. It is subdivided into two distinct subunits on the basis of variations in the relative proportions of carbonate and clay:

	Hole 661A	*Hole 661B*
Subunit IA	0–20.6 mbsf	0–15.2 mbsf
Subunit IB	20.6–72.55 mbsf	15.2–81.7 mbsf

Subunit IA is composed of interbedded muddy nannofossil ooze and nannofossil-bearing and nannofossil silty clay. The muddy nannofossil ooze is the most common sediment type in Subunit IA and is commonly brown or light gray to dark gray. The silty clay is the less common sediment type in Subunit IA and is found only in Cores 108-661A-2H and -661A-3H. It is commonly light to dark gray and contains minor to major amounts of nannofossils. Both sediment types are moderately

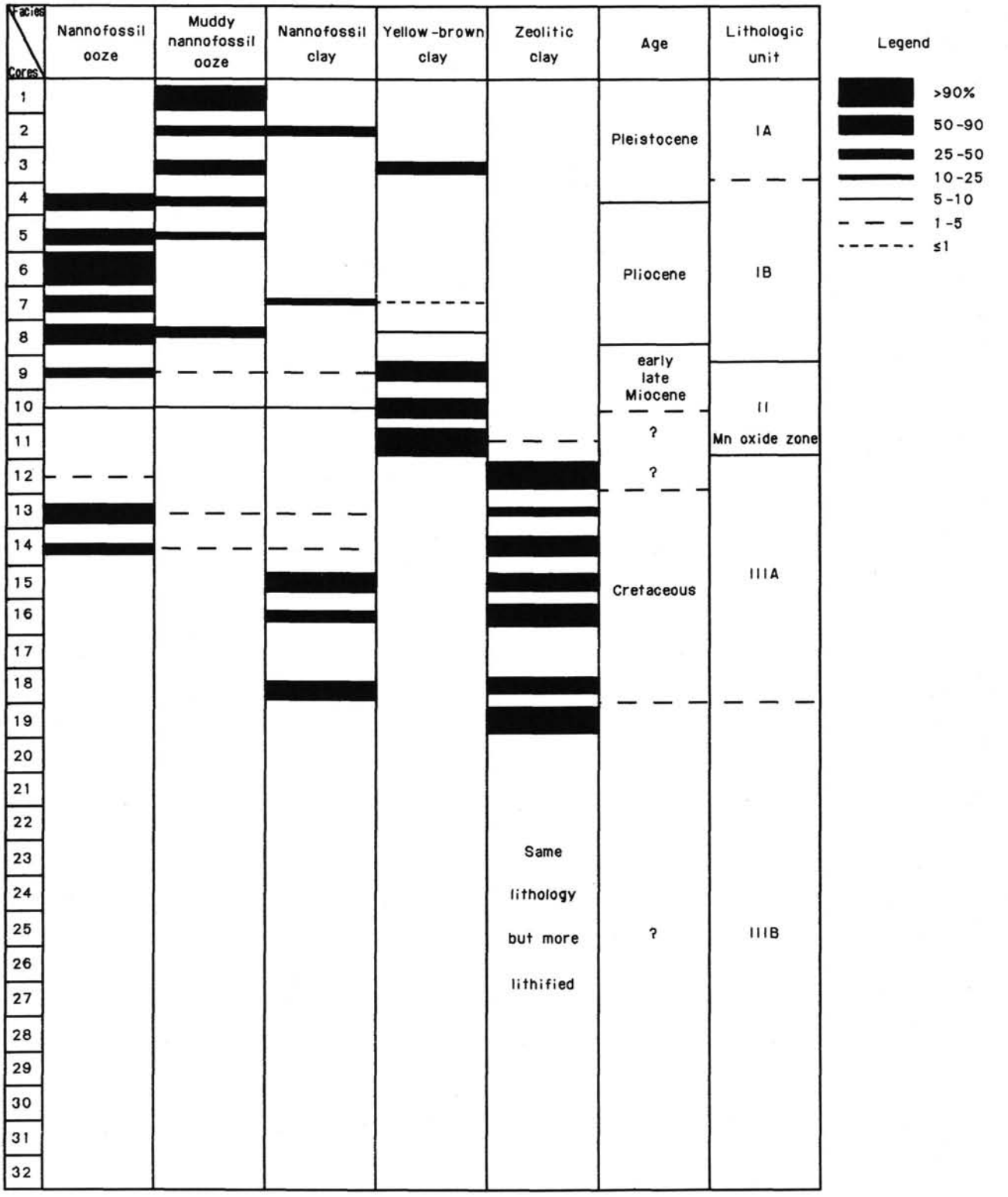

Figure 4. Summary of lithofacies for Hole 661A.

bioturbated and contain numerous dark greenish gray laminations. The entire subunit is characterized by a general downward increase in measured carbonate content (Fig. 5), which reflects the common occurrence of silty clay in its upper part. The silty clay consists mainly of quartz and kaolinite (Fig. 6).

Subunit IB is composed of interbedded nannofossil ooze, muddy nannofossil ooze, and silty clay. The nannofossil ooze is the most common sediment type in Subunit IB. It is commonly white to olive gray and contains major to minor amounts of foraminifers and minor amounts of clay. The muddy nannofossil

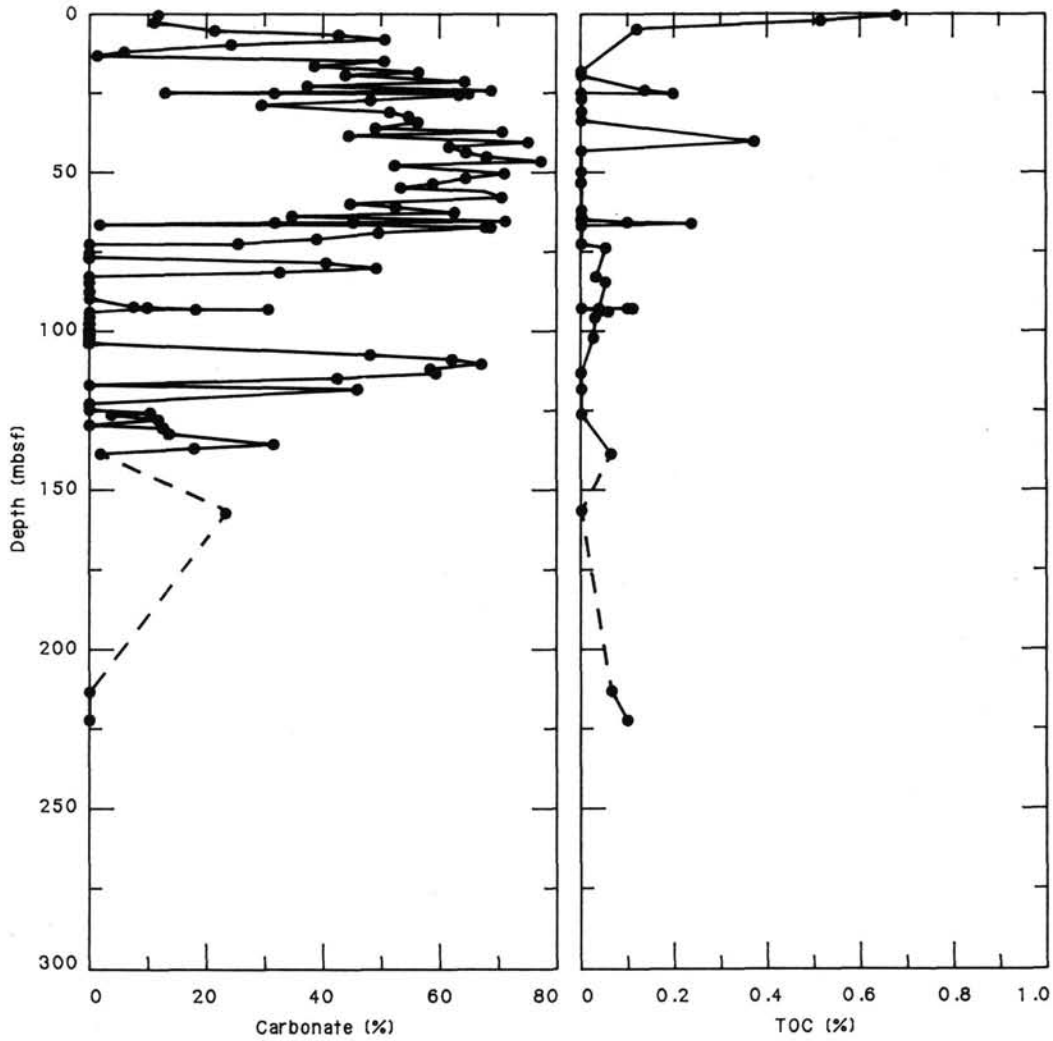

Figure 5. Carbonate and total-organic-carbon (TOC) contents of sediments from Hole 661A.

ooze is less common in Subunit IB. It is commonly light gray and also contains major to minor amounts of foraminifers. The silty clay is the least common sediment type in Subunit IB and is found only in the lower three cores of Subunit IB. It is yellowish brown and contains minor to major amounts of nannofossils. All three sediment types are moderately bioturbated; in addition, the nannofossil ooze and muddy nannofossil ooze contain numerous green and black laminae and are commonly stained black or gray with pyrite. The entire subunit is generally characterized by a high (up to 80%) measured carbonate content (Fig. 5) and a low quartz content (Fig. 6). However, the measured carbonate content decreases slightly in the lower three cores of Subunit IB, in which silty clay is more common.

Unit II

Cores 108-661A-9H-3, 145 cm, to -661A-11H-3, 80 cm; depth, 72.55–90.8 mbsf; thickness, 18.25 m; age, latest Miocene and possibly older (lower part of unit is barren).

Unit II is composed of interbedded silty clay and nannofossil ooze and is characterized by a relatively low carbonate content (0%–50%; Fig. 5). The silty clay is generally brown or yellow and commonly contains minor amounts of nannofossils. The nannofossil ooze is reddish yellow to pink and contains minor amounts of clay. Both sediment types are extensively bioturbated.

Unit III

Cores 108-661A-11H-3, 80 cm, through -661A-32X; depth, 90.8–296.1 m; thickness, 205.3 m; age, Late Cretaceous and possibly younger (upper part of unit is barren).

Unit III is composed of clay and claystone, with lesser amounts of nannofossil ooze, and is characterized by a general downward decrease in measured carbonate content (Fig. 5). It is divided into two subunits:

	Hole 661A
Subunit IIIA	90.8–163.1 mbsf
Subunit IIIB	163.1–296.1 mbsf

Subunit IIIA is composed of interbedded silty clay, nannofossil ooze, and nannofossil clay. Its top is marked by the occurrences of (1) iron nodules with minor amounts of copper, cobalt, chromium, nickel, and titanium (Fig. 7); (2) variegated sediments containing some dolomite and manganese oxides; and (3) sharp, presumably erosional, bedding planes, all of which occur in Sections 108-661A-11H-3 through -661A-11H, CC. The silty clay is principally composed of quartz, illite, montmorillonite, and clinoptilolite (heulandite) (Fig. 6), as well as major to minor amounts of nannofossils and minor to trace amounts of quartz, accessory minerals, and pyrite. It is greenish gray,

Core	Q	K	I	M	Z	Age
1	●●●●●●●	●●	-	-	-	Pleistocene
2	●●●●●●	●	-	-	-	
3	●●●●	●●	-	-	-	
4	●●	●●	-	-	-	
5	●	●	-	-	-	Pliocene
6	●	●	-	-	-	
7	●	●	-	-	-	
8	●	●●	-	-	-	
9	●●●●	●●●●	-	-	-	late Miocene
10	●●●	●●	-	-	-	
11	●●●●	●●●●	●●	●●●●	●●●●	?
12	●●●	●●	●●●	●●●●	●●	
13	●●●	-	-	●	-	Maestrichtian
14	●●●●	●	●●	●●	●●	
15	●●●●	●	●	●●	●	
16	●●●●	•	●●●	●	-	
17						
18	●●●●	•	●●●	●	-	
19	●●●●	●	●●●	●●	-	?
20	●●●●	-	●●	●●	●	
21	●●●●	-	●●	●●	●●	
22	●●●●	-	●●	●●●	●●	
23	●●●●	-	●●	●●●	●●	
24	●●●	-	●	●●	●●	
25	●●●	-	●	●●	●●	
26	●●●	-	●●	●●	●	
27	●●●	-	●●	●●	●	
28	●●●●	-	●●	●●	●	

Figure 6. X-ray-diffraction data from bulk-sediment samples from Hole 661A (qualitative estimates). Q = quartz; K = kaolinite; I = illite; M = montmorillonite; Z = zeolite (clinoptilolite/heulandite).

slightly bioturbated to massive, and contains scattered grayish green laminae. The nannofossil ooze is restricted to the upper part of Subunit IIIA (Cores 108-661A-13H and -661A-14H). It is greenish gray to light greenish gray, contains minor amounts of clay (in Core 108-661A-13H), and is slightly to moderately bioturbated. The nannofossil clay is restricted to the lower part of Subunit IIIA (Cores 108-661A-15H, -661A-16H, and -661A-18H). It is light olive brown to grayish green and slightly to moderately bioturbated. The entire subunit is characterized by a general downward decrease in measured carbonate content (Fig. 5).

Subunit IIIB is composed of clay and claystone. The clay (stone) is greenish gray, massive, and contains scattered nodules of pyrite. It is composed of clay minerals, zeolites (in the upper part of the subunit), and banded anhydrite (in the lower part) and is characterized by an extremely low (approaching 0%) measured carbonate content (Fig. 5).

Depositional History

The depositional history of the stratigraphic interval that was recovered at Site 661 began with accumulation of a thick section of clay during the Late Cretaceous Period. The site was initially below the carbonate compensation depth (CCD) during the earlier parts of this first depositional phase (Subunit IIIB), but gradually evolved to a relative position above the CCD (Subunit IIIA). The second depositional phase preserved at this site began some time before the late Miocene, after a considerable hiatus, and was characterized by deposition of calcareous pelagic sediment and lesser amounts of terrigenous brown silt and clay (Unit II). The third and last depositional phase took place during the Pliocene-Pleistocene and was characterized by deposition of calcareous pelagic sediment, an increased (but variable) influx of terrigenous silt and clay, and/or an increased dissolution of calcareous sediment (Unit I).

BIOSTRATIGRAPHY

Two holes were cored at Site 661, which is situated along the eastern slope of Kane Gap under waters of relatively high productivity. Hole 661A was cored to a depth of 296.1 mbsf, and Hole 661B to a depth of 81.7 mbsf. Age and zonal assignments are shown in Figures 8 and 9. The interval from 0 to 82.6 mbsf (Hole 661A) is fossiliferous and ranges in age from late Miocene to Holocene. Based on nannofossil and planktonic-foraminifer stratigraphies, the Miocene/Pliocene boundary is placed between 67 and 68.2 mbsf. The stratigraphic interval from 83.6 to 105.3 mbsf is barren of calcareous and siliceous microfossils; as a result, no age could be determined for this interval. The interval from 105.3 to 163.1 mbsf is Late Cretaceous in age, based on calcareous nannofossils. The only microfossils recognized below 163.1 m were rare pyritized radiolarians and diatoms.

Although the water depth at Site 661 has resulted in considerable carbonate dissolution, the $CaCO_3$ content is generally

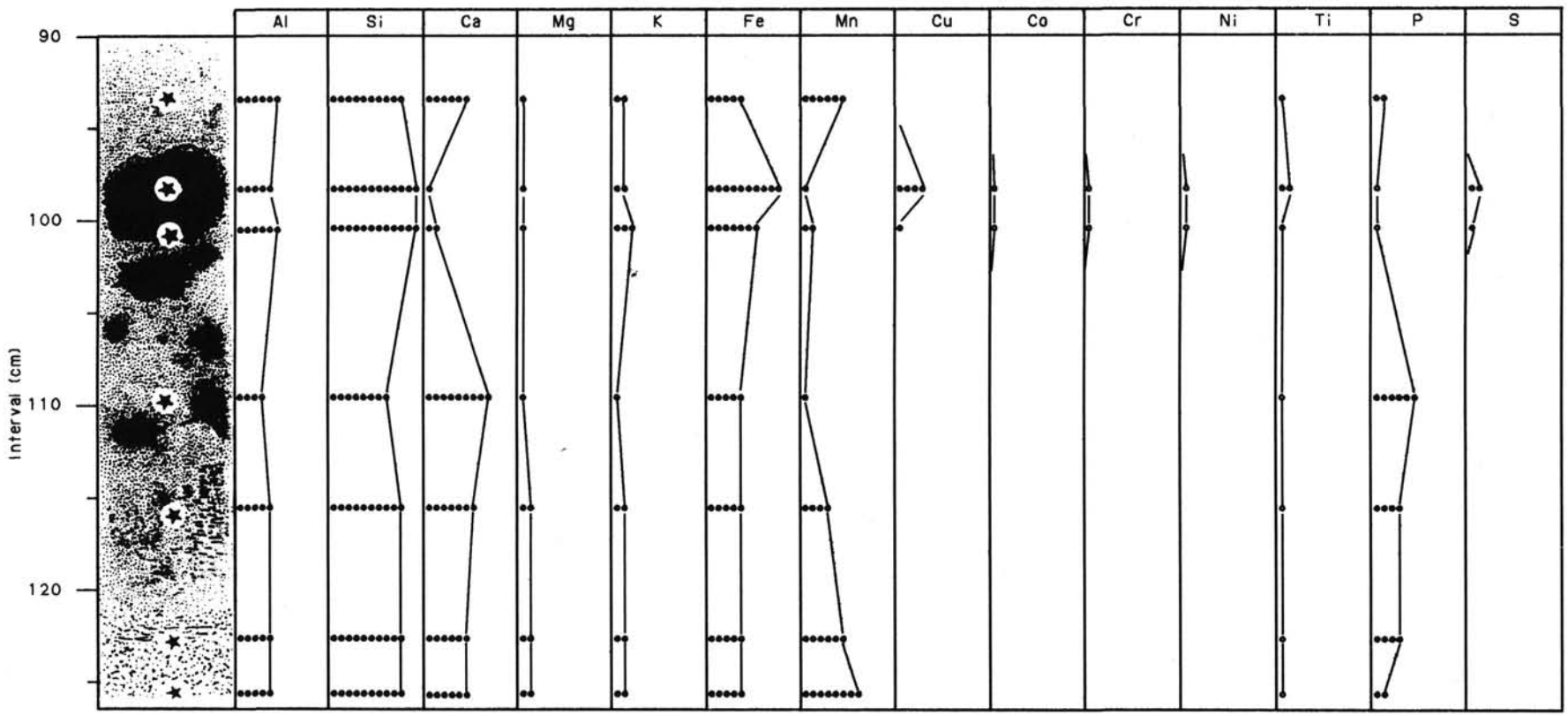

Figure 7. X-ray-fluorescence data from bulk sediment of Sample 108-661A-11H-4, 90–125 cm (qualitative estimates based on noncalibrated intensity values). Open dots indicate intensity values slightly higher than the noise level. Stars mark sample positions.

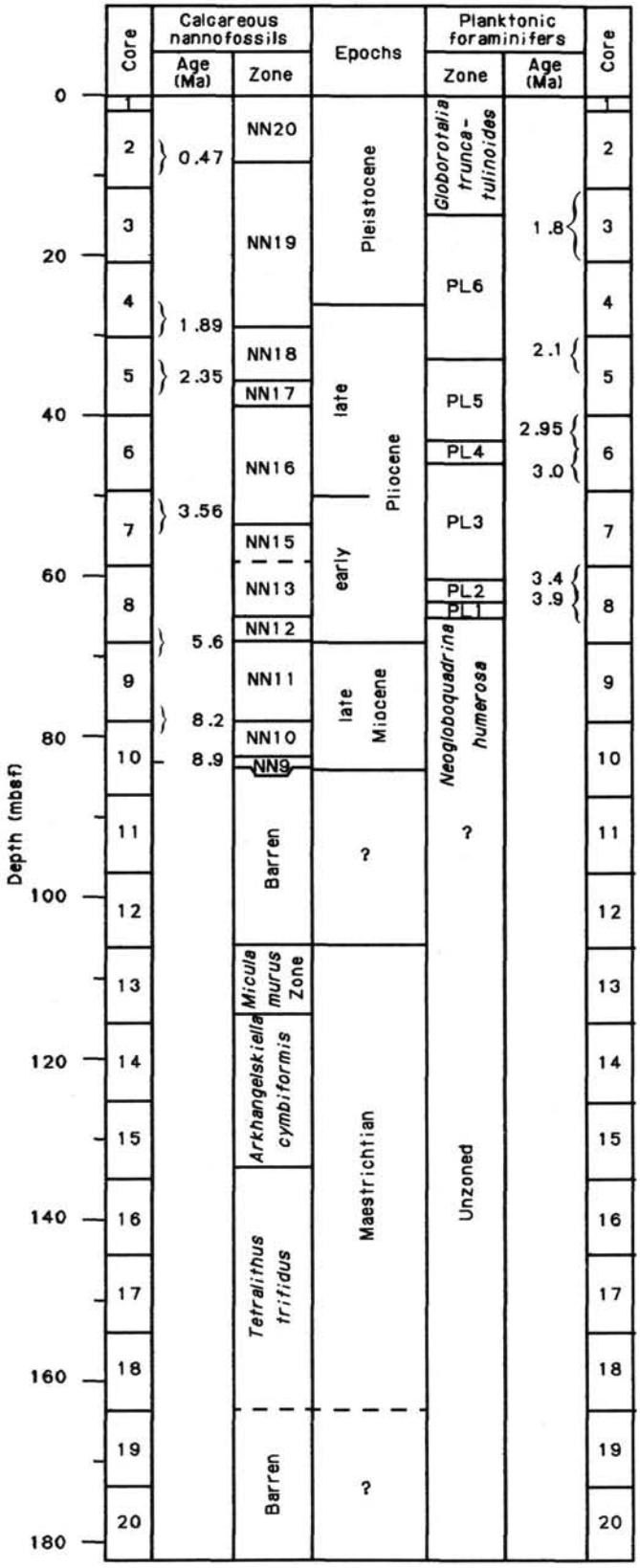

Figure 8. Zonal assignments for core recovered from Hole 661A. The interval representing calcareous-nannofossil Zone NN14 was not identified in this hole.

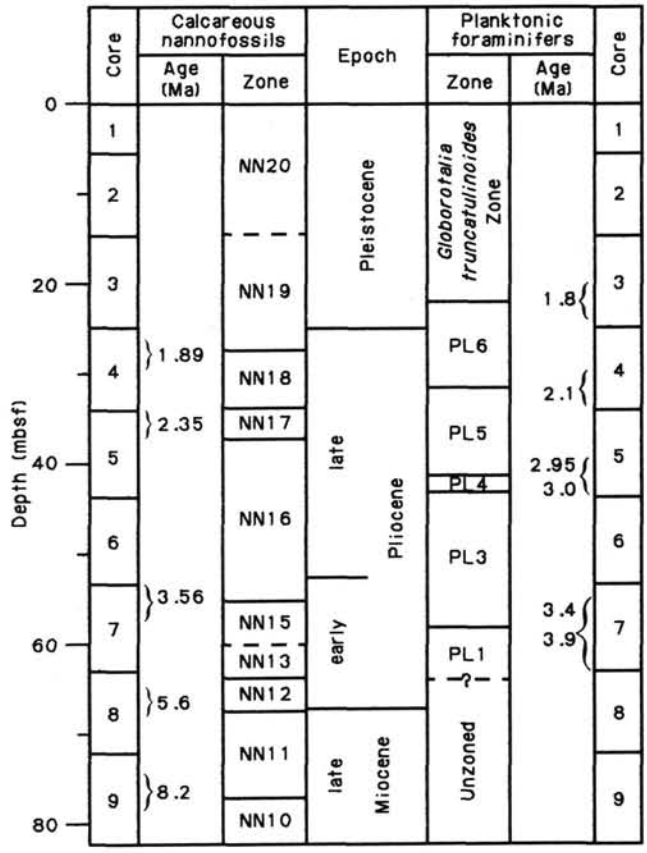

Figure 9. Zonal assignments for core recovered from Hole 661B. The interval representing calcareous-nannofossil Zone NN14 was not identified in this hole.

greater than at the deeper Site 660. At Site 661, $CaCO_3$ dissolution is greater in the Pliocene and Miocene than in the Pleistocene. Nevertheless, well-preserved discoasters are observed throughout the upper Miocene and Pliocene interval.

The planktonic foraminifers are characteristic of low latitudes and are generally abundant and moderately well preserved through the Pliocene and Pleistocene. As with the calcareous nannofossils, preservation of the planktonic foraminifers deteriorates in the upper Miocene. Planktonic foraminifers are absent from the unzoned red clays and zeolitic silts and from the Cretaceous sediments.

Although diatoms generally were not observed, scattered samples contained rare, biostratigraphically unimportant species. Rare pyritized radiolarians and diatoms were observed in a few samples from the lowermost part of Hole 661A.

Calcareous Nannofossils

Site 661 is a companion site to Site 660, and correlation of the seismic stratigraphy indicated that the stratigraphic records would be virtually identical. The slightly shallower water depth (~300 m) of Site 661 suggested the recovery of sediment with a higher calcium carbonate content. Therefore, while the oldest nannofossil-bearing sediment at Site 660 belonged to the later part of Zone NN11 (5.6–6.5 Ma), the oldest (nannofossil-bearing) Cenozoic sediment at Site 661 was referred to Zone NN9 and assigned an age close to 9 Ma. Quite surprising was the recovery of nannofossil-bearing sediment of Late Cretaceous age (Maestrichtian and perhaps latest Campanian) at Site 661 between about 106 and 163 mbsf. Although Site 660 was drilled to a depth of 163 mbsf, nannofossils were not observed below 76.8 m.

At Site 661, the Pleistocene sediments alternate between dark muds and yellowish oozes, with the dark muds barren of nannofossils or showing poorly preserved assemblages. Preservation improves in sediment of late Pliocene and early Pleistocene age but is preceded by increased dissolution of lower Pliocene assemblages and severe dissolution of upper Miocene assemblages. Miocene placoliths are largely reduced to more dissolution-resistant forms, whereas discoasters generally still display a great deal of morphological detail. The Upper Cretaceous assemblages are all severely dissolved, displaying large amounts of fragmented placolith rims and placoliths with dissolved central areas.

Pleistocene

Pseudoemiliania lacunosa disappears between Sections 108-661A-2H-3 and -661A-2H-5. In Hole 661B the NN20/NN19 zonal boundary occurs in Core 108-661B-2H. The early Pleistocene disappearance of *Calcidiscus macintyrei* provides an easily recognizable event, occurring between Samples 108-661A-4H-1, 80 cm, and -661A-4H-2, 80 cm, and in the lower part of Section 108-661B-3H-6.

Pliocene

The late Pliocene succession of discoaster events provides good biostratigraphic control at Site 661, partly because of high abundances and partly because reworking is negligible. The extinctions of *Discoaster brouweri* and *Discoaster triradiatus* were observed in Sections 108-661A-4H-6 and -661B-4H-3. The most abundant species at these levels are small placoliths (<4 μm), belonging either to *Gephyrocapsa* or *Reticulofenestra*. Their taxonomic affinities have to be determined using electron-microscope techniques. The increase in proportion of *D. triradiatus* relative to *D. brouweri* occurs between Cores 108-661A-6H and -661A-7H and in the lower part of Core 108-661B-4H. This event subdivides Zone NN18 into two parts of virtually equal duration.

The extinctions of *Discoaster pentaradiatus* and *Discoaster surculus* occur in the lower half of Core 108-661A-5H (upper half of Core 108-661B-5H). These are followed by the disappearance of *Discoaster tamalis* (Sections 108-661A-6H-2 and -661B-5H-6). The boundary between the late and early Pliocene approximates the extinction of the sphenoliths in Sections 108-661A-7H-3 and -661B-7H-1. This event is, in turn, shortly preceded (about 1 to 2 m) by the disappearance of *Reticulofenestra pseudoumbilica*. Amaurolithids disappear in Section 108-661A-7H-5; the first occurrence (FO) of *Discoaster asymmetricus* has not been determined. Perfectly preserved specimens of *Ceratolithus acutus* occur in Section 108-661A-8H-6 but not in one section upcore, where *Ceratolithus rugosus* is present. In Hole 661B the transition from *C. acutus* to *C. rugosus* occurs in Section 108-661B-8H-3.

Miocene

Generally, Miocene assemblages are characterized by well-preserved discoasters and poorly preserved placoliths. Reticulofenestrids dominate the placoliths. *Triquetrorhabdulus rugosus* survives *Discoaster quinqueramus* for a brief interval, but their exact biochronologic relationship still remains ambiguous. The extinction of *D. quinqueramus* occurs in Sections 108-661A-9H-1 and -661B-8H-4. The appearance of amaurolithids occurs in Sections 108-661A-9H-4 and -661B-8H-6 (Section 108-661B-9H-1 was severely disturbed by drilling and was not investigated; Section 108-661B-9H-2 was barren of nannofossils), and the appearance of *Discoaster berggrenii* occurs in Sections 108-661A-10H-1 and -661B-9H-4 (base of Zone NN11). *Discoaster bollii* disappears shortly above (1 to 2 m) the extinction of *Discoaster hamatus*. The latter event, defining the top of Zone NN9, was observed at the bottom of Section 108-661A-10H-3. Hole 661B ends about 1 m below the extinction of *D. bollii*. Investigation of two core-catcher samples from Core 108-661B-9H did not yield *Discoaster hamatus*, indicating that this core reaches down to the basal part of Zone NN10. A single reworked Eocene specimen of *Discoaster barbadiensis* was observed in Sample 108-661B-9H-CC, 11 cm.

Cenozoic nannofossils were not observed below Sample 108-661A-10H-4, 45 cm. This sample still contained *D. hamatus*, indicating Zone NN9, together with abundant middle to late Miocene discoasters and *Catinaster calyculus*, but without *Catinaster coalitus*. Thus, this sample represents an age of about 8.9 to 9.0 Ma.

About 50 samples were investigated between Samples 108-661A-10H-4, 140 cm, and -661A-12H-6, 103 cm, but all were barren of nannofossils. Thus, only about 22 m of sediment separates the upper Miocene from the Upper Cretaceous, representing a time interval of about 57 to 58 m.y.

Mesozoic (Maestrichtian–Campanian)

Upper Cretaceous sediments recovered from Hole 661A contain severely dissolved nannofossils. Calcite overgrowth is especially common on specimens of the dissolution-resistant genus *Micula*, which, with *Tetralithus* spp., provides the stratigraphic control. Other species provide poor biostratigraphic resolution because of their long stratigraphic ranges.

Sample 108-661A-12H-6, 121 cm, contains few, moderately well-preserved specimens including *Micula staurophora, M. murus, M. prinsii*, and *Watznaueria barnesae*. Samples 108-661A-12H-6, 122 cm, and -661A-12H-6, 124 cm, contain a marked increase in abundance of *M. staurophora*. In addition, *Micula murus, M. praemura, W. barnesae, Arkhangelskiella cymbiformis, Cribrosphaerella ehrenbergii, Prediscosphaera cretacea, Zygodiscus spiralis*, and *Microrhabdulus stradneri* were also observed. This assemblage is characteristic of the upper part of the *M. murus* Zone. *Micula prinsii*, the marker species for the top of the Maestrichtian, has its FO in Sample 108-661A-13H-1, 90 cm.

The FO of *M. murus* was observed in Sample 108-661A-13H-6, 100 cm. This biostratigraphic event marks the base of the *Micula murus* Zone, which is defined as the interval representing the total stratigraphic range of *M. murus*. Only the *Micula murus* Zone could be identified at Site 661, because *Nephrolithus frequens*, another useful late Maestrichtian marker, was not observed. Similar to the findings of Perch-Nielsen (1977) and Stradner and Steinmetz (1984) from the South Atlantic, the absence of *N. frequens* at Site 661 most likely results from ecological exclusion.

Stratigraphically below the FO of *M. murus*, the preservation of the assemblage deteriorated, and only rare, poorly preserved fragments (only one wing) of *L. quadratus* were observed. Because of the poor preservation, the *Lithraphidites quadratus* Zone could not be identified. Therefore, only the basal part of the *Arkhangelskiella cymbiformis* Zone, represented by the LO of *Tetralithus trifidus*, was recognized. The FOs of *M. murus* and *M. praemura* mark the top of the *Arkhangelskiella cymbiformis* Zone.

The interval between Samples 108-661A-14H-8, 84 cm, and -661A-18X, CC represents the early Maestrichtian *Tetralithus trifidus* Zone. This zone is characterized by the occurrence of *T. trifidus, Tetralithus gothicus, M. staurophora*, and *Ceratolithoides aculeus*. Partially dissolved specimens of *Reinhardites levis* were observed in Section 108-661A-17X, CC, and specimens of *Lithraphidites praequadratus* were observed in Section 108-661A-16X, CC. Abundant and well-preserved specimens of *T. gothicus* occur in Sections 108-661A-17X, CC and -661A-18X, CC.

The LO of *Eiffellithus eximius* is considered by Monechi and Thierstein (1985) to represent the Maestrichtian/Campanian

boundary. This species was observed in Section 108-661A-18X, CC, which consequently approximates this boundary.

The absence of *Lucianorhabdus cayeuxi* (typical nearshore indicator) and the abundance of *T. trifidus* and *T. gothicus* indicate that the Maestrichtian nannofossil assemblage at Site 661 is a typical low-latitude, pelagic assemblage similar to that described by Stradner and Steinmetz (1984) from Site 530 (South Atlantic).

Planktonic Foraminifers

Site 661 compares closely with Site 660 in the nature and distribution of its foraminifer fauna. The main differences are better preservation in the Pleistocene and a late Neogene record extending back slightly farther in time at Site 661. Planktonic foraminifers are abundant and moderately well preserved through the Pliocene and Pleistocene, but in the uppermost Miocene preservation rapidly deteriorates, with only the more carbonate-rich samples having any fauna. Below the uppermost Miocene, all samples were barren.

The fauna has a tropical aspect, as at Site 660, with *Globigerinoides sacculifer* and *Globigerinoides trilobus* being fairly common throughout. Other tropical species, such as *Pulleniatina* spp., *Sphaerodinella dehiscens*, and several species of *Globorotalia*, are present in many samples.

The Pleistocene proved impossible to subdivide, and even the zonal fossil *Globorotalia truncatulinoides* is rare at this site, with its deepest occurrences in Samples 108-661A-1H, CC and -661B-3H-3, 110 cm. The Pleistocene fauna contains common *Globigerinoides ruber, G. sacculifer, G. trilobus*, and *Neogloboquadrina dutertrei*.

The PL6 Zone is found between Samples 108-661A-3H, CC and -661A-5H-1, 136 cm, and between Samples 108-661B-3H, CC and -661B-4H-4, 29 cm. The PL5 Zone extends to Sample 108-661A-6H-1, 135 cm, and to Sample 108-661B-5H-4, 29 cm. *Globorotalia puncticulata* has its LO at the top of the PL5 Zone, with the FO of *Globorotalia inflata* just above the base of the PL6 Zone. The short PL4 Zone was identified in Samples 108-661A-6H-3, 135 cm, and -661B-5H-5, 120 cm. The PL3 Zone extends down to Samples 108-661A-7H, CC and -661B-7H-4, 30 cm. The upper Pliocene fauna contains numerous *G. trilobus, G. sacculifer, Globigerinoides obliquus, Globigerina decoraperta*, and globorotaliids.

The early Pliocene PL2 Zone is very short and was observed only in Sample 108-661A-8H-3, 90 cm. The accumulation-rate curve ("Sediment-Accumulation Rates" section, this chapter) shows that this is due to the absence of *Globorotalia margaritae* rather than a hiatus. This is surprising because dissolution is not severe in this interval, and *G. margaritae* is regarded as a reliable marker in tropical regions (Bolli and Saunders, 1985). Zone PL1, marked by the overlap of *G. margaritae* with *Globigerina nepenthes* above the LO of *Globoquadrina dehiscens*, occurs in Samples 108-661A 8H-3, 90 cm, and -661B-7H, CC. The lower Pliocene fauna contains common *G. trilobus, G. obliquus, Globorotalia limbata, Sphaeroidinellopsis seminulina*, and *Neogloboquadrina humerosa*.

Samples 108-661A-8H, CC and -661A-9H-2, 14 cm, probably belong to the *Neogloboquadrina humerosa* Zone, based on the absence of *G. margaritae*, but this may be due to dissolution. As at previous sites, there is no overlap of *G. margaritae* with *G. dehiscens*, and the latter may have a restricted range in this area. *G. dehiscens* occurs only in Section 108-661A-8H, CC. Sections 108-661A-9H, CC and -661B-9H, CC contain poorly preserved faunas, and below these samples both holes are barren.

Benthic Foraminifers

Benthic foraminifers at Site 661 are roughly divided into two assemblages. The upper one is from core-catcher Sections 108-661A-1H to -661A-8H, which contain rare to common and moderately well-preserved specimens. This assemblage is characterized by several species that indicate middle bathyal to abyssal depths, such as *Melonis pompilioides, Gyroidinoides soldanii, Laticarinina pauperata*, and *Planulina wuellerstorfi*. The lower assemblage occurs from core-catcher Sections 108-661A-13H to -661A-20X and contains few to rare specimens exhibiting poor to moderate preservation. This lower assemblage is characterized by the common occurrence of agglutinated forms such as *Bathysiphon* spp., *Glomospira charoides, Rzehakina epigona*, and *Hormosina* sp. In addition, this assemblage includes abundant specimens of *Globorotalites conicus, Globorotalites spineus, Aragonia ouezzanensis, Gyroidina* sp., and *Reussella* sp. Their faunal association is essentially similar to that of the Upper Cretaceous sediments in the Southeast Atlantic Ocean reported by Beckmann (1978). No specimens were observed in core-catcher samples from Cores 108-661A-9H to -661A-12H and from Cores 108-661A-21X to -661A-32X.

Diatoms

With the exception of few diatoms in Section 108-661A-1H, CC and rare diatoms in Cores 108-661A-25X, -661A-27X, -661B-1H, -661B-3H, and -661B-4H, all core-catcher samples examined from Site 661 were barren of diatoms.

Core 108-661A-1H contains the following species, none of which is age-diagnostic: *Nitzschia marina, Thalassiothrix longissima, Thalassionema nitzschioides*, and the freshwater species *Cyclotella* sp., *Melosira* spp., and *Stephanodiscus astraea*.

Cores 108-661A-25X and -661A-27X contain rare, pyritized specimens of several *Triceratium* spp. and *Hemiaulus* spp. The primitive morphology of all species observed suggests a possible Cretaceous age for these samples. Any age assignment, however, should be considered extremely tentative because of the small number of specimens observed and their state of preservation.

Section 108-661B-1, CC contains rare specimens of *T. nitzschioides* and freshwater *Melosira* spp. Specimens of several freshwater *Melosira* spp. also occur in Sections 108-661B-3H, CC and -661B-4H, CC.

PALEOMAGNETISM

Magnetostratigraphy

Continuous core measurements were obtained on archive halves from sections of Cores 108-661A-1H to -661A-13H. All sections were demagnetized to 50 Oe. The results from Hole 661A archive halves were of exceptional quality, documenting the polarity sequence through Chron C2r in Core 108-661A-6H. A new surprise awaited us in Core 108-661A-7H: a post-splitting remanence. Severe discrepancy among discrete samples and the archive and working halves led us to the conclusion that Core 108-661A-7H had been remagnetized in the splitting room and subsequently during sampling. Presumably, the core had also been remagnetized during coring, tripping, cutting, and capping and will be remagnetized again during transport, storage, and resampling. We surmise that the low shear strength ("Physical Properties" section, this chapter) of the sediment contained in Core 108-661A-7H was responsible for the excessive mobility of the magnetic grains. This phenomenon cannot be entirely excluded in other cores, but we feel confident that cores with higher shear strengths will retain a pre-coring remanence.

Two to three subsamples were taken from Hole 661A core sections and one sample per core section was taken from Hole 661B. In most cases, a stable component was isolated by demagnetization to 100 Oe. In certain Hole 661B samples, however, there was a large and stable overprint, which was removed only after demagnetization to 300 or 400 Oe.

In Figures 10 and 11 we present our inclination data from the upper 50 mbsf of Hole 661A and all the Hole 661B data. The Hole 661A results are of acceptable quality, and we correlate the polarity log to the time scale without hesitation. The inclination values closely approximate the expected dipole inclination of 20° for the site latitude. Inclinations steeper than 50° are considered unreliable, as shown by the dashed lines which connect them to the rest of the data. Below about 50 mbsf the specimens show the same behavior as was observed below 60 mbsf at Site 660: general unreliability.

The data obtained from Hole 661B are good down to about 23 mbsf and correlate quite well with those of Hole 661A. Below this point, the persistence of positive inclinations renders the data suspect, as indicated by the question marks. We suspect that the overprinting exhibited by sediments in Hole 661A has proceeded to a greater extent in Hole 661B and that inclination data alone cannot be used for polarity determination.

Magnetic Susceptibility

We measured the whole-core volume susceptibility of most of the recovered interval from Holes 661A and 661B at a 3-cm spacing. In lithologic Unit III (see below) we increased the spacing to 6 cm.

In lithologic Unit I (Hole 661A, 0–72.6 mbsf; 661B, 0–81.7 mbsf: interbedded nannofossil ooze, muddy nannofossil ooze, and rare nannofossil clay of latest Miocene to Pleistocene age) susceptibilities average about 200 × 10^{-6} SI units and exhibit a pattern of high-frequency fluctuations. In lithologic Unit II (Hole 661A, 72.55–90.8 mbsf: interbedded silty clay and nannofossil ooze of latest Miocene age) susceptibilities average about 400 × 10^{-6} SI units and generally show little high-frequency variation. Over most of lithologic Unit III (Hole 661A, 90.8–296.1 mbsf: clay and claystone of Late Cretaceous and possibly younger age) the values are uniform and average about 100 to 200 × 10^{-6} SI units.

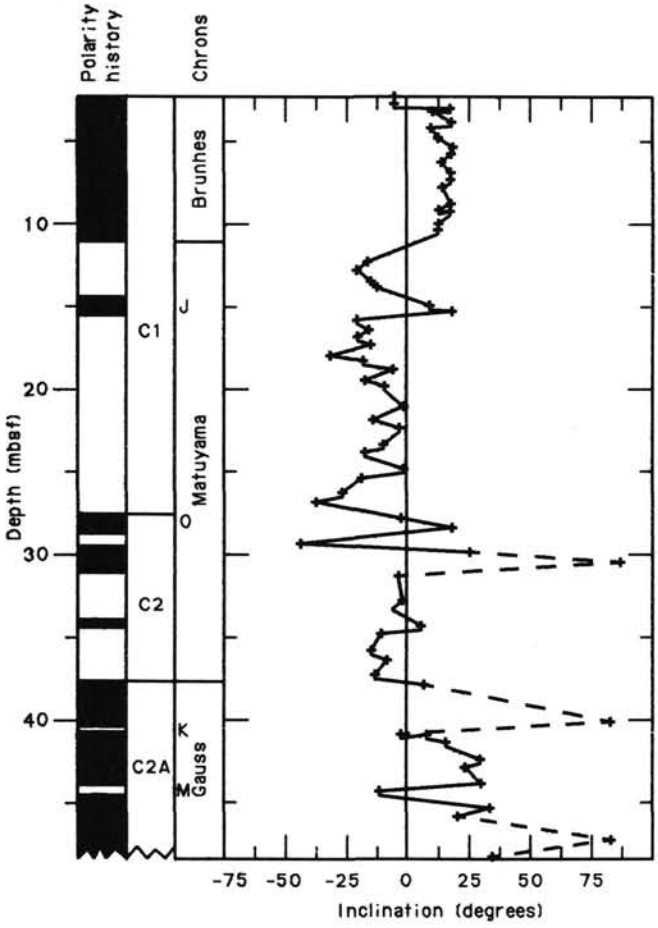

Figure 10. Inclination data from Hole 661A.

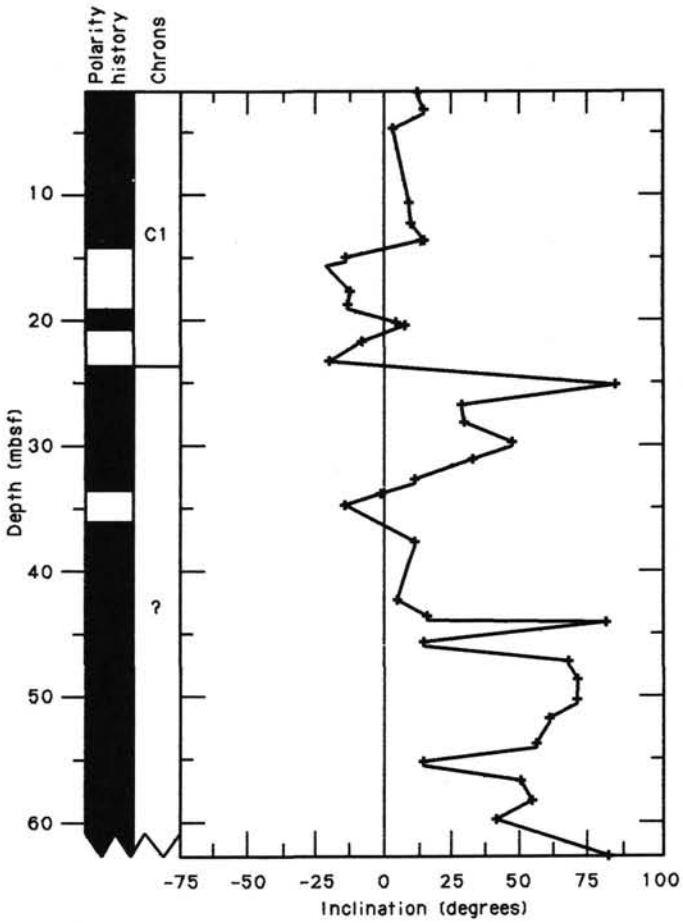

Figure 11. Inclination data from Hole 661B.

Detailed between-hole correlations are possible, and we have identified about 250 correlatable features over the interval 0 to 80 mbsf. We have also attempted to correlate parts of the susceptibility record from this site with that from Site 661. Figure 12 shows the suggested correlation of a composite-depth section for Site 660 (30–82 mbsf) with a composite-depth section for Site 661 (20–76 mbsf). Figure 13 plots depth versus depth for the two composite-depth sections based on the correlation of the susceptibility features.

SEDIMENT-ACCUMULATION RATES

Accumulation rates for Site 661 were calculated for Hole 661A. Figures 14 and 15 combine data from nannofossils, planktonic foraminifers, and paleomagnetics (Table 3). Figure 14 shows the late Neogene (0 to 10 Ma) in detail. The curve has two components; from 0 to 63 m (0 to 4.2 Ma) the accumulation rate averaged 16 m/m.y., and from 63 to 82 m (4.2 to 8.9 Ma) the rate averaged 4 m/m.y. Between 82 and 105.3 m the sediments were barren, with Late Cretaceous nannofossils beneath. Because the barren interval is only 23 m long and represents over 57 m.y. (Fig. 15), it probably contains at least one major hiatus.

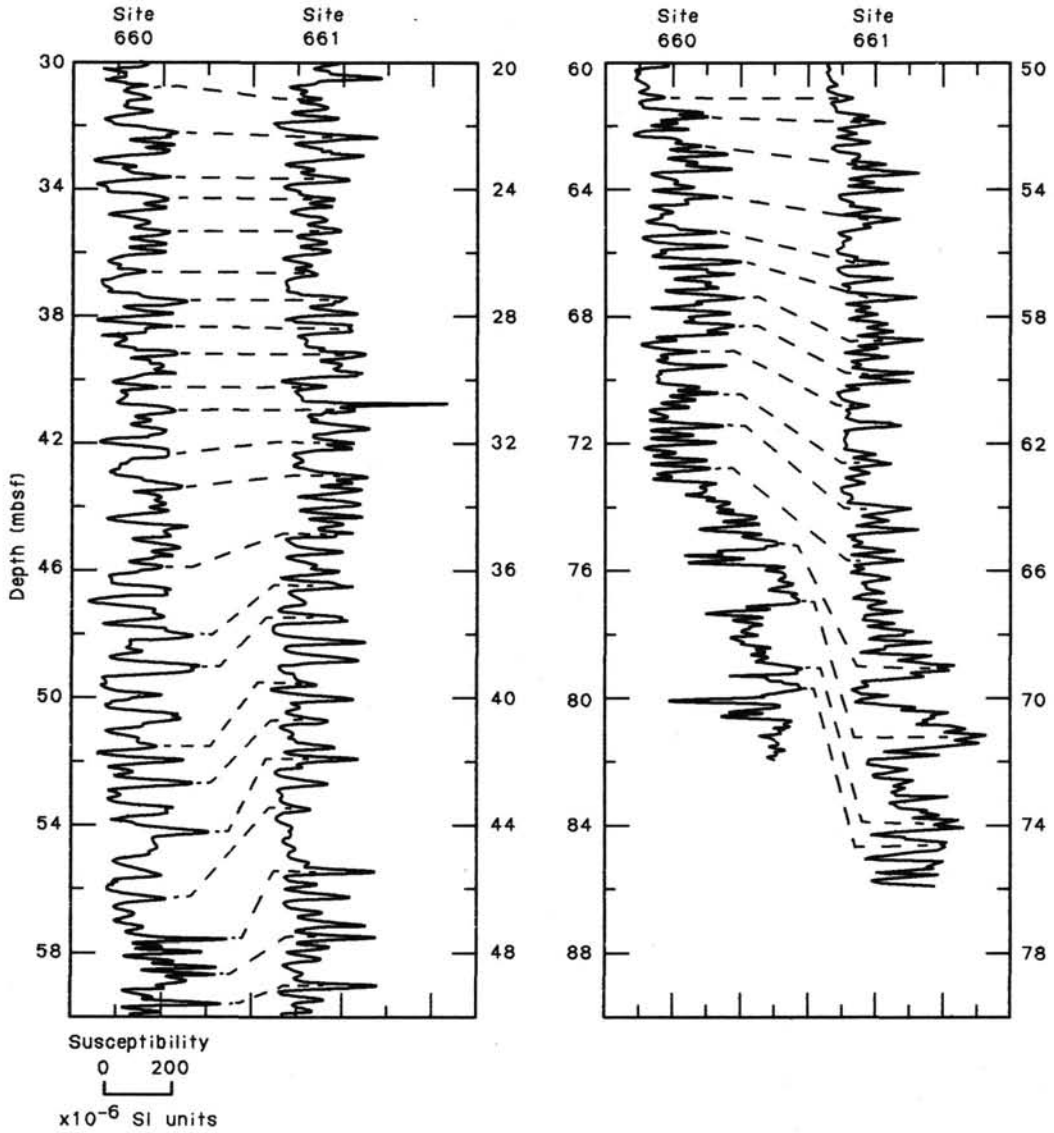

Figure 12. Suggested susceptibility correlations between Site 660 and Site 661.

The recovery of Cretaceous sediments during Leg 108 was unexpected, and for this reason we have not listed Cretaceous species events in Table 1 of the "Introduction and Explanatory Notes" chapter (this volume). Four such events were used to reconstruct Cretaceous sedimentation rates (Table 3; Fig. 15). The age assignments of these four species events represent the averages of age values assigned by recent studies which make direct correlations of the events to the geomagnetic polarity scale. Age assignments of anomalies 30 through 33 were taken from Berggren et al. (1985) to be consistent with the Cenozoic marine magnetic-anomaly time scale used at other Leg 108 sites.

Monechi et al. (1985) estimated the age of the FO of *Micula prinsii* at 66.50 Ma in DSDP Hole 577 and at 66.58 Ma in Hole 577A, whereas an estimate of 66.8 Ma was calculated from DSDP Hole 530A, using data shown by Stradner and Steinmetz (1984). Hence, a mean value of 66.6 Ma was used for the FO of *M. prinsii*.

Monechi et al. (1985) derived an age of 68.25 Ma from DSDP Hole 577A for the FO of *Micula murus*. Stradner and Steinmetz (1984) data gave an age of 69.2 Ma. Kent and Gradstein (1985) suggested an age of about 68.5 Ma for the FO of *Nephrolithus frequens*, which Thierstein (1976) considered synchronous with the *M. murus* event. Thus, the mean value of 68.7 Ma was used here.

Monechi and Thierstein (1985) associated the LO of *Tetralithus trifidus* with the upper part of anomaly 32 (estimated age 71.9 Ma). Data taken from Stradner and Steinmetz (1985) suggested an age of 72.0 Ma, whereas Kent and Gradstein (1985) gave an age of 73.0 Ma for this datum. The mean age was estimated to be 72.3 Ma.

The core-catcher sample of Core 108-661A-18X was the deepest nannofossil-bearing sediment retrieved from Hole 661A. Since *T. trifidus* was present, the age of that level has to be younger than the evolutionary first occurrence of *T. trifidus*. Using the mean value of estimates from Kent and Gradstein (1985; 75.5 Ma), Stradner and Steinmetz (1984; 76.5 Ma), and Monechi and Thierstein (1985; 76.0 Ma), we place the FO of *T. trifidus* at 76.0 Ma.

Using the above datums, sedimentation rates in the later part of the Maestrichtian are estimated to have varied between 4.1 m/m.y. (between FOs of *M. prinsii* and *M. murus*) and 2.6 m/m.y. (between the FO of *M. murus* and the LO of *T. trifidus*).

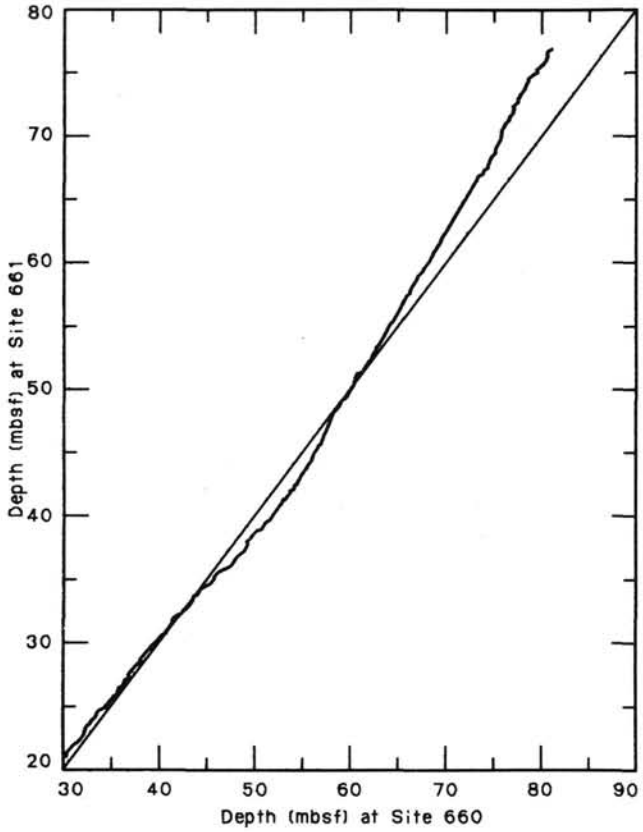

Figure 13. Depth at Site 660 plotted against depth at Site 661 on the basis of susceptibility correlations.

The sedimentation rate of the early Maestrichtian and late Campanian(?) had to be higher than 10.3 m/m.y., as indicated by the stratigraphic distribution of *T. trifidus*.

Figure 16 displays possible accumulation rates in the latest Maestrichtian. If we use the maximum accumulation rate allowable by the data (6.2 m/m.y., based on the minimum age of the FO of *M. murus* and maximum age of the FO of *M. prinsii*) and extrapolate this rate, the position of the Cretaceous/Tertiary boundary would lie 0.8 m (=0.13 m.y.) above the last occurrence of $CaCO_3$ in the section. As no Paleocene nannofossils have been identified in the carbonate-bearing sediment, the Cretaceous/Tertiary boundary may lie within this 0.8-m interval, assuming there are no hiatuses. In the absence of any opaline or calcareous microfossils, we cannot constrain the position of the Cretaceous/Tertiary boundary or verify that Paleocene sediments are even present.

INORGANIC GEOCHEMISTRY

Interstitial-water samples were squeezed from seven sediment samples taken routinely from approximately every 50 m in Hole 661A. Values for pH and alkalinity were measured in conjunction, using a Metrohm 605 pH-meter followed by titration with 0.1N HCl. Salinities were measured using an optical refractometer, and chlorinities determined by titration with silver nitrate to a potassium chromate end-point.

Magnesium and sulfate analyses were carried out by ion chromatography on a Dionex 2120i instrument. Results from all these analyses are presented in Table 4.

ORGANIC GEOCHEMISTRY

At Site 661, 97 samples from Hole 661A were investigated for organic-carbon and carbonate contents. Because of the generally very low organic-carbon content, no Rock-Eval analyses were performed.

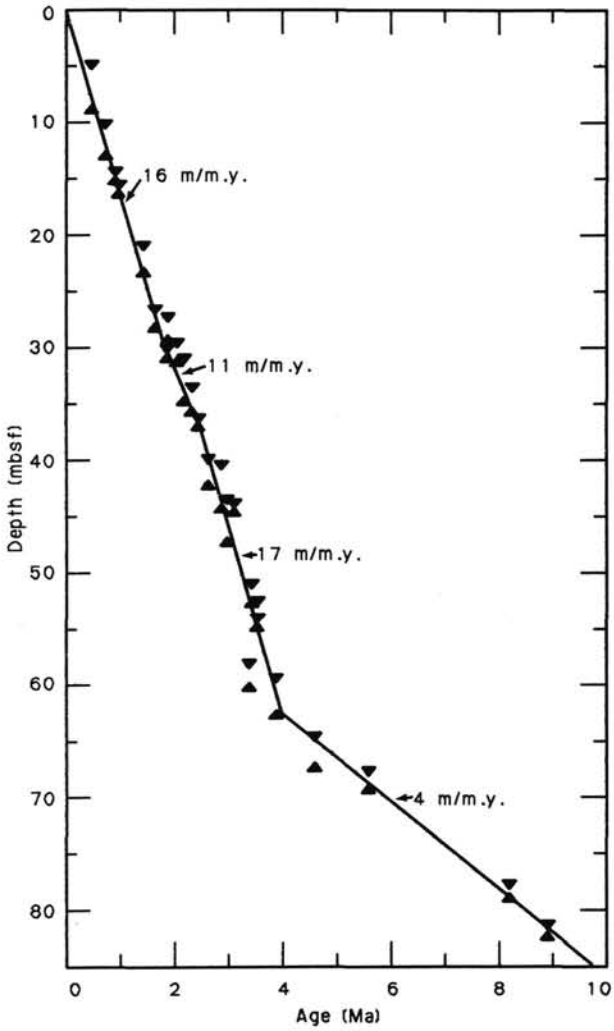

Figure 14. Late Neogene sedimentation rates for Hole 661A.

Organic and Inorganic Carbon

The inorganic-carbon (IC) content was determined using the Coulometrics Carbon Dioxide Coulometer, while the total-carbon (TC) content was measured by means of the Perkin Elmer 240C Elemental Analyser. Total-organic-carbon (TOC) values were calculated by difference. Analytical methods are discussed and data listed in the chapter entitled, "Total Organic Carbon and Carbonate Analyses, ODP Leg 108" (this volume).

In general, the TOC values determined at Site 661 are very low (i.e., less than 0.25%), with two exceptions: (1) in Sample 108-661A-6H-1, 105–106 cm, a value of 0.38% was measured, and (2) the uppermost two samples of this site have TOC values of 0.68% (Sample 108-661A-1H-1, 105–107 cm) and 0.51% (Sample 108-661A-2H-1, 105–107 cm), respectively (Fig. 17).

According to the carbonate content, the sediment sequence at Site 661 can be divided into three parts that correspond partly to the lithologic units and/or subunits (Fig. 17; see "Lithostratigraphy and Sedimentology" section, this chapter). Unit I (0 to 72.55 mbsf) is characterized by high-amplitude variations of $CaCO_3$ between less than 10% and 70% in the upper half (Cores 108-661A-1H to -661A-3H, corresponding to Subunit IA) and generally high $CaCO_3$ values between about 40% and 80% in

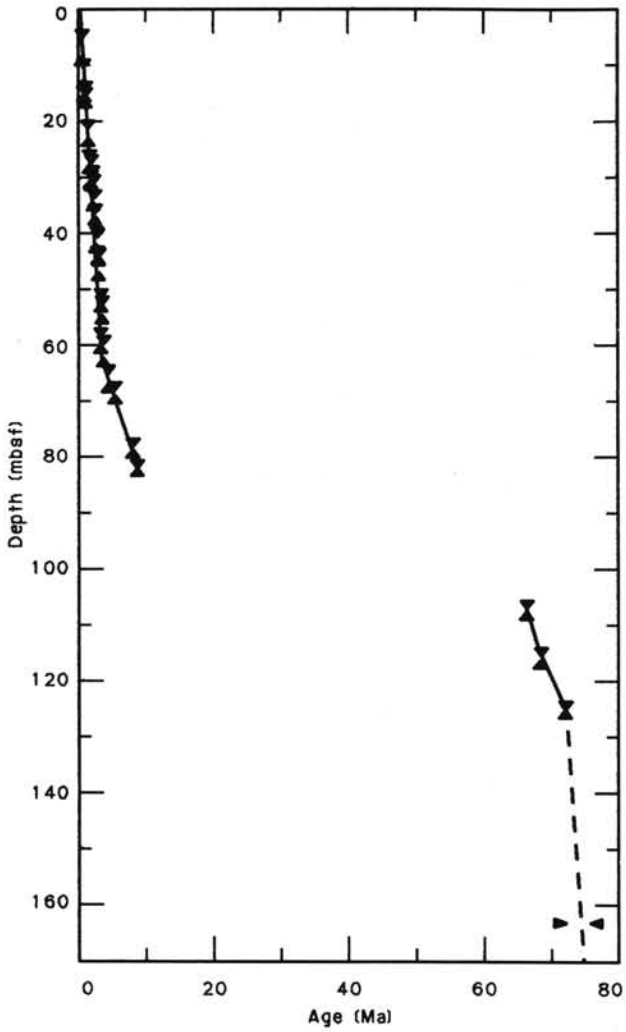

Figure 15. Neogene and Cretaceous sedimentation rates for Hole 661A.

the lower half (Cores 108-661A-5H to -661A-8H, corresponding to Subunit IB). Units II and III (below 72.55 mbsf) are characterized by generally low $CaCO_3$ values ranging from 0% to about 30%. Within this sequence, two short intervals of higher carbonate content occur in Core 108-661A-10H (40% to 50% $CaCO_3$) and in Core 108-661A-13H (about 40% to 70% $CaCO_3$). Below 163.1 mbsf (Core 661A-19X downward), i.e., in Subunit IIIB, the carbonate content is zero.

Discussion

The sediments at Site 661 are generally characterized by very low TOC values (less than 0.4%), typical of open-marine environments (e.g., Müller et al., 1983). However, these values are less than modern TOC values reported from the site area (cf. Tiedemann, 1985), except for the two uppermost values (0.5% and 0.7% TOC). Although both Site 661 and nearby Site 660 lie below the upwelling of the North Equatorial Divergence Zone, higher TOC values were recorded only at Site 660 (see "Organic Geochemistry" section, Site 660 chapter, this volume). If these higher TOC values are interpreted in terms of higher productivity and/or higher preservation of organic matter (see "Organic Geochemistry" section, Site 660 chapter, this volume), additional mechanisms near the seafloor must have influenced the accumulation of organic matter at Site 661. Since Site 661 lies on a plateau at 4000 m, i.e., shallower than Site 660 (4300 m), more oxygen-rich bottom water at 4000-m water depth may have oxidized most of the organic matter, and/or (slow) currents may have winnowed the organic matter originally supplied.

The short-term fluctuations in amount of carbonate (Fig. 17) may reflect glacial/interglacial changes in carbonate dissolution and/or input of both biogenic silica and terrigenous matter. The lack of carbonate in depths below 160 mbsf suggests a permanent position of Site 661 below the CCD during the Late Cretaceous.

Table 3. Biostratigraphic and magnetostratigraphic events, their stratigraphic placement, and their estimated ages.

Datum	Depths (mbsf)	Age (Ma)
LO *Pseudoemiliania lacunosa*	5.3–8.5	0.47
Brunhes/Matuyama	10.6–12.6	.73
Matuyama/Jaramillo	14.8–14.8	.91
Jaramillo/Matuyama	16.0–16.0	.98
LO *Calcidiscus macintyrei*	21.4–22.9	1.45
Olduvai/Matuyama	27.0–27.8	1.66
Matuyama/Olduvai	30.5–30.6	1.88
LO *Discoaster brouweri*	27.7–28.9	1.89
FO *D. triradiatus* acme	30.0–30.9	2.07
LO *Globorotalia miocenica*	31.4–34.4	2.20
LO *Discoaster pentaradiatus*	33.9–35.4	2.35
Matuyama/Gauss	36.7–36.8	2.47
LO *D. tamalis*	40.4–41.9	2.65
LO *D. altispira*	40.9–43.9	2.90
LO *Saphaeroidinellopsis seminulina*	43.9–46.9	3.00
Mammoth (within)	44.3–44.3	3.13
LO *Globorotalia margaritae*	58.6–59.9	3.40
LO *Sphenolithus* spp.	51.5–52.4	3.45
LO *Reticulofenestra pseudoumbilica*	53.0–54.5	3.56
LO *Globigerina nepenthes*	59.9–62.3	3.9
FO *Ceratolithus rugosus*	65.1–67.0	4.6
LO *Discoaster quinqueramus*	68.2–69.0	5.6
FO *D. berggrenii*	78.3–78.7	8.2
LO *D. hamatus*	81.9–82.1	8.9
FO *Micula prinsii*	107.0–107.6	66.6
FO *M. murus*	115.5–116.3	68.7
LO *Tetralithus trifidus*	125.1	72.3
T. trifidus present	163.1	72.3–76.0

FO = first occurrence. LO = last occurrence.

PHYSICAL PROPERTIES

The techniques used for the shipboard physical-property measurements at Site 661 are outlined in the "Introduction and Explanatory Notes" chapter (this volume). Index-properties, thermal-conductivity, and shear-strength measurements were made only on cores from Holes 661A and 661B. Table 5 shows the index-property and vane-shear-strength data for Hole 661A. Table 6 shows the thermal-conductivity data and a synthesis of the *P*-wave-logger data for Hole 661A. Most of the data for Hole 661A are presented graphically in Figures 18 through 22 (the calcium carbonate profile is shown in Fig. 20 for comparison with the other properties). All the data presented in this section are unscreened for any bad data points. All the whole-core sections were continuously logged using the GRAPE.

The wet-bulk density increases relatively steadily through lithologic Unit I ("Lithostratigraphy and Sedimentology" section, this chapter) from 1.25 g/cm^3 at the mud line to about 1.6 g/cm^3 at a depth of 70 mbsf (Fig. 18). Below 70 m, in Units II and III, the density profile is erratic, reflecting the large fluctuations in carbonate content (Fig. 20). The other index properties reveal a similar erratic behavior below 70 m, whereas the grain density (Fig. 20) remains relatively constant.

The shear-strength profile (Fig. 21) shows a marked increase in strength in the clay-rich lithologies. Shear strengths of up to 150 kPa were recorded around 130 mbsf in the zeolite-rich clay of Unit III.

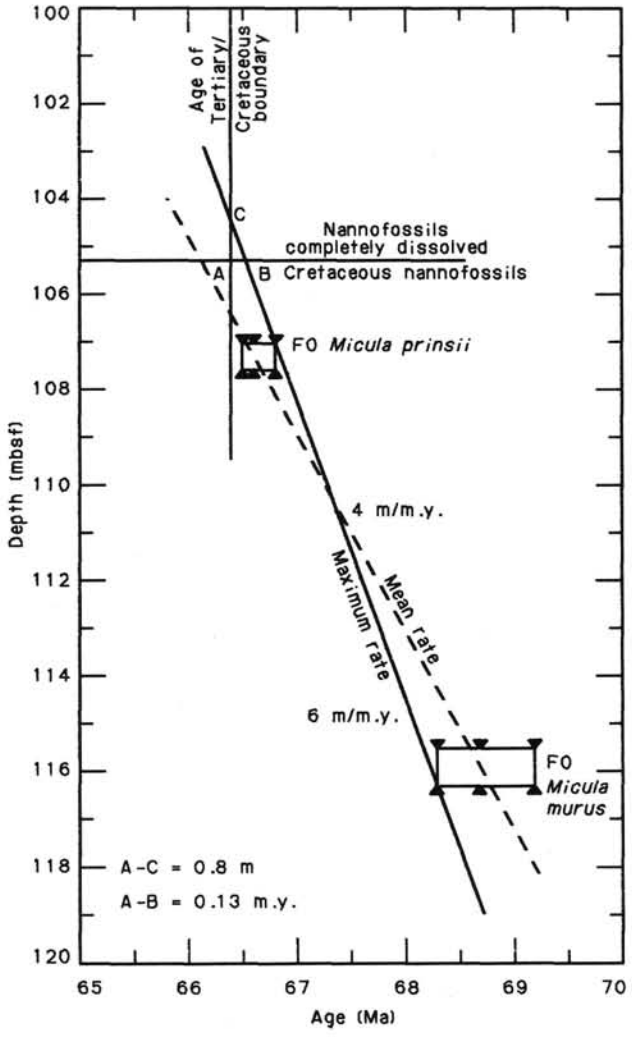

Figure 16. Alternative interpretations of sedimentation rates in the latest Maestrichtian for Hole 661A.

Thermal conductivity varies between about 0.8 and 1.3 W/m/°C throughout most of Hole 661A (Fig. 21). There is some correlation between high thermal-conductivity values (Fig. 21) and high carbonate values (Fig. 20). Downhole temperature measurements (Fig. 23) were obtained from Hole 661B on Cores 108-661B-2H, -661B-4H, -661B-6H, and -661B-8H (5.7–15.2, 24.7–34.2, 43.7–53.2, and 62.7–72.2 mbsf). The linear vertical thermal gradient in Hole 661B is about 0.06°C/m depth.

The *P*-wave-logger velocity profile (Fig. 22) shows only a small positive velocity gradient down to 100 mbsf. Thereafter it fluctuates erratically, as does the carbonate content (Fig. 20).

SEISMIC STRATIGRAPHY

The seismic reflection profiles of *JOIDES Resolution* (20- to 500-Hz water gun, 3.5 and 12 kHz; see "Background and Objectives" section, this chapter) are the only seismic lines recorded at Site 661. The water-gun profile is characterized by four different seismic units situated above the seismic basement (Fig. 24 and Table 7). Unit 1 extends to 0.134 s (approximately 102.5 m) bsf and is largely transparent except for two artifact reflectors below the seafloor and two faint reflectors. Unit 2 consists of a sequence of reflectors of varying intensity occurring between 0.134 and 0.292 s (approximately 102.5 to 227.4 m) bsf. Unit 3 is almost transparent from 0.292 to 0.416 sbsf. Below, layered unit 4 overlies the presumed seismic basement at 0.674 sbsf.

Similar to previous sites, *P*-wave velocities determined from sediment cores (see "Physical Properties" section, this chapter) enabled us to correlate several reflectors with major stratigraphic and/or lithologic changes in the sedimentary record. The details of our seismic correlation for Site 661 are summarized in Table 7.

The base of largely transparent seismic unit 1 correlates well with the top part of the Maestrichtian nannofossil ooze in uppermost lithologic Unit III. Reflector 7, within layered seismic unit 2, corresponds in sub-bottom depth to the lowermost carbonate layer interbedded with zeolitic clay and the base of lithologic Subunit IIIA at about 160 mbsf, which occurs near the Campanian/Maestrichtian boundary. Most of the other reflectors at this site do not correspond in depth to any particular feature of the lithologic record. The seismic unit 2/3 boundary is not reflected in the sedimentary record. Neither the base of seismic unit 3 nor 4 was reached at Site 661, the total penetration of which was limited to 300 mbsf.

COMPOSITE-DEPTH SECTION

The lithologic units recovered from Hole 661A (Cores 108-661A-1H through -661A-10H) and Hole 661B (Cores 108-661B-1H through -661B-9H), which lie about 15 m apart, are essentially identical (see "Lithostratigraphy and Sedimentology" section, this chapter). We succeeded in fully correlating between most core pairs in each hole by comparing continuous magnetic-susceptibility curves, which are characterized by short-term cyclic fluctuations. Analogous results were achieved by comparing continuous *P*-wave log curves for the same cores (see "Physical Properties" and "Magnetic Susceptibility" section, this chapter).

Similar to previous Sites 657 through 660, the nominal sub-bottom depth (based on the drilling record) of most susceptibility features is offset by 1 m or more between Holes 661A and 661B (Fig. 25). The offset direction becomes reversed several times downhole. This irregular displacement is regarded as an artifact, because the gains and losses in core length are generally tied to the breaks between succeeding cores (Fig. 25). Thus, the offsets are attributed to the coring process and the ODP conventions of recording sub-bottom depths.

In Table 8, we adjusted the core depths in the two holes in order to arrive at a composite-depth section of complete and uncontorted core sections. The following criteria and rationales define our procedure:

1. Both Cores 108-661A-1H and -661B-1H reveal identical susceptibility records in the uppermost sediment sections. We chose the sediment record of Hole 661A as the reference section for generating a composite-depth profile at this site.
2. Points in the undisturbed proportion of the sediment record that approximate the upper and lower boundaries of each core in both holes were used as switch-points to generate a continuous "pathway" of between-hole correlation.
3. The continuous correlation of cores with staggered penetration depths resulted in composite-depth numbers that persistently increase relative to the nominal sub-bottom depth of both holes down to about 70 mbsf, where the cumulative gain in penetration depth amounts to more than 4 m. Farther below, the adjustment of core boundaries leads to losses of nominal penetration depth, probably because of flow-in processes predominantly near the lower core end.
4. Our correlations and adjustments lead to a complete overlap of sections of "good core" between the holes down to a composite depth of 84.6 mbsf, except for the correlation of lower Core 108-661B-2H with upper Core 108-661A-3H and lowermost Core 108-661A-2H. This link is problematical for unknown reasons.

The composite-depth section (Table 8) presents the closest approximation to the *in-situ* stratigraphy and should reveal the

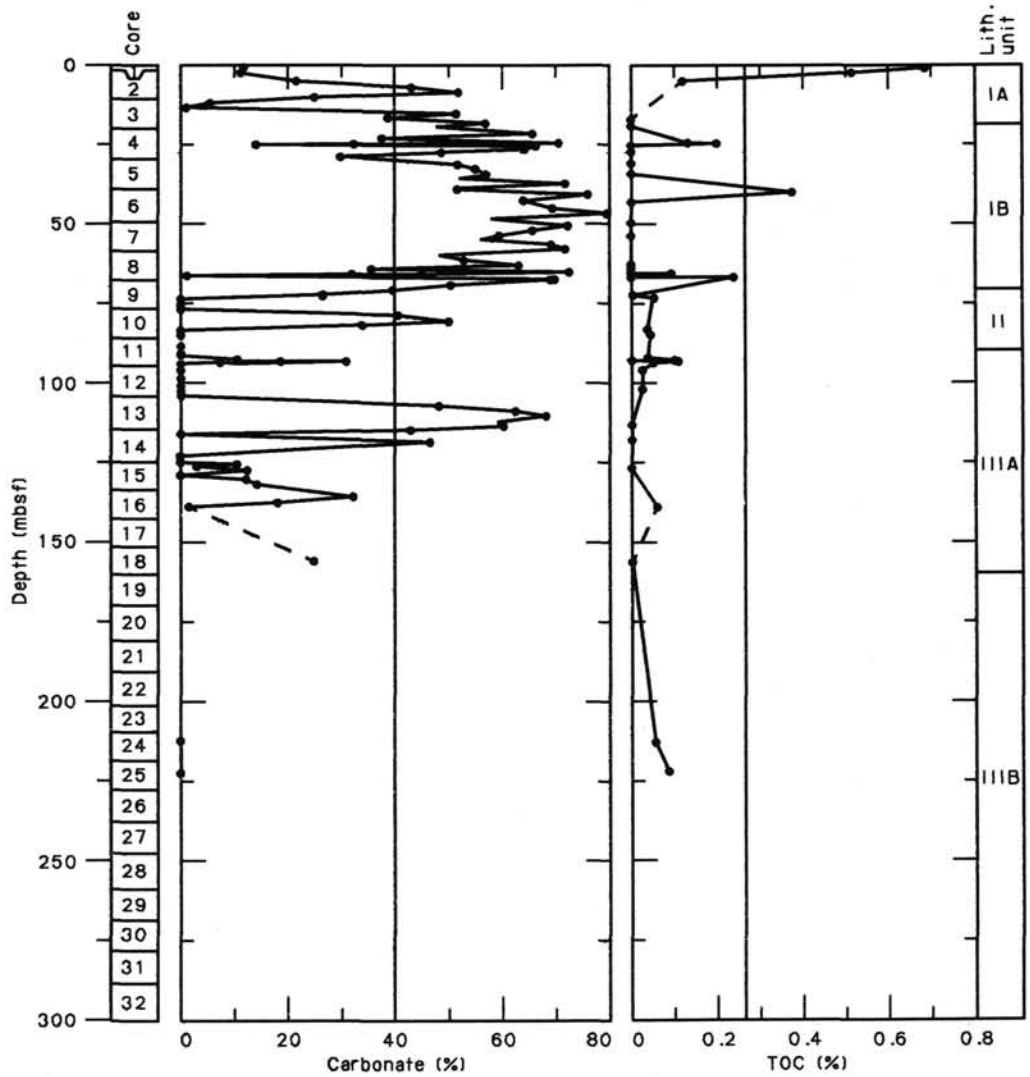

Figure 17. Carbonate and total-organic-carbon (TOC) records of Hole 661A.

Table 4. Results of inorganic geochemical analyses conducted for Site 661.

Section	pH	Alkalinity (meq/dm^3)	Salinity (‰)	Chlorinity (mmol/L)	SO_4^{2-} (mmol/L)	Mg^{2+} (mmol/L)	Ca^{2+} (mmol/L)
2H-4	7.51	3.48	34.2	571	27.00	55.37	**
6-5	7.38	3.26	34.5	584	25.30	58.22	**
11-5	7.68	3.85	32.8	571	21.48	62.91	**
16-4	*	*	33.7	573	19.51	52.38	**
21-1	7.73	4.07	33.8	575	19.67	50.39	**
26-3	7.79	7.10	31.8	556	10.93	46.41	**
31-2	7.67	6.31	32.0	569	11.72	45.63	**
Surface	8.18	2.22	34.9	593	28.57	60.21	**

* An insufficient amount of water was obtained for these determinations.
** No data are available from this site for calcium because of instrumentation problems.

best estimates of sedimentation rates (Fig. 26) as well as the best match with seismic stratigraphy. In addition, it shows how voids and contorted sections in cores with poor recovery can be successfully bypassed by sampling the companion hole.

LOGGING

Two logging runs and testing of the new side-entry subunit were planned for Hole 661A. Unfortunately, the latter could not be completed because of operational difficulties. Instead, conventional logging techniques (over the crown) were used, even though the shallow sub-bottom depth (296.1 mbsf) and the poor hole conditions created uncertainties as to how successful any logging attempt would be.

At 0700 UTC, the dual-induction (CDIL), gamma-ray (GR), long-spaced-sonic (LSS), and caliper (CAL) tools were rigged up. They were started in the hole at 0815 hr. The logging tools were out of the drill pipe and into the open hole by 0930 hr. A

Table 5. Data for index properties and shear strength, Hole 661A.

Section	Interval (cm)	Depth (mbsf)	Grain density (g/cm^3)	Wet water content (%)	Dry water content (%)	Wet-bulk density (g/cm^3)	Dry-bulk density (g/cm^3)	Porosity (%)	Vane shear strength (kPa)
1H-1	106	1.06	2.48	63.05	170.66	1.30	0.52	80.84	8.5
2-1	106	2.66	2.78	63.43	173.42	1.33	0.52	82.78	14.0
2-2	106	4.16	2.60	61.96	162.86	1.33	0.54	80.85	6.0
2-3	106	5.66	2.55	62.02	163.29	1.32	0.54	80.55	8.0
2-4	106	7.16	2.63	56.97	132.41	1.39	0.63	77.59	14.0
2-5	106	8.66	2.63	58.44	140.64	1.37	0.62	78.59	11.0
2-6	106	10.16	2.36	62.32	165.37	1.30	0.52	79.52	26.0
3-1	106	12.05	2.16	71.66	252.85	1.20	0.38	84.58	6.0
3-2	106	13.55	2.45	61.54	159.99	1.31	0.54	79.59	15.0
3-3	106	15.05	2.53	59.63	147.73	1.34	0.58	78.81	12.0
3-4	106	16.55	2.44	61.30	158.38	1.32	0.69	79.38	17.0
3-5	106	18.05	2.43	54.31	118.85	1.39	0.56	74.18	15.0
3-6	102	19.51	2.84	50.19	100.17	1.50	0.69	73.93	13.0
4-1	106	21.61	2.89	55.98	127.19	1.43	0.68	78.50	16.0
4-2	106	23.06	2.60	53.88	116.82	1.42	0.69	75.09	12.0
4-3	106	24.56	2.46	59.08	144.41	1.34	0.59	77.93	13.0
4-4	106	26.06	2.72	56.05	127.51	1.41	0.66	77.51	27.0
4-5	106	27.56	2.73	53.41	114.65	1.44	0.72	75.63	19.0
4-6	106	29.06	2.58	52.26	109.49	1.43	0.73	73.71	24.0
5-1	106	31.10	2.55	51.71	107.08	1.44	0.74	73.03	20.0
5-2	106	32.60	2.57	50.79	103.23	1.45	0.76	72.47	31.0
5-3	106	34.10	2.57	50.98	103.99	1.45	0.76	72.58	38.0
5-4	106	35.60	2.37	53.00	112.78	1.39	0.70	72.61	27.0
5-5	106	37.10	2.58	52.42	110.16	1.43	0.73	73.82	31.0
5-6	106	38.60	2.59	49.42	97.71	1.47	0.79	71.50	31.0
6-1	106	40.66	2.33	50.35	101.40	1.42	0.74	70.13	43.0
6-2	103	42.13	2.62	48.87	95.58	1.48	0.81	71.27	23.0
6-3	106	43.66	2.74	47.18	89.33	1.53	0.86	70.79	17.0
6-4	106	45.16	2.58	49.58	98.35	1.47	0.80	71.55	11.0
6-5	106	46.66	2.85	49.87	99.49	1.50	0.80	73.72	27.0
7-1	106	50.16	2.58	50.10	100.41	1.46	0.77	71.96	6.0
7-2	106	51.66	2.61	44.78	81.10	1.54	0.90	67.65	10.0
7-3	106	53.16	2.57	41.75	71.68	1.57	0.97	64.57	13.0
7-4	106	54.66	2.67	42.36	73.48	1.58	0.97	65.97	10.0
7-5	106	56.16	2.62	44.17	79.12	1.55	0.90	67.23	11.0
7-6	106	57.66	2.70	45.61	83.86	1.54	0.89	69.15	8.0
8-1	106	59.66	2.73	40.97	69.42	1.62	0.99	65.17	32.0
8-2	106	61.16	2.02	52.76	111.68	1.33	0.79	69.22	22.0
8-3	106	62.66	2.62	41.86	72.00	1.58	0.96	65.11	24.0
8-4	106	64.16	2.56	41.00	69.50	1.58	0.99	63.78	37.0
8-5	106	65.66	2.61	41.11	69.80	1.59	0.98	64.27	37.0
8-6	106	67.16	2.66	43.19	76.01	1.57	0.95	66.62	34.0
9-1	106	69.16	2.69	40.91	69.24	1.61	1.01	64.81	33.0
9-2	106	70.66	2.58	39.27	64.68	1.61	1.03	62.26	39.0
9-3	106	72.16	2.70	38.31	62.11	1.65	1.07	62.32	54.0
9-4	106	73.66	2.58	41.60	71.24	1.58	0.97	64.50	55.0
9-5	106	75.16	2.57	41.38	70.58	1.58	0.98	64.21	54.0
9-6	106	76.66	2.60	42.28	73.25	1.57	0.95	65.34	52.0
10-1	106	78.66	2.76	38.13	61.63	1.67	1.09	62.69	43.0
10-2	106	80.16	2.58	40.01	66.68	1.60	1.01	62.95	30.0
10-3	106	81.66	2.65	39.42	65.07	1.63	1.04	62.99	53.0
10-4	106	83.16	2.61	41.21	70.10	1.59	0.98	64.40	58.0
10-5	106	84.66	2.54	37.52	60.05	1.63	1.09	60.13	58.0
11-1	106	88.16	2.55	42.15	72.86	1.56	0.69	64.74	68.0
11-2	106	89.66	2.63	43.01	75.48	1.57	1.16	66.23	77.0
11-3	106	91.16	2.64	31.33	45.62	1.76	0.97	54.32	87.0
11-5	106	94.16	2.55	49.23	96.95	1.47	0.91	71.01	87.0
12-1	110	97.70	2.53	54.41	119.35	1.40	0.70	74.95	100.0
12-2	106	99.16	2.63	46.21	85.92	1.52	0.89	69.11	110.0
12-3	106	100.66	2.62	45.73	84.26	1.52	0.89	68.56	110.0
12-4	106	102.16	2.64	46.39	86.53	1.52	0.86	69.30	115.0
12-5	106	103.66	2.71	47.83	91.68	1.51	0.83	71.08	117.5
12-6	97	105.07	2.64	43.78	77.89	1.56	0.92	67.07	130.0
13-1	106	107.14	2.67	36.54	57.58	1.68	1.10	60.24	85.0
13-2	106	108.64	2.62	33.70	50.83	1.71	1.18	56.76	60.0
13-3	106	110.14	2.60	31.80	46.63	1.74	1.24	54.50	80.0
13-4	106	111.64	2.67	32.83	48.88	1.74	1.22	56.30	90.0
13-5	106	113.14	2.63	31.85	46.74	1.75	1.24	54.77	100.0
13-6	106	114.64	2.63	37.15	59.10	1.66	1.09	60.54	125.0
14-1	106	116.66	2.68	42.13	72.79	1.59	0.96	65.88	140.0
14-2	106	118.16	2.69	33.13	49.54	1.74	1.38	56.76	125.0
14-5	106	120.52	2.61	40.03	66.76	1.61	1.02	63.24	122.5
14-6	106	122.02	2.67	38.56	62.75	1.65	1.06	62.37	120.0
14-7	106	123.52	2.57	36.58	57.69	1.65	1.12	59.47	145.0
15-1	106	126.10	2.64	40.31	67.53	1.61	1.00	63.77	125.0
15-2	106	127.60	2.71	37.01	58.77	1.68	1.11	61.12	118.7
15-3	106	129.10	2.68	40.87	69.13	1.61	0.99	64.71	115.0
15-4	106	130.60	2.55	37.52	60.06	1.63	1.08	60.17	155.0
15-5	106	132.10	2.56	36.88	58.44	1.64	1.10	59.61	145.0
16-1	103	135.17	2.61	38.97	63.86	1.62	1.04	62.24	50.0
16-2	104	136.68	2.64	40.57	68.25	1.61	1.00	64.03	87.5
16-3	104	138.18	2.76	43.12	75.81	1.59	0.93	67.39	100.0
18-2	106	156.16	2.75	37.74	60.61	1.68	1.08	62.23	125.0

Table 6. Data for thermal conductivity and compressional-wave velocity, Hole 661A.

	Thermal conductivity			*P*-wave velocity	
Section	Interval (cm)	Depth (mbsf)	(W/m/°C)	Depth (mbsf)	(km/s)
1H-1	120	1.20	0.9470	1.00	1.505
2-1	120	2.80	0.9310	2.10	1.548
2-2	120	4.30	0.9150	2.60	1.528
2-3	120	5.80	0.9073	3.60	1.521
2-4	120	7.30	1.0290	3.90	1.533
2-5	100	8.60	1.0430	4.60	1.516
2-6	120	10.30	1.5750	5.60	1.510
3-1	120	12.19	0.9130	7.10	1.504
3-2	120	13.69	0.9430	7.60	1.522
3-3	120	15.19	0.9470	8.60	1.500
3-4	120	16.69	0.9960	12.10	1.520
3-5	120	18.19	1.0290	13.40	1.534
3-6	110	19.59	1.0550	14.10	1.510
4-1	120	21.75	1.0220	15.10	1.521
4-2	120	23.20	1.0360	16.60	1.541
4-3	120	24.70	0.9800	17.10	1.516
4-4	120	26.20	0.8730	19.10	1.505
4-5	120	27.70	1.1750	21.10	1.507
4-6	120	29.20	1.0250	21.60	1.532
4-7	30	29.80	1.0280	23.60	1.522
5-1	120	31.24	1.0560	24.60	1.520
5-2	120	32.74	1.0040	25.60	1.519
5-3	120	34.24	0.9840	26.30	1.522
5-4	120	35.74	1.0300	27.10	1.504
5-5	100	37.04	0.9210	28.60	1.508
5-6	100	38.54	0.9950	29.60	1.510
6-1	120	40.80	1.0410	32.10	1.515
6-2	120	42.30	0.9710	33.60	1.514
6-3	120	43.80	1.0690	34.10	1.512
6-4	120	45.30	1.0940	34.80	1.534
6-5	120	46.80	0.9650	35.10	1.501
6-6	120	48.30	0.8240	36.60	1.518
7-1	120	50.30	1.0990	38.60	1.510
7-2	120	51.80	1.0420	40.60	1.525
7-3	120	53.30	1.1320	42.60	1.518
7-4	120	54.80	1.1030	43.60	1.518
7-5	120	56.30	1.0880	44.60	1.512
7-6	120	57.80	1.1610	45.60	1.520
8-1	120	59.80	1.1140	46.60	1.520
8-2	120	61.30	1.1820	47.60	1.510
8-3	100	62.60	1.1130	50.10	1.520
8-4	100	64.10	1.0860	51.10	1.510
8-5	100	65.60	1.1650	52.10	1.518
8-6	100	67.10	1.0050	53.10	1.510
9-1	100	69.10	1.1690	54.20	1.534
9-2	100	70.60	1.1310	54.30	1.511
9-3	100	72.10	1.1760	55.20	1.543
9-4	100	73.60	1.0780	55.70	1.508
9-5	100	75.10	1.0450	56.90	1.528
9-6	100	76.60	0.9660	57.60	1.513
10-1	100	78.60	1.1310	59.60	1.530
10-2	100	80.10	1.1650	60.60	1.527
10-3	100	81.60	1.1680	61.60	1.537
10-4	100	83.10	1.0390	62.50	1.512
10-5	100	84.60	1.1280	63.10	1.541
10-6	80	85.90	1.0370	64.60	1.511
11-1	80	87.90	0.9120	65.60	1.530
11-2	80	89.40	0.9930	66.90	1.540
11-3	80	90.90	0.9680	67.10	1.514
11-4	80	92.40	0.9700	68.60	1.536
11-5	120	94.30	0.9120	69.00	1.514
11-6	120	95.80	0.8680	71.10	1.537
12-1	120	97.80	0.9110	72.60	1.557
12-2	120	99.30	0.9500	73.80	1.528
12-3	22	99.82	0.9040	75.00	1.547
12-4	100	102.10	1.0080	77.10	1.537
12-5	100	103.60	0.8890	80.10	1.540
12-6	100	105.10	1.0070	80.40	1.522
13-1	100	107.08	1.0930	80.50	1.550
13-2	100	108.58	1.2730	81.30	1.519
13-3	100	110.08	1.3060	82.90	1.548
13-4	100	111.58	1.0520	84.10	1.523
13-5	100	113.08	1.2570	85.30	1.563
13-6	100	114.58	0.9610	90.60	1.533
14-1	100	116.60	0.9620	92.60	1.530

Table 6 (continued).

	Thermal conductivity			*P*-wave velocity	
Section	Interval (cm)	Depth (mbsf)	(W/m/°C)	Depth (mbsf)	(km/s)
14-2	120	118.30	1.1430	92.70	1.650
14-3	50	119.10	0.9030	93.40	1.528
14-5	120	120.66	0.9880	93.50	1.648
14-6	120	122.16	0.9920	93.80	1.547
14-7	100	123.46	1.1210	95.10	1.531
14-8	80	124.76	1.2110	97.60	1.556
15-1	120	126.24	0.9580	98.60	1.555
15-2	120	127.74	1.0740	100.00	1.519
15-3	120	129.24	1.0050	101.60	1.558
15-4	120	130.74	1.0320	103.60	1.548
15-5	120	132.24	1.2400	105.20	1.563
15-6	50	133.04	1.2880	107.10	1.560
16-1	120	135.34	1.1240	109.10	1.582
16-2	120	136.84	0.9900	110.20	1.588
16-3	120	138.34	0.9400	112.10	1.580
16-4	110	139.74	1.0560	113.30	1.602
16-5	120	141.34	1.1550	121.60	1.560
16-6	120	142.71	1.0800	123.00	1.606
17-1	120	145.30	1.0790	124.40	1.636
18-1	100	154.60	1.0160	127.60	1.600
18-2	100	156.10	1.0990	130.90	1.622
19-5	120	164.80	1.0130	132.70	1.541
19-6	120	166.30	1.0990	135.10	1.524
				135.60	1.570
				137.60	1.555
				139.60	1.565
				140.10	1.525
				142.10	1.549
				142.80	1.504
				145.10	1.502
				154.60	1.552
				171.10	1.525
				173.60	1.540
				179.10	1.555
				182.80	1.555
				183.90	1.608
				193.30	1.605
				202.10	1.625
				204.60	1.574
				211.90	1.565
				212.50	1.670
				213.80	1.575
				216.20	1.623
				220.60	1.639
				221.30	1.547
				230.60	1.594
				233.50	1.559
				236.70	1.673
				240.10	1.570
				241.40	1.680

sediment bridge was encountered just below the end of the drill pipe, but the tools were worked through the bridge and down to an approximate depth of 196 mbsf. Hole conditions were poor, and later review of the caliper data indicated that in many intervals the hole had a diameter of only 11.5 cm.

At 1000 hr, a decision was made to make a wiper trip to clean out the hole and to try the same logging suite again. After a partially successful logging run with the CDIL, GR, LSS, and CAL, the tools were pulled out of the hole and on deck by 1230 hr.

At 1235 hr, a decision was made not to make a wiper trip but to run the next tool suite, composed of the litho-density (LDT), compensated-neutron (CNT), and natural-spectroscopy gamma-ray (NGT) tools. The logging tools were started in the hole at 1330 hr. The bottom of the drill pipe was reached at 1500 hr, but the logging tools could not get into the open hole; apparently the hole had closed. The logging tools were pulled out of the hole and were on deck by 1645 hr. At 1730 hr, procedures were under way for coring Hole 661B.

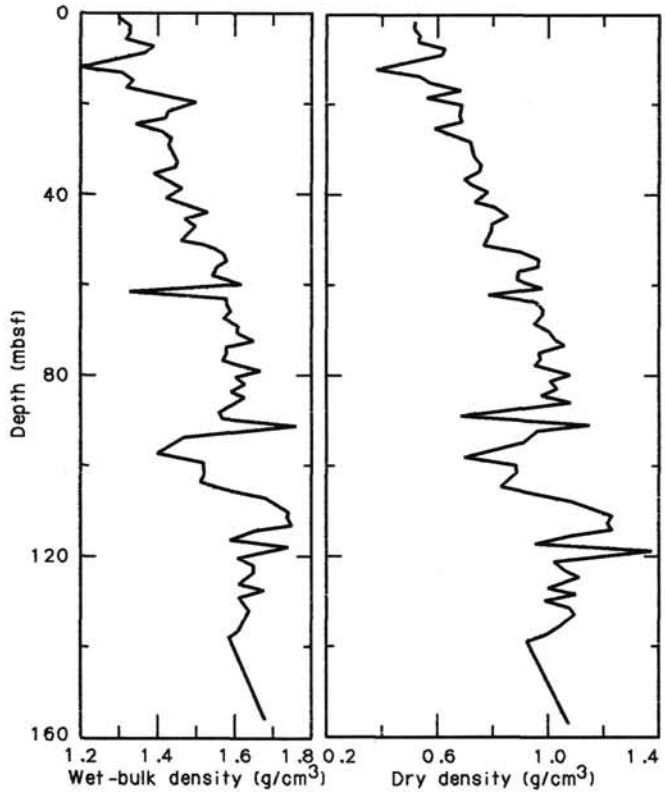

Figure 18. Wet- and dry-bulk-density profiles for Hole 661A.

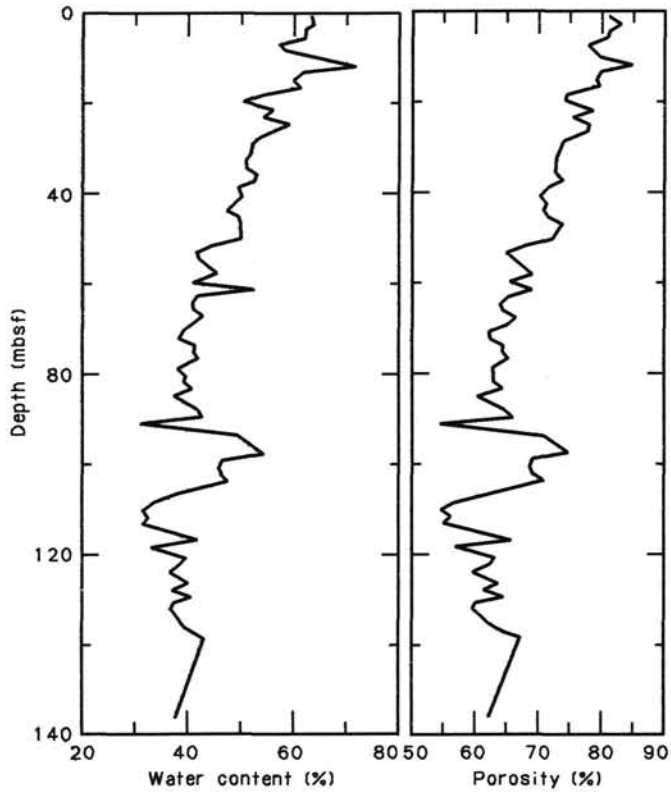

Figure 19. Water-content and porosity profiles for Hole 661A.

REFERENCES

Beckmann, J. P., 1978. Late Cretaceous smaller benthic foraminifers from Sites 363 and 364, DSDP Leg 40, Southeast Atlantic Ocean. *In* Bolli, H. M., Ryan, W.B.F., et al., *Init. Repts. DSDP*, 40: Washington (U.S. Govt. Printing Office), 759–781.

Berggren, W. A., Kent, D. V., Flynn, J. J., and Van Couvering, J. A., 1985. Cenozoic geochronology. *Geol. Soc. Amer. Bull.*, 96:1407–1418.

Bolli, H. M., and Saunders, J. B., 1985. Oligocene to Holocene low latitude planktic foraminifera. *In* Bolli, H. M., Saunders, J. B., and Perch-Nielsen, K. (Eds.), *Plankton Stratigraphy*: Cambridge (Cambridge Univ. Press), 165–262.

Brassel, S. C., Eglinton, G., Marlowe, I. T., Pflaumann, U., and Sarnthein, M., 1986. Molecular stratigraphy: a new tool for climatic assessment. *Nature*, 320:129–133.

Jones, E.J.W., and Mgbatogu, C.C.S., 1982. The structure and evolution of the West African continental margin off Guine Bissau, Guinee, and Sierra Leone. *In* Scrutton, R. A., and Talwani, M. (Eds.), *The Ocean Floor*: New York (Wiley), 165–202.

Kent, D. V., and Gradstein, F. M., 1985. A Cretaceous and Jurassic geochronology. *Geol. Soc. Amer. Bull.*, 96:1419–1427.

Lancelot, Y., Seibold, E., et al., 1978. Site 366: Sierra Leone Rise. *In* Lancelot, Y., Seibold, E., et al., *Init. Repts. DSDP*, 41: Washington (U.S. Govt. Printing Office), 21–46.

Mienert, J., 1986. Akustostratigraphie im äquatorialen Ostatlantik: Zur Entwicklung der Tiefenwasserzirkulation der letzten 3.5 millionen Jahre. *"Meteor" Forsch. Eng.*, C14:19–86.

Monechi, S., Bleil, U., and Backman, J., 1985. Magnetobiochronology of Late Cretaceous–Paleogene and late Cenozoic pelagic sedimentary sequences from the northwest Pacific (Deep Sea Drilling Project, Leg 86, Site 577). *In* Heath, G. R., Burckle, L. H., et al., *Init. Repts. DSDP*, 86: Washington (U.S. Govt. Printing Office), 787–797.

Monechi, S., and Thierstein, H. R., 1985. Late Cretaceous–Eocene nannofossil and magnetostratigraphic correlations near Gubbio, Italy. *Mar. Micropaleontol.*, 9:419–440.

Müller, P., Erlenkeuser, H., and von Grafenstein, R., 1983. Glacial-interglacial cycles in oceanic productivity inferred from organic carbon contents in eastern North Atlantic sediment cores. *In* Thiede, J., and Suess, E. (Eds.), *Coastal Upwelling: Its Sediment Record*, Part B: New York (Plenum), 365–398.

Perch-Nielsen, K., 1977. Albian to Pleistocene calcareous nannofossils from the western South Atlantic, DSDP Leg 39. *In* Supko, P. R., Perch-Nielsen, K., et al., *Init. Repts. DSDP*, 39: Washington (U.S. Govt. Printing Office), 699–823.

Stradner, H., and Steinmetz, J., 1984. Cretaceous calcareous nannofossils from the Angola Basin, Deep Sea Drilling Project Site 530. *In* Hay, W. W., Sibuet, J.-C., et al., *Init. Repts. DSDP*, 75: Washington (U.S. Govt. Printing Office): 565–649.

Thierstein, H. R., 1976. Mesozoic calcareous nannoplankton biostratigraphy of marine sediments. *Mar. Micropaleontol.*, 1:325–362.

Tiedemann, R., 1985. Verteilung von organischem Kohlenstoff in Oberflächensedimenten und die örtliche Primärproduktion im äquatorialen Ostatlantik, 0–20°N, 15–25°W [M.S. thesis]. Univ. Kiel.

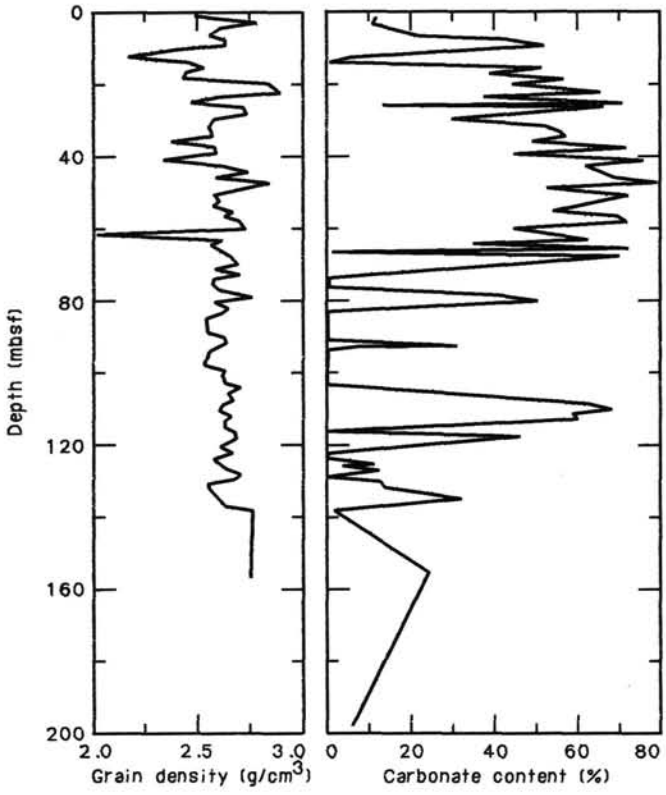

Figure 20. Grain-density and calcium carbonate-content profiles for Hole 661A.

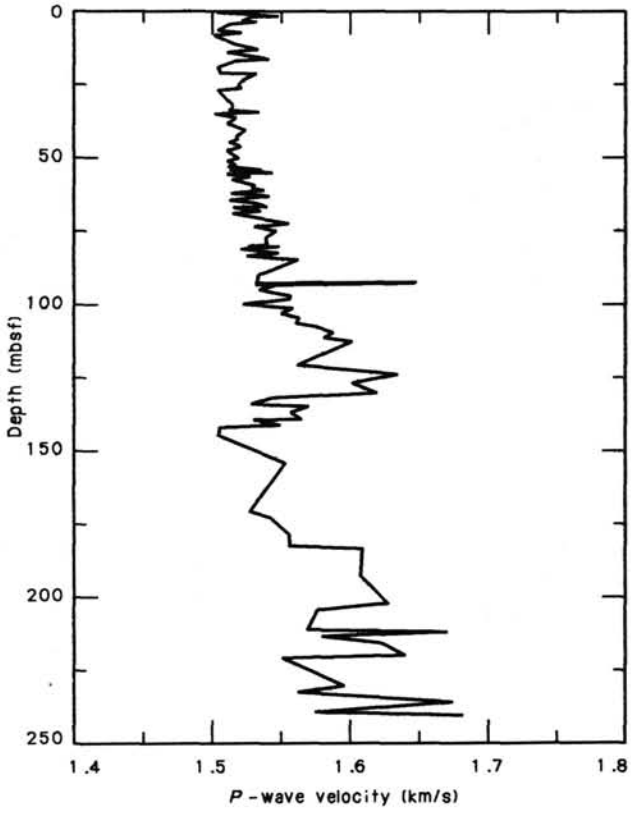

Figure 22. *P*-wave-velocity profile for Hole 661A.

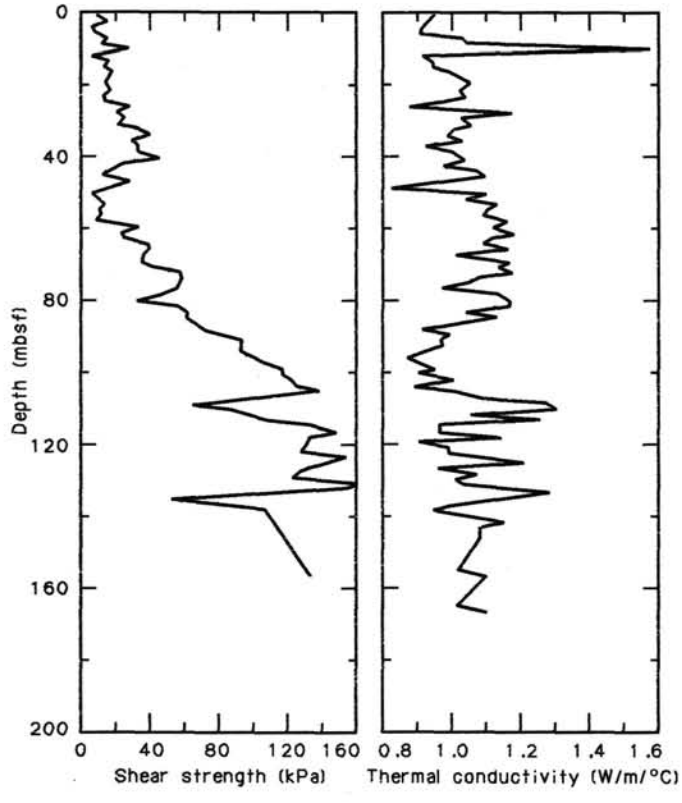

Figure 21. Vane-shear-strength and thermal-conductivity profiles for Hole 661A.

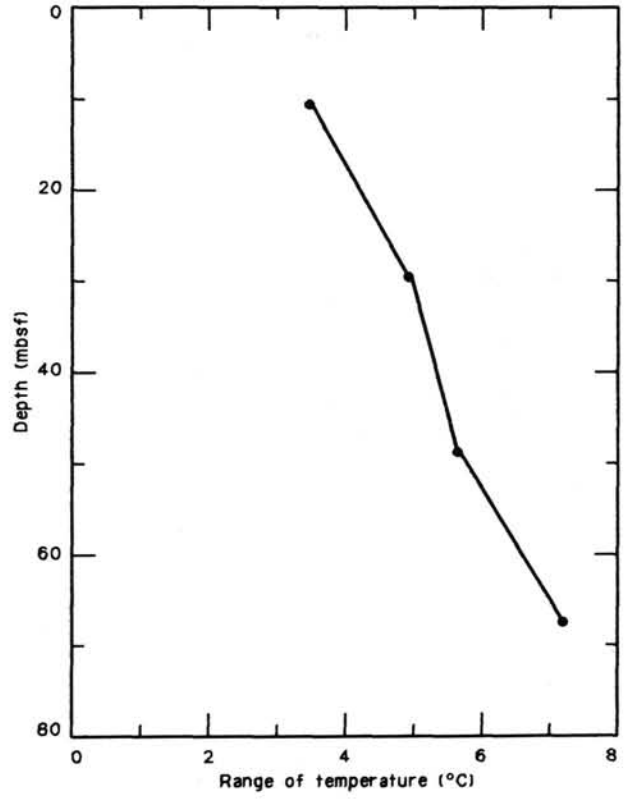

Figure 23. Vertical, *in-situ* sediment-temperature profile for Hole 661B. The linear vertical thermal gradient is about 0.06°C per 1 m depth.

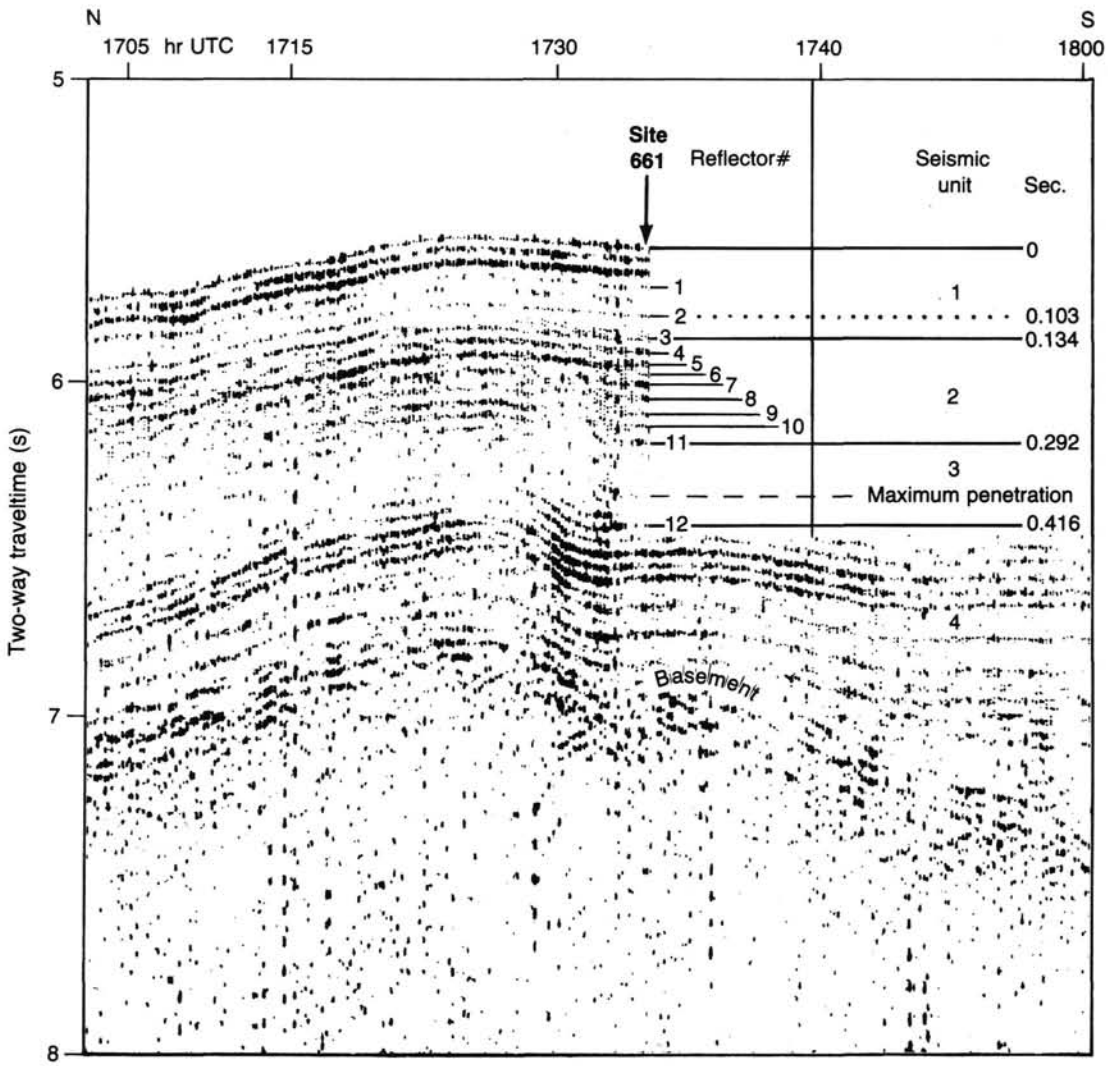

Figure 24. Reflection profile (20 to 500 Hz) over Site 661, showing the seismic sequence described in the text and Table 7.

Table 7. Seismic correlations (50 to 500 Hz), Site 661.

Seismic unit	Reflector (no.)	Reflector (sbsf)	Reflector depth 1525 m/s (mbsf)	1530 m/s (mbsf)	1590 m/s (mbsf)	1600 m/s (mbsf)	Cumulative depth (mbsf)	Source	Age	Lithostratigraphic unit
	1	0.060	45.2				45.7			
1	2	0.103	32.8				78.5	$CaCO_3$ peak	ca. 9 Ma	I, II
	3	0.134		24.0			102.5	Top $CaCO_3$ beds	ca. K/T boundary →	
	4	0.153			15.1		117.6			
	5	0.174			16.7		134.3			IIIA
	6	0.192		14.0			148.3			
2	7	0.205		10.0			158.3	Base of $CaCO_3$	Campanian/ Maestrichtian →	
	8	0.226		16.25			174.6			
	9	0.253				21.6	196.2			IIIB
	10	0.268				12.0	208.2			
	11	0.292				19.2	227.4			
							296.1		Total penetration →	
3										
	12	0.416				99.2	326.6			
4										
Basement		0.674				191.4	518.0			

Note: K = Cretaceous; T = Tertiary.

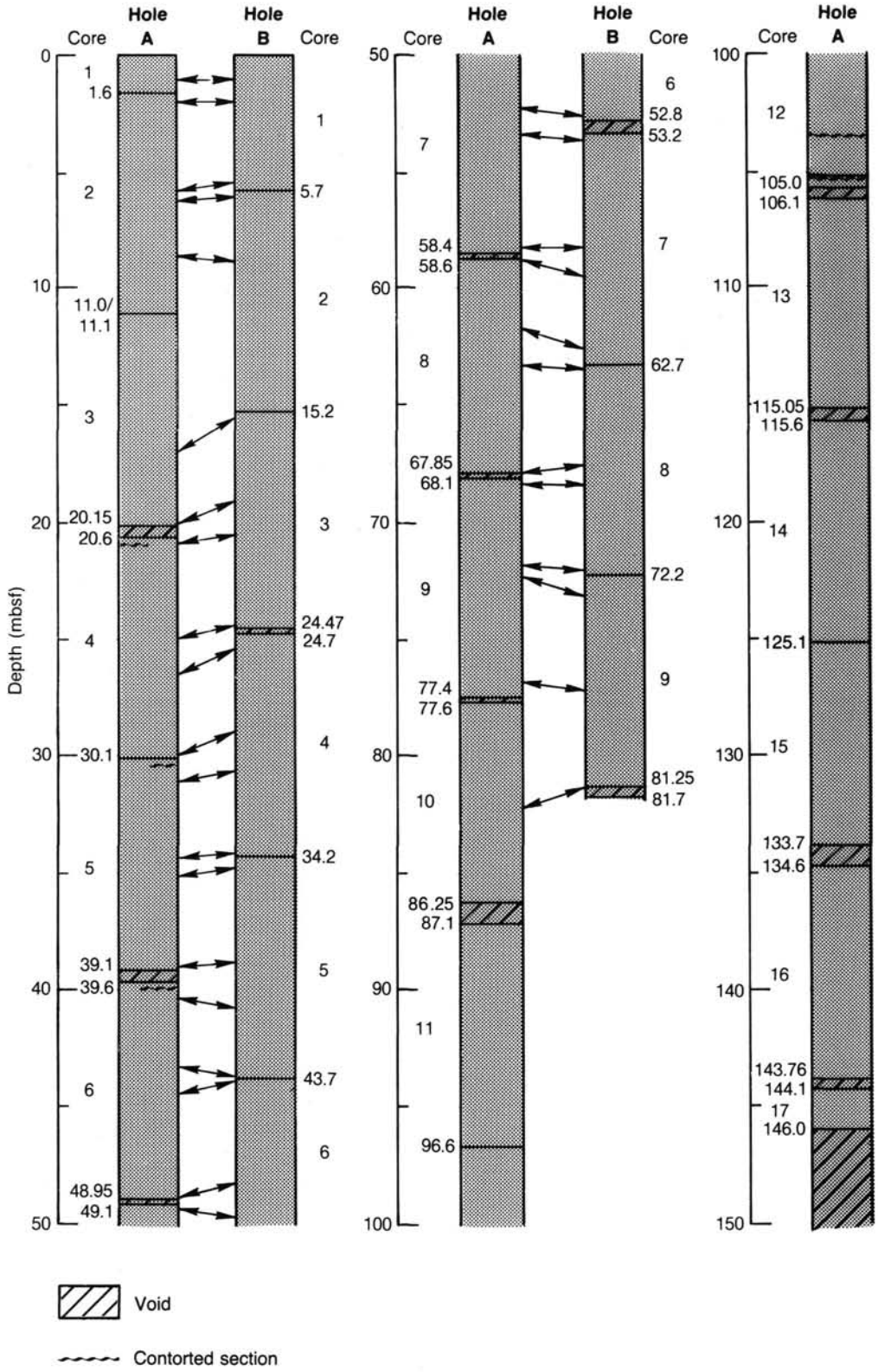

Figure 25. Depth correlation between Holes 661A and 661B.

Table 8. Composite-depth levels used to correlate cores from Holes 661A and 661B.

Composite depth (mbsf)	Gain/loss (m)	Cumulative gain (m)	Hole 661A (mbsf)	Hole 661B (mbsf)
0			0	0
8.6			8.6	8.85
16.95			16.95	15.5
20.1			20.1	18.6
22.0	+1.2	1.20	20.8	20.5
26.2			25.0	24.4
31.15			29.95	28.9
32.85	+0.65	1.85	31.0	30.7
40.75			38.9	38.75
42.7	+0.55	2.4	40.3	40.7
51.15			48.75	48.25
52.5	+0.8	3.2	49.3	49.6
61.4			58.2	58.2
62.6	+0.6	3.8	58.8	59.4
62.6			58.8	59.4
71.55			67.75	67.5
72.4	+0.35	4.15	68.25	68.35
76.35			72.2	73.0
80.45	−0.6	3.55	76.9	77.1

Note: Gains and losses of sediment at core breaks are presented relative to Hole 661A and are derived by subtracting the differences of sub-bottom depth between two succeeding switch-points in the two holes, respectively. The total stratigraphic thickness recovered is increased by approximately 4.5%.

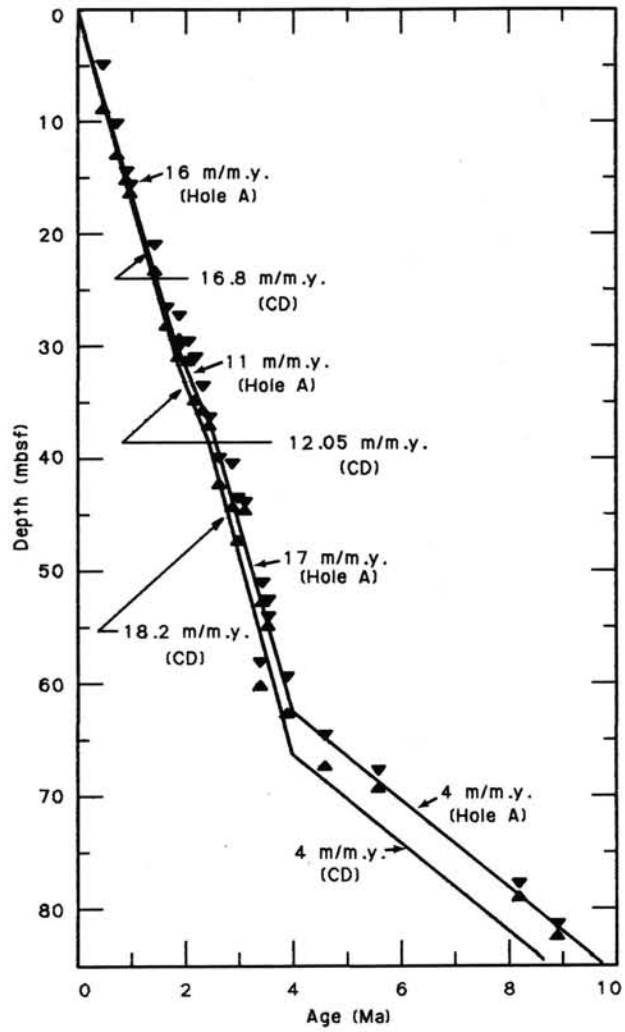

Figure 26. Age-depth section of Site 661 using biostratigraphic data from "Biostratigraphy" section (this chapter), comparing age-depth curves based on nominal depths in Hole 661A and based on new composite-depth estimates. *CD* = composite depth.

SITE 661 HOLE A CORE 1 H CORED INTERVAL 4012.7-4014.3 mbsl; 1-1.6 mbsf

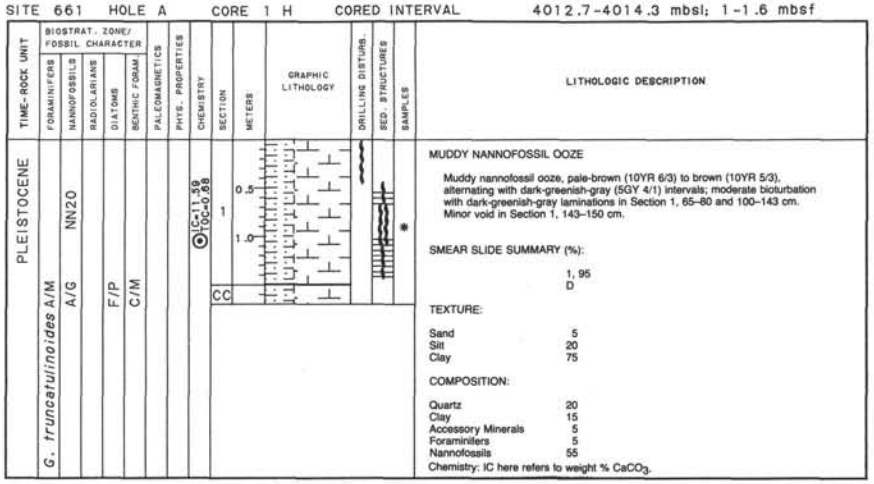

LITHOLOGIC DESCRIPTION

MUDDY NANNOFOSSIL OOZE

Muddy nannofossil ooze, pale-brown (10YR 6/3) to brown (10YR 5/3), alternating with dark-greenish-gray (5GY 4/1) intervals; moderate bioturbation with dark-greenish-gray laminations in Section 1, 65–80 and 100–143 cm. Minor void in Section 1, 143–150 cm.

SMEAR SLIDE SUMMARY (%):

	1, 95 D
TEXTURE:	
Sand	5
Silt	20
Clay	75
COMPOSITION:	
Quartz	20
Clay	15
Accessory Minerals	5
Foraminifers	5
Nannofossils	55

Chemistry: IC here refers to weight % $CaCO_3$.

SITE 661 HOLE A CORE 2 H CORED INTERVAL 4014.3-4023.8 mbsl; 1.6-11.1 mbsf

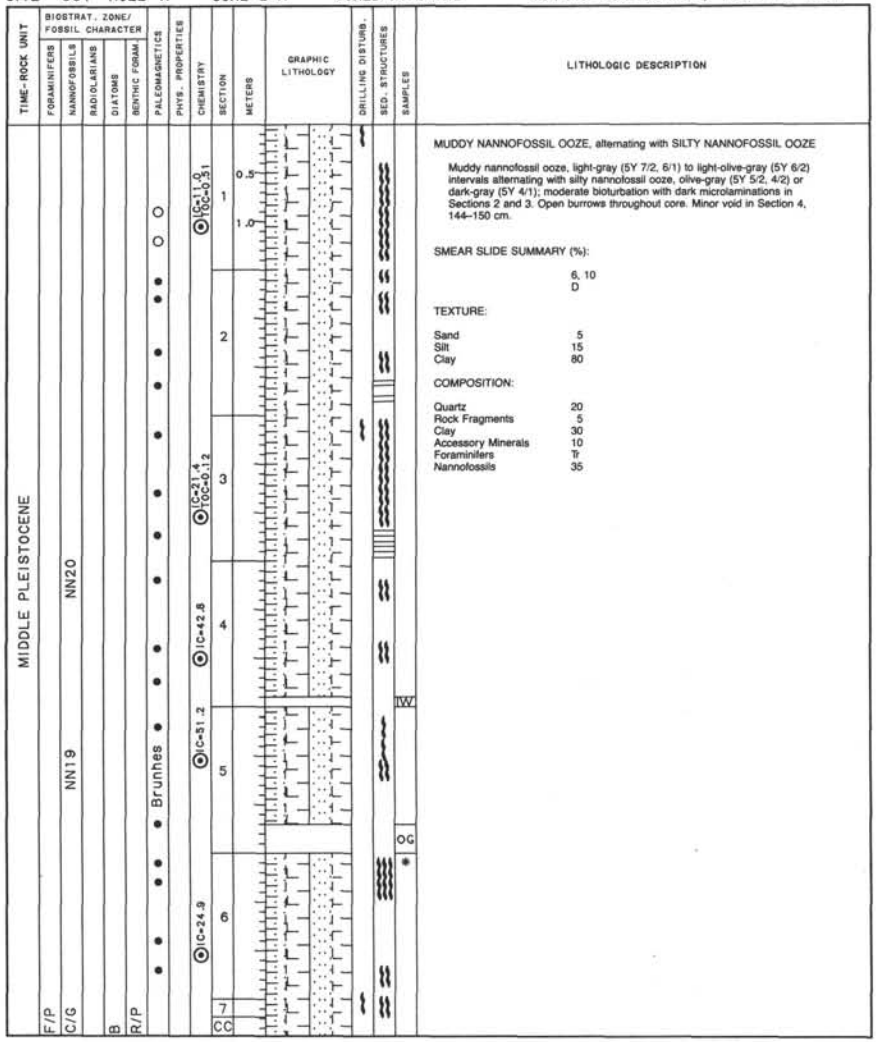

LITHOLOGIC DESCRIPTION

MUDDY NANNOFOSSIL OOZE, alternating with SILTY NANNOFOSSIL OOZE

Muddy nannofossil ooze, light-gray (5Y 7/2, 6/1) to light-olive-gray (5Y 6/2) intervals alternating with silty nannofossil ooze, olive-gray (5Y 5/2, 4/2) or dark-gray (5Y 4/1); moderate bioturbation with dark microlaminations in Sections 2 and 3. Open burrows throughout core. Minor void in Section 4, 144–150 cm.

SMEAR SLIDE SUMMARY (%):

	6, 10 D
TEXTURE:	
Sand	5
Silt	15
Clay	80
COMPOSITION:	
Quartz	20
Rock Fragments	5
Clay	30
Accessory Minerals	10
Foraminifers	Tr
Nannofossils	35

SITE 661 HOLE A CORE 3 H CORED INTERVAL 4023.8–4033.3 mbsl; 11.1–20.6 mbsf

TIME-ROCK UNIT: UPPER PLIOCENE / LOWER PLEISTOCENE

BIOSTRAT. ZONE/FOSSIL CHARACTER: FORAMINIFERS: PL6; NANNOFOSSILS: NN19; RADIOLARIANS: A/M; DIATOMS: A/M; BENTHIC FORAM.: F/M

PALEOMAGNETICS: O O O O Mat. O O O O ● J. ● O O O O Matuyama

PHYS. PROPERTIES: IC=43.8 00 / IC=38.7 00

CHEMISTRY: IC=38.3 / IC=51.2 / IC=0.6 / IC=5.7

SECTION: 1 2 3 4 5 6 CC

METERS: 0.5 1.0

GRAPHIC LITHOLOGY: VOID

DRILLING DISTURB.

BED. STRUCTURES

SAMPLES

LITHOLOGIC DESCRIPTION

NANNOFOSSIL-BEARING, SILTY CLAY, alternating with MUDDY NANNOFOSSIL OOZE

Nannofossil-bearing, silty clay, gray (5Y 5/2) to dark-gray (5Y 4/1) intervals, alternating with muddy nannofossil ooze, light-gray (5Y 7/1, 7/2) to gray (5Y 6/1), moderate bioturbation with large burrows throughout core. Dark greenish-gray microlaminations in Sections 3 and 4.

SMEAR SLIDE SUMMARY (%):

	2, 30 M	4, 20 D	6, 50 D
TEXTURE:			
Sand	—	10	—
Silt	40	20	—
Clay	60	70	—
COMPOSITION:			
Quartz	20	5	30
Rock fragments	5	—	—
Clay	60	30	50
Accessory Minerals	10	5	10
Foraminifers	—	10	—
Nannofossils	5	50	10
Diatoms	—	Tr	—

SITE 661 HOLE A CORE 4 H CORED INTERVAL 4033.3–4042.8 mbsl; 20.6–30.1 mbsf

TIME-ROCK UNIT: UPPER PLIOCENE

BIOSTRAT. ZONE/FOSSIL CHARACTER: FORAMINIFERS: PL6; NANNOFOSSILS: NN19 / NN18; RADIOLARIANS: A/M / C/P; DIATOMS: B; BENTHIC FORAM.: F/M

PALEOMAGNETICS: O O ● O O O O O O O O O O O O

PHYS. PROPERTIES: IC=29.3 / IC=48.6 00 / IC=0.0 00

CHEMISTRY: IC=70.0 / IC=37.1 / IC=65.1

SECTION: 1 2 3 4 5 6 7 CC

METERS: 0.5 1.0

GRAPHIC LITHOLOGY

DRILLING DISTURB.

BED. STRUCTURES

SAMPLES

LITHOLOGIC DESCRIPTION

CLAYEY, NANNOFOSSIL-FORAMINIFER OOZE, alternating with CLAY-BEARING, NANNOFOSSIL-FORAMINIFER OOZE

Clayey, nannofossil-foraminifer ooze, light-gray (5Y 7/1, 7/2), alternating with clay-bearing, nannofossil-foraminifer ooze, gray (5Y 6/1, 5/1) to olive-gray (5Y 5/2); moderately bioturbated with thin greenish to black layers, in Sections 1 through 3. Minor void in Section 1, 147–150 cm.

SMEAR SLIDE SUMMARY (%):

	1, 53 D	2, 93 D	3, 82 D	4, 82 D
TEXTURE:				
Sand	—	25	30	Tr
Silt	20	25	15	10
Clay	80	50	55	90
COMPOSITION:				
Quartz	10	5	5	5
Clay	30	25	25	35
Foraminifers		10	35	40
Nannofossils	10	50	35	30

SITE 661 HOLE A CORE 5 H CORED INTERVAL 4042.8-4052.3 mbsl; 30.1-39.6 mbsf

TIME-ROCK UNIT: UPPER PLIOCENE

BIOSTRAT. ZONE/FOSSIL CHARACTER

	FORAMINIFERS	NANNOFOSSILS	RADIOLARIANS	DIATOMS	BENTHIC FORAM.	PALEOMAGNETICS	PHYS. PROPERTIES	CHEMISTRY	SECTION	METERS	GRAPHIC LITHOLOGY	DRILLING DISTURB.	SED. STRUCTURES	SAMPLES
A/M	PL5	A/M	PL5	A/M	PL6									
A/M	NN16	NN17	NN18											
B														
F/M														
					•									
	•	O	O	O	O									
					•	•								
								IC-71.5						
					O	O		IC-57.1 TOC-0.00						
								IC-48.7						
								IC-55.5						
								IC-44.4						
	•	•	•	•					CC		VOID			

LITHOLOGIC DESCRIPTION

CLAYEY, NANNOFOSSIL-FORAMINIFER OOZE and CLAY-BEARING NANNOFOSSIL OOZE

Clayey, nannofossil-foraminifer ooze, light gray (5Y 7/1, 7/2); alternating with clay-bearing nannofossil ooze, light olive-gray (5Y 6/2) to olive-gray (5Y 5/2); moderate bioturbation and pyrite staining.

SMEAR SLIDE SUMMARY (%):

	4, 4 D	4, 34 D	4, 44 D
TEXTURE:			
Sand	20	30	tr
Silt	30	20	20
Clay	50	50	80
COMPOSITION:			
Quartz	tr	5	10
Clay	30	20	15
Accessory Minerals	—	—	5
Pyrite	—	—	5
Foraminifers	45	40	—
Nannofossils	25	35	65

SITE 661 HOLE A CORE 6 H CORED INTERVAL 4052.3-4061.8 mbsl; 39.60-49.10 mbsf

TIME-ROCK UNIT: UPPER PLIOCENE

BIOSTRAT. ZONE/FOSSIL CHARACTER

	FORAMINIFERS	NANNOFOSSILS	RADIOLARIANS	DIATOMS	BENTHIC FORAM.	PALEOMAGNETICS	PHYS. PROPERTIES	CHEMISTRY	SECTION	METERS	GRAPHIC LITHOLOGY	DRILLING DISTURB.	SED. STRUCTURES	SAMPLES
A/M	PL3	A/G	PL3	A/G	PL4	A/M	PL5							
A/M		NN16												
B														
F/M														
							•							
							•							
							•							
							•	IC-76.0 TOC-0.38						
							•	TOC-61.7						
							•	IC-65.1 TOC-0.0						
						O	•	IC-68.3						
							•	IC-79.0						
	•	•	•	•			•	IC-52.1						
									CC					

LITHOLOGIC DESCRIPTION

FORAMINIFER-NANNOFOSSIL OOZE

Foraminifer-nannofossil ooze, white (5Y 8/1), light-gray (5Y 7/1, 7/2) and light-olive-gray (5Y 6/2); moderate bioturbation; pyrite staining throughout core.

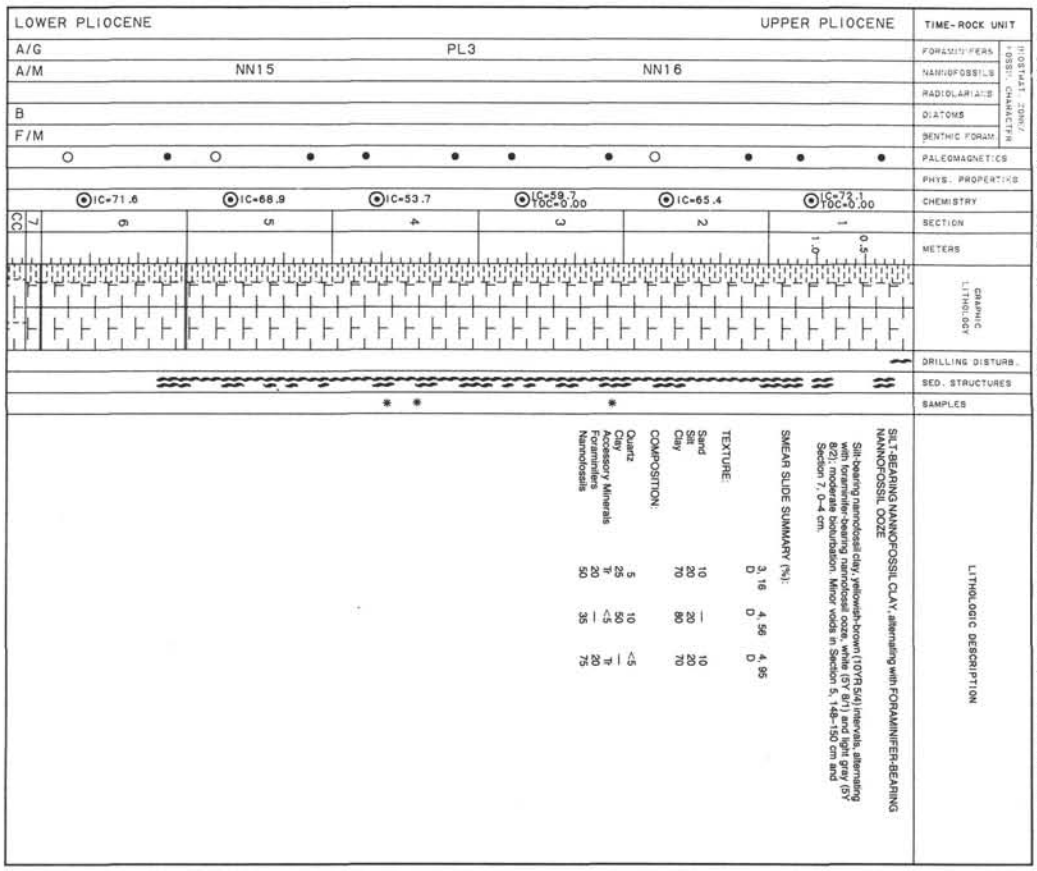
SITE 661 HOLE A CORE 7 H CORED INTERVAL 4061.8-4071.3 mbsl; 49.10-58.6 mbsf
LOWER PLIOCENE
UPPER PLIOCENE
TIME-ROCK UNIT
A/G
PL3
FORAMINIFERS
A/M
NN15
NN16
NANNOFOSSILS
RADIOLARIANS
DIATOMS
B
F/M
BENTHIC FORAM.
BIOSTRAT. ZONE/ FOSSIL CHARACTER
PALEOMAGNETICS
PHYS. PROPERTIES
IC=71.6
IC=68.9
IC=53.7
IC=59.7 TOC=0.00
IC=65.4
IC=72.1 TOC=0.00
CHEMISTRY
CC
7
6
5
4
3
2
1
SECTION
METERS
1.0
0.5
GRAPHIC LITHOLOGY
DRILLING DISTURB.
SED. STRUCTURES
SAMPLES
LITHOLOGIC DESCRIPTION
SILT-BEARING NANNOFOSSIL CLAY, alternating with FORAMINIFER-BEARING NANNOFOSSIL OOZE
Silt-bearing nannofossil clay, yellowish-brown (10YR 5/4) intervals, alternating with foraminifer-bearing nannofossil ooze, white (5Y 8/1) and light gray (5Y 8/2); moderate bioturbation. Minor voids in Section 5, 148–150 cm and Section 7, 0–4 cm.
SMEAR SLIDE SUMMARY (%):
TEXTURE:
Sand
Silt
Clay
COMPOSITION:
Quartz
Clay
Accessory Minerals
Foraminifers
Nannofossils
3, 16 D
4, 56 D
4, 95 D
5
25
Tr
20
50
10
20
70
—
10
50
<5
—
20
80
<5
—
10
20
70
—
Tr
20
75

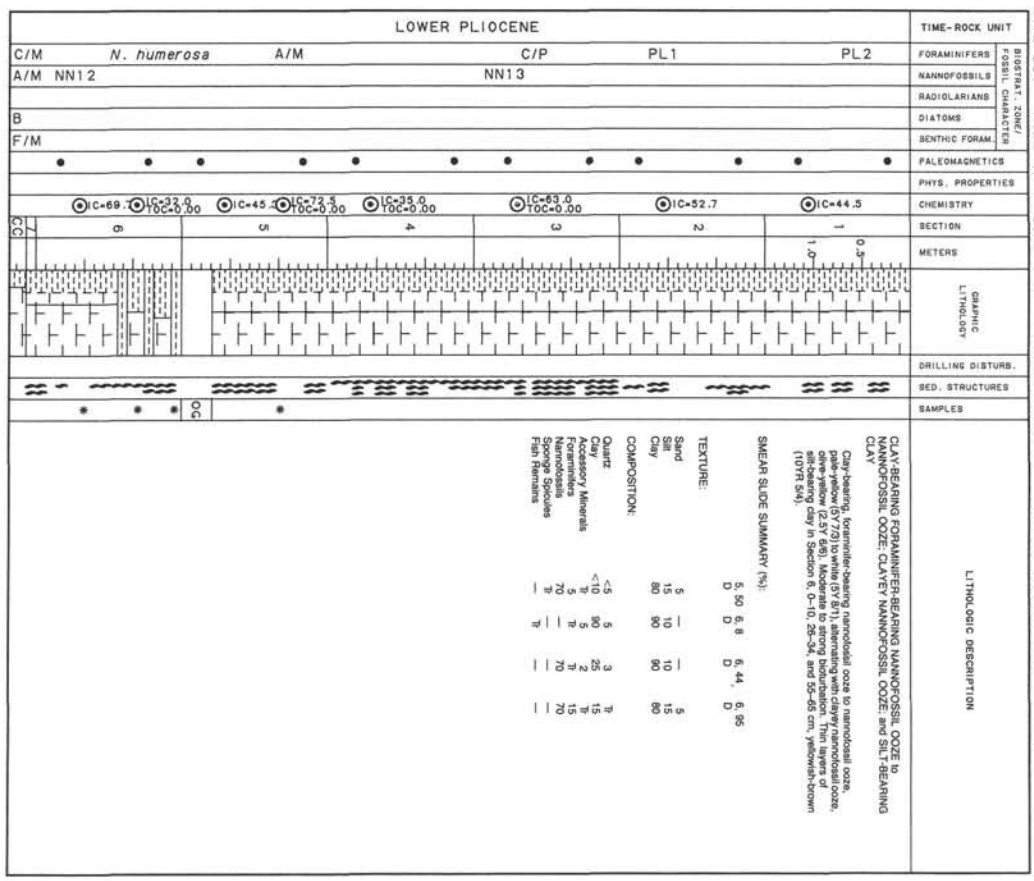
SITE 661 HOLE A CORE 8 H CORED INTERVAL 4071.3-4080.8 mbsl; 58.6-68.10 mbsf
LOWER PLIOCENE
TIME-ROCK UNIT
C/M
N. humerosa
A/M
C/P
PL1
PL2
FORAMINIFERS
A/M
NN12
NN13
NANNOFOSSILS
RADIOLARIANS
DIATOMS
B
F/M
BENTHIC FORAM.
BIOSTRAT. ZONE/ FOSSIL CHARACTER
PALEOMAGNETICS
PHYS. PROPERTIES
IC=69.7
IC=32.0 TOC=0.00
IC=45.3
IC=72.5 TOC=0.00
IC=35.0 TOC=0.00
IC=63.0 TOC=0.00
IC=52.7
IC=44.5
CHEMISTRY
CC
6
5
4
3
2
1
SECTION
METERS
1.0
0.5
GRAPHIC LITHOLOGY
DRILLING DISTURB.
SED. STRUCTURES
SAMPLES
OG
LITHOLOGIC DESCRIPTION
CLAY-BEARING FORAMINIFER-BEARING NANNOFOSSIL OOZE to NANNOFOSSIL OOZE; CLAYEY NANNOFOSSIL OOZE; and SILT-BEARING CLAY
Clay-bearing, foraminifer-bearing nannofossil ooze to nannofossil ooze, pale-yellow (5Y 7/3) to white (5Y 8/1), alternating with clayey nannofossil ooze, light-yellow (2.5Y 8/4). Moderate to strong bioturbation. Thin layers of silt-bearing clay in Section 6, 0–10, 28–34, and 50–65 cm; yellowish-brown (10YR 5/4).
SMEAR SLIDE SUMMARY (%):
TEXTURE:
Sand
Silt
Clay
COMPOSITION:
Quartz
Clay
Accessory Minerals
Foraminifers
Nannofossils
Sponge Spicules
Fish Remains
5, 50 D
6, 8 D
6, 44 D
6, 95 D
5
15
80
—
10
90
3
25
2
15
70
—
Tr
15
70
—
5
15
80
—
<5
<10
5
70
Tr
—
5
5
90
Tr
—
—
Tr
Tr
—
—

SITE 661 HOLE A CORE 9 H CORED INTERVAL 4080.8-4090.3 mbsl; 68.10-77.6 mbsf

NANNOFOSSIL OOZE, alternating with SILT-BEARING, NANNOFOSSIL-BEARING CLAY to SILT-BEARING CLAY

Nannofossil ooze, light gray (10YR 7/1) in Section 1, 80 cm, through Section 3, 145 cm, alternating with silt-bearing, nannofossil-bearing clay to silt-bearing clay, yellowish-brown (10YR 5/4, 5/6, 5/8) to pale-olive (5Y 6/3, 6/4); moderate to strong bioturbation.

Minor lithology: Section 1, 0–80 cm, and Section 4 to CC: silt-bearing, nannofossil-bearing clay to silt-bearing clay, yellowish-brown (10YR 5/4) to olive-yellow (5Y 6/6); moderate bioturbation.

SMEAR SLIDE SUMMARY (%):

	3, 123 D	5, 130 D
TEXTURE:		
Sand	—	—
Silt	20	10
Clay	80	90
COMPOSITION:		
Quartz	5	10
Clay	70	90
Accessory Minerals	5	Tr
Nannofossils	20	Tr

SITE 661 HOLE A CORE 10 H CORED INTERVAL 4090.3-4099.8 mbsl; 27.6-87.10 mbsf

CLAY-BEARING NANNOFOSSIL OOZE and NANNOFOSSIL-BEARING, SILTY CLAY

Clay-bearing nannofossil ooze, reddish-yellow (7.5YR 6/6, 7/6) to pink (7.5YR 7/4), alternating with nannofossil-bearing, silty clay, light brown (7.5YR 6/4) to strong brown (7.5YR 5/6); moderate to strong bioturbation throughout core.

SMEAR SLIDE SUMMARY (%):

	4, 12 M	4, 69 D
TEXTURE:		
Sand	—	Tr
Silt	—	30
Clay	100	70
COMPOSITION:		
Quartz	Tr	20
Rock Fragments	—	60
Clay	10	—
Accessory Minerals	—	10
Foraminifers	Tr	Tr
Nannofossils	90	<10

SITE 661 HOLE A CORE 11 H CORED INTERVAL 4099.8–4109.3 mbsl; 87.10–91.60 mbsf

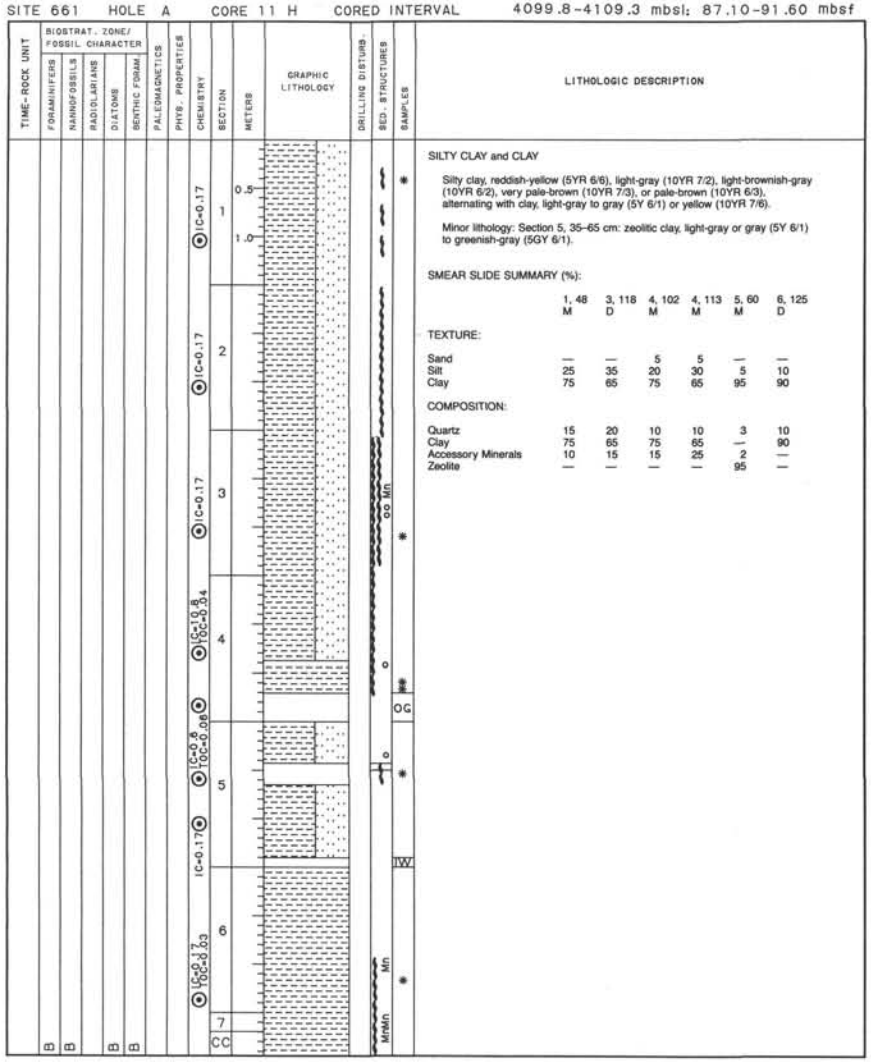

LITHOLOGIC DESCRIPTION

SILTY CLAY and CLAY

Silty clay, reddish-yellow (5YR 6/6), light-gray (10YR 7/2), light-brownish-gray (10YR 6/2), very pale-brown (10YR 7/3), or pale-brown (10YR 6/3), alternating with clay, light-gray to gray (5Y 6/1) or yellow (10YR 7/6).

Minor lithology: Section 5, 35–65 cm: zeolitic clay, light-gray or gray (5Y 6/1) to greenish-gray (5GY 6/1).

SMEAR SLIDE SUMMARY (%):

	1, 48 M	3, 118 D	4, 102 M	4, 113 M	5, 60 M	6, 125 D
TEXTURE:						
Sand	—	—	5	5	—	—
Silt	25	35	20	30	5	10
Clay	75	65	75	65	95	90
COMPOSITION:						
Quartz	15	20	10	10	3	10
Clay	75	65	75	65	—	90
Accessory Minerals	10	15	15	25	2	—
Zeolite	—	—	—	—	95	—

SITE 661 HOLE A CORE 12 H CORED INTERVAL 4109.3–4118.8 mbsl; 96.60–106.1 mbsf

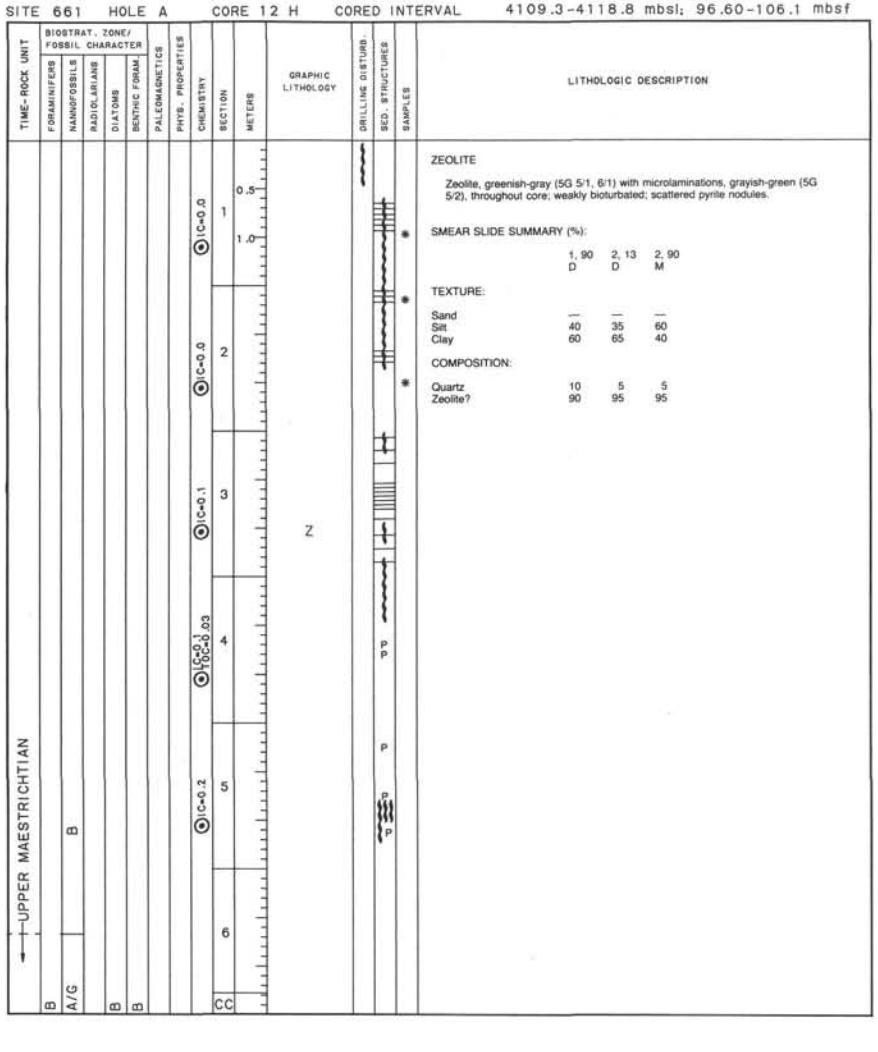

LITHOLOGIC DESCRIPTION

ZEOLITE

Zeolite, greenish-gray (5G 5/1, 6/1) with microlaminations, grayish-green (5G 5/2), throughout core; weakly bioturbated; scattered pyrite nodules.

SMEAR SLIDE SUMMARY (%):

	1, 90 D	2, 13 D	2, 90 M
TEXTURE:			
Sand	—	—	—
Silt	40	35	60
Clay	60	65	40
COMPOSITION:			
Quartz	10	5	5
Zeolite?	90	95	95

SITE 661 HOLE A CORE 13 H CORED INTERVAL 4118.8-4128.3 mbsl; 106.10-115.60 mbsf

TIME-ROCK UNIT: UPPER MAESTRICHTIAN

BIOSTRAT. ZONE/FOSSIL CHARACTER: FORAMINIFERS: B; A/M–A. cymbiformis; M. mura; NANNOFOSSILS: A/M–A. cymbiformis; RADIOLARIANS: F/M; DIATOMS: F/M; BENTHIC FORAM.: F/M; PALEOMAGNETICS

PHYS. PROPERTIES: IC=43.2; IC=58.6; IC=68.1; IC=62.4; IC=48.3

CHEMISTRY: IC=59.1 / IC=59.30

SECTION: 1, 2, 3, 4, 5, 6, CC

METERS: 0.5, 1.0

GRAPHIC LITHOLOGY: Z

DRILLING DISTURB.

SED. STRUCTURES: *

SAMPLES

LITHOLOGIC DESCRIPTION

CLAYEY NANNOFOSSIL OOZE

Clayey nannofossil ooze, light-greenish-gray (5BG 7/1) alternating with intervals of (5G 7/1); weak to moderate bioturbation; dark-microlaminations in Section 6. Minor void in Section 1, 29–32 cm.

Minor lithology: Section 1, 0–85 cm: zeolitic nannofossil ooze, light-greenish-gray (5G 7/1) to greenish-gray (5G 7/1).

SMEAR SLIDE SUMMARY (%):

	1, 70 D	2, 80 D
TEXTURE:		
Sand	—	—
Silt	40	30
Clay	60	70
COMPOSITION:		
Quartz	5	5
Rock Fragments	5	—
Clay	—	20
Accessory Minerals	—	5
Zeolite?	90	—
Nannofossils	—	70

SITE 661 HOLE A CORE 14 H CORED INTERVAL 4128.3-4137.8 mbsl; 115.60-125.10 mbsf

TIME-ROCK UNIT: UPPER MAESTRICHTIAN

BIOSTRAT. ZONE/FOSSIL CHARACTER: FORAMINIFERS: B; A/P; NANNOFOSSILS: A. cymbiformis; RADIOLARIANS: B; DIATOMS: B; BENTHIC FORAM.: F/M; PALEOMAGNETICS

PHYS. PROPERTIES: IC=11.3

CHEMISTRY: IC=0.2; IC=0.25; IC=48.3 / IC=49.30; IC=0.4

SECTION: 1, 2, 3, 4, 5, 6, 7, 8

METERS: 0.5, 1.0

GRAPHIC LITHOLOGY: Z; VOID

DRILLING DISTURB.

SED. STRUCTURES: P; *

SAMPLES: OC

LITHOLOGIC DESCRIPTION

NANNOFOSSIL OOZE and ZEOLITE

Nannofossil ooze, light-greenish-gray (5G 7/1) to greenish-gray (5G 8/1), alternating with zeolite, greenish-gray (5G 5/1, 5GY 6/1, 5GY 5/1); dark microlaminations in Sections 2, 5, and 7; strongly bioturbated in Sections 1 and 2. Minor void in Section 2, 148–150 cm.

SMEAR SLIDE SUMMARY (%):

	1, 120 D	2, 80 D
TEXTURE:		
Sand	—	—
Silt	35	5
Clay	65	95
COMPOSITION:		
Quartz	<5	2
Accessory Minerals	—	3
Zeolite?	95	—
Nannofossils	—	95

SITE 661 HOLE A CORE 15 H CORED INTERVAL 4137.8–4147.3 mbsl; 125.10–134.6 mbsf

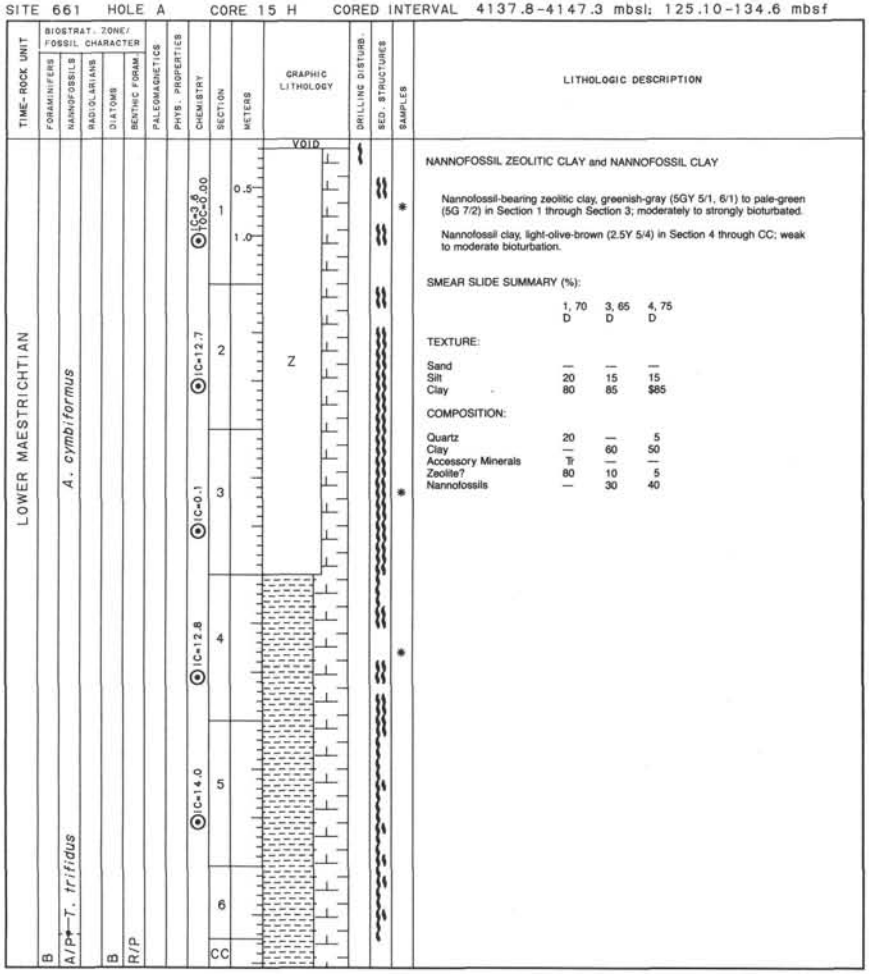

NANNOFOSSIL ZEOLITIC CLAY and NANNOFOSSIL CLAY

Nannofossil-bearing zeolitic clay, greenish-gray (5GY 5/1, 6/1) to pale-green (5G 7/2) in Section 1 through Section 3; moderately to strongly bioturbated.

Nannofossil clay, light-olive-brown (2.5Y 5/4) in Section 4 through CC; weak to moderate bioturbation.

SMEAR SLIDE SUMMARY (%):

	1, 70 D	3, 65 D	4, 75 D
TEXTURE:			
Sand	—	—	—
Silt	20	15	15
Clay	80	85	\$85
COMPOSITION:			
Quartz	20	—	5
Clay	—	60	50
Accessory Minerals	tr	—	—
Zeolite?	80	10	5
Nannofossils	—	30	40

SITE 661 HOLE A CORE 16 X CORED INTERVAL 4147.3–4156.8 mbsl; 134.6–146.1 mbsf

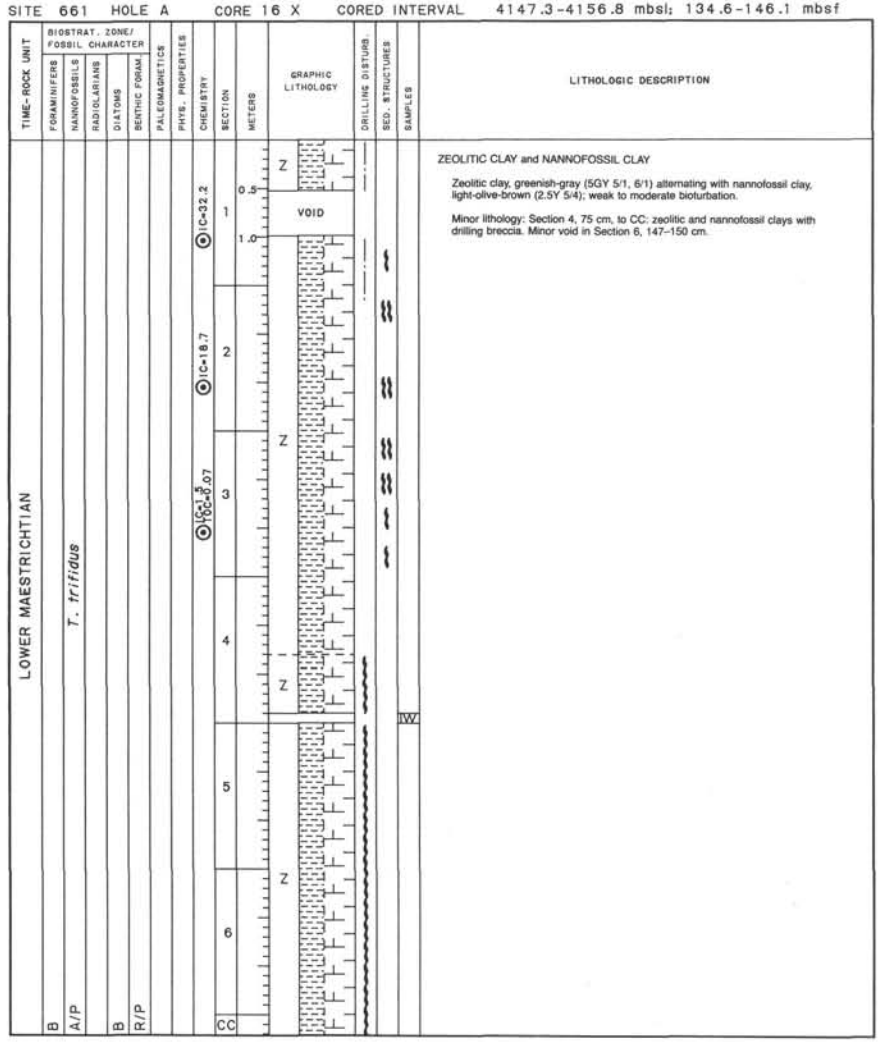

ZEOLITIC CLAY and NANNOFOSSIL CLAY

Zeolitic clay, greenish-gray (5GY 5/1, 6/1) alternating with nannofossil clay, light-olive-brown (2.5Y 5/4); weak to moderate bioturbation.

Minor lithology: Section 4, 75 cm, to CC: zeolitic and nannofossil clays with drilling breccia. Minor void in Section 6, 147–150 cm.

SITE 661 HOLE A CORE 17 X CORED INTERVAL 4156.8-4166.3 mbsl; 146.1-153.6 mbsf

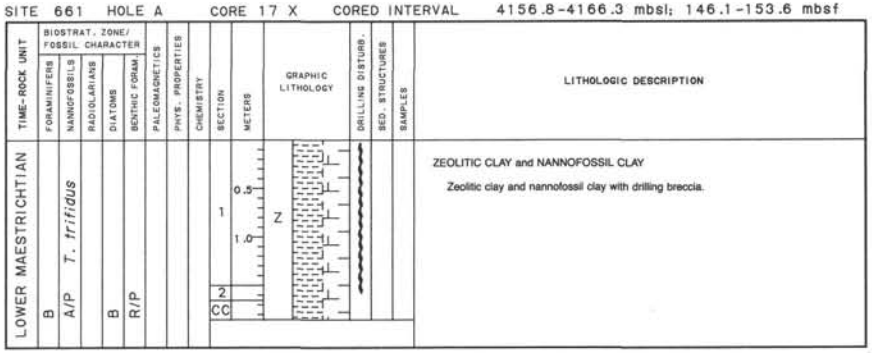

SITE 661 HOLE A CORE 18 X CORED INTERVAL 4166.3-4175.8 mbsl; 153.6-163.10 mbsf

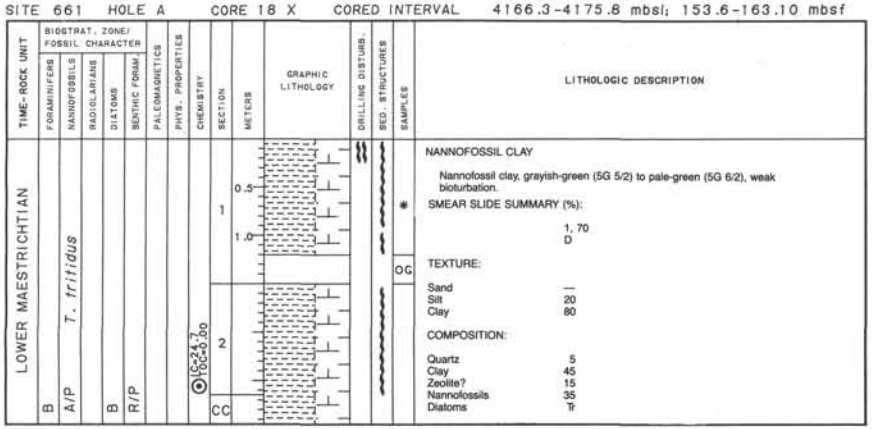

SITE 661 HOLE A CORE 19 X CORED INTERVAL 4175.8-4185.3 mbsl; 163.1-172.6 mbsf

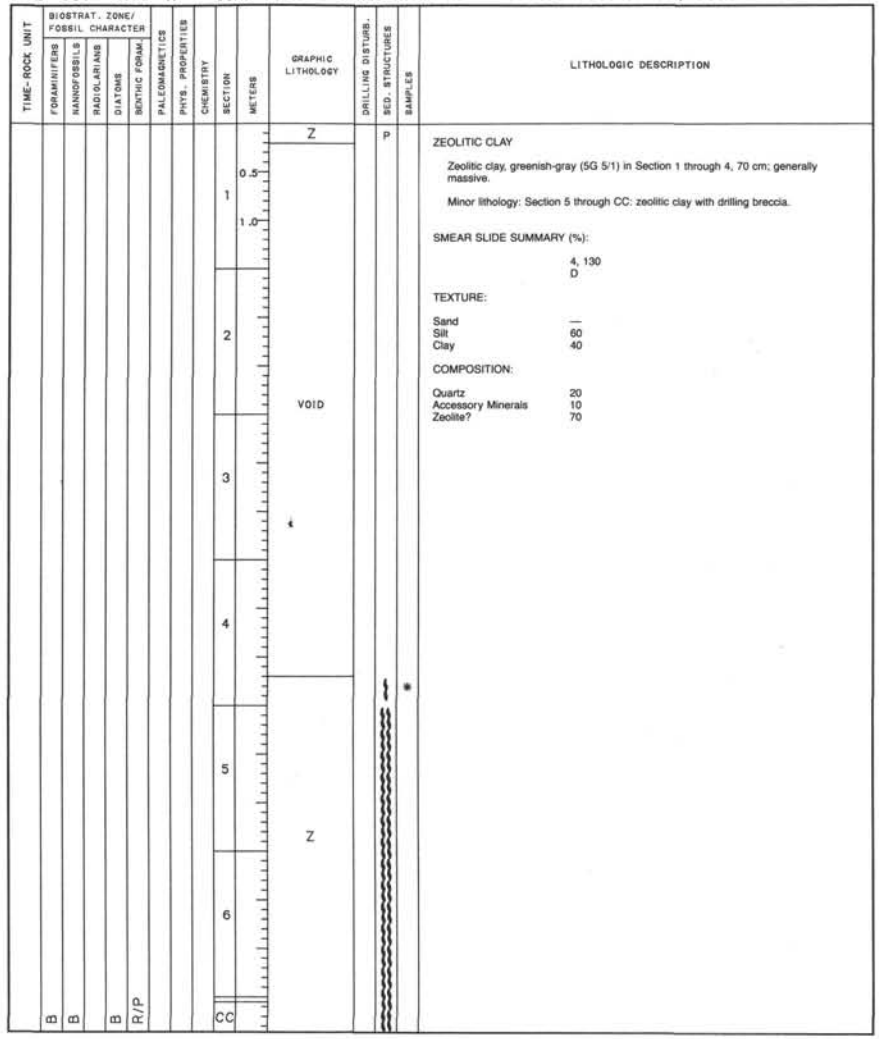

SITE 661 HOLE A CORE 20 X CORED INTERVAL 4185.3-4194.8 mbsl; 172.6-182.1 mbsf

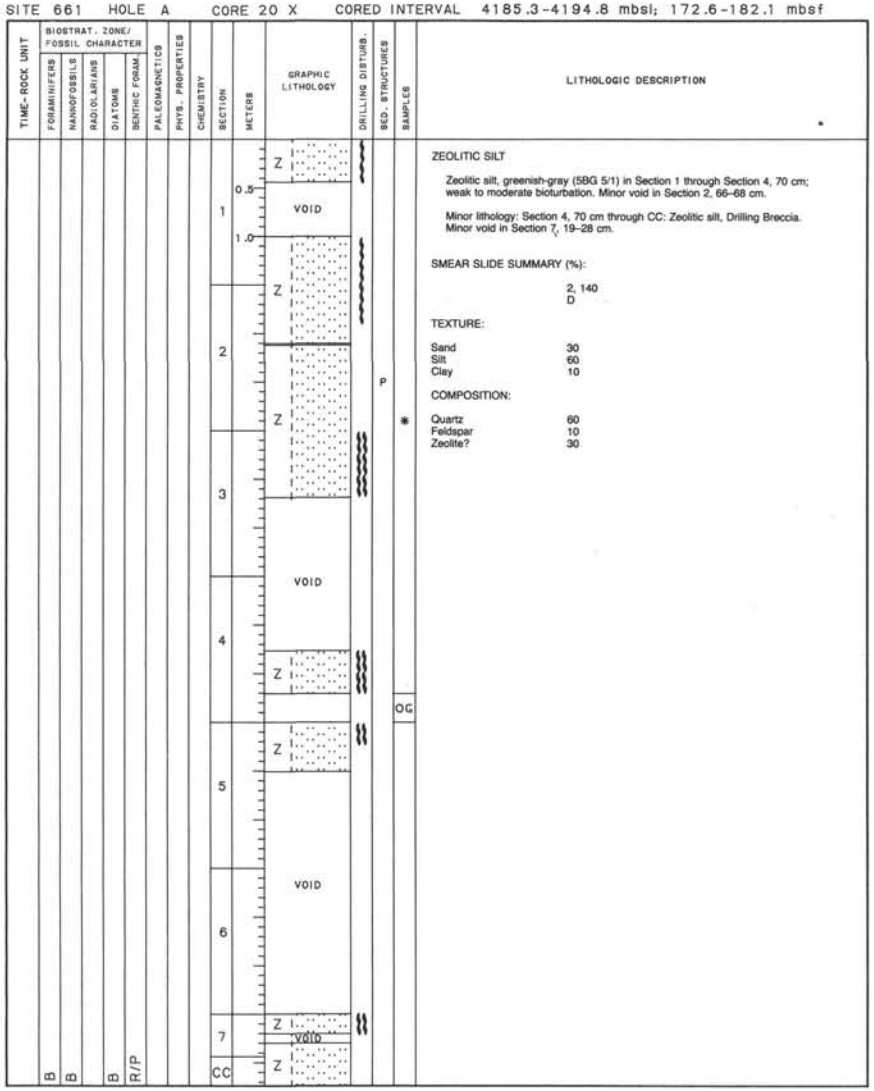

ZEOLITIC SILT

Zeolitic silt, greenish-gray (5BG 5/1) in Section 1 through Section 4, 70 cm; weak to moderate bioturbation. Minor void in Section 2, 66–68 cm.

Minor lithology: Section 4, 70 cm through CC: Zeolitic silt, Drilling Breccia. Minor void in Section 7, 19–28 cm.

SMEAR SLIDE SUMMARY (%):

	2, 140 D
TEXTURE:	
Sand	30
Silt	60
Clay	10
COMPOSITION:	
Quartz	60
Feldspar	10
Zeolite?	30

SITE 661 HOLE A CORE 21 X CORED INTERVAL 4194.8-4204.3 mbsl; 182.1-191.6 mbsf

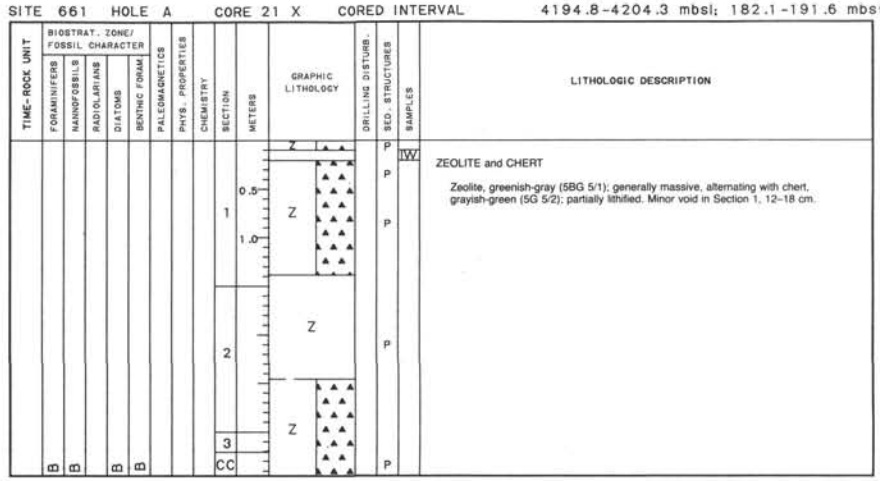

ZEOLITE and CHERT

Zeolite, greenish-gray (5BG 5/1); generally massive, alternating with chert, grayish-green (5G 5/2); partially lithified. Minor void in Section 1, 12–18 cm.

SITE 661 HOLE A CORE 22 X CORED INTERVAL 4204.3-4213.8 mbsl; 191.6-201.1 mbsf

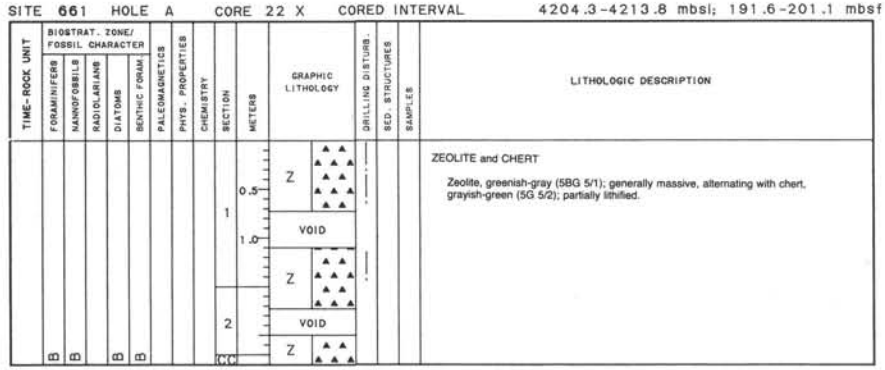

ZEOLITE and CHERT

Zeolite, greenish-gray (5BG 5/1); generally massive, alternating with chert, grayish-green (5G 5/2); partially lithified.

SITE 661 HOLE A CORE 23 X CORED INTERVAL 4213.8-4223.3 mbsl; 201.1-210.6 mbsf

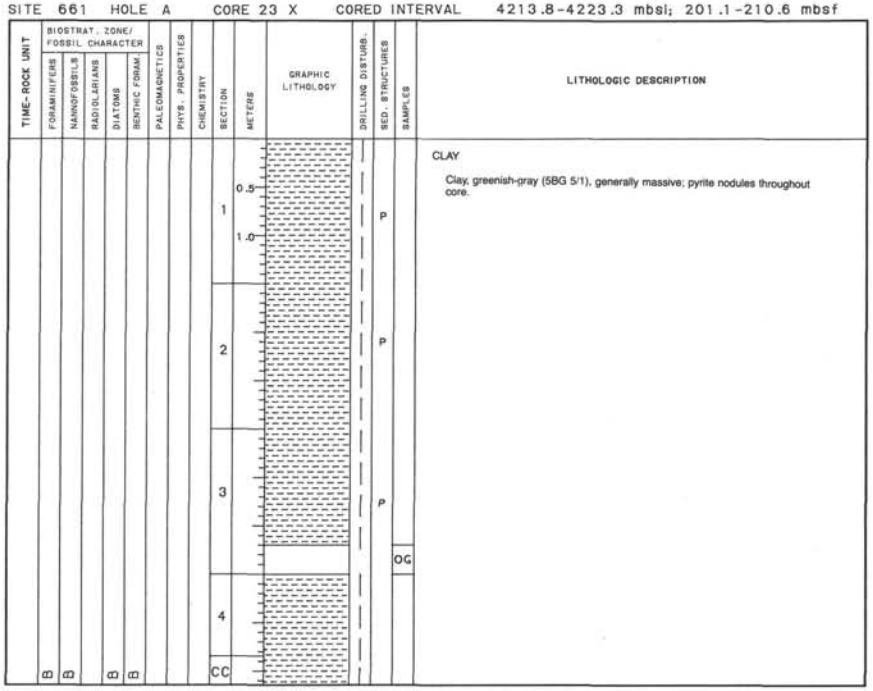

CLAY

Clay, greenish-gray (5BG 5/1), generally massive; pyrite nodules throughout core.

SITE 661 HOLE A CORE 24 X CORED INTERVAL 4223.3-4232.8 mbsl; 210.6-220.1 mbsf

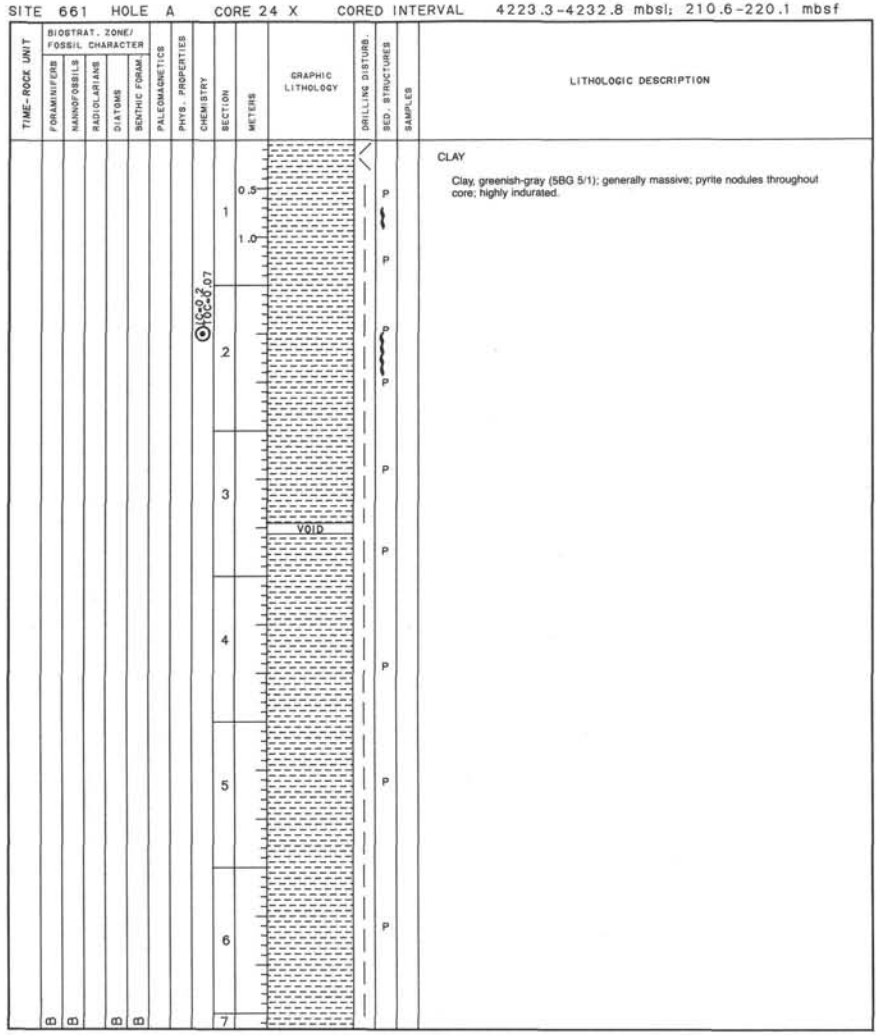

CLAY

Clay, greenish-gray (5BG 5/1); generally massive; pyrite nodules throughout core; highly indurated.

SITE 661 HOLE A CORE 25 X CORED INTERVAL 4232.8-4242.3 mbsl; 220.1-229.6 mbsf

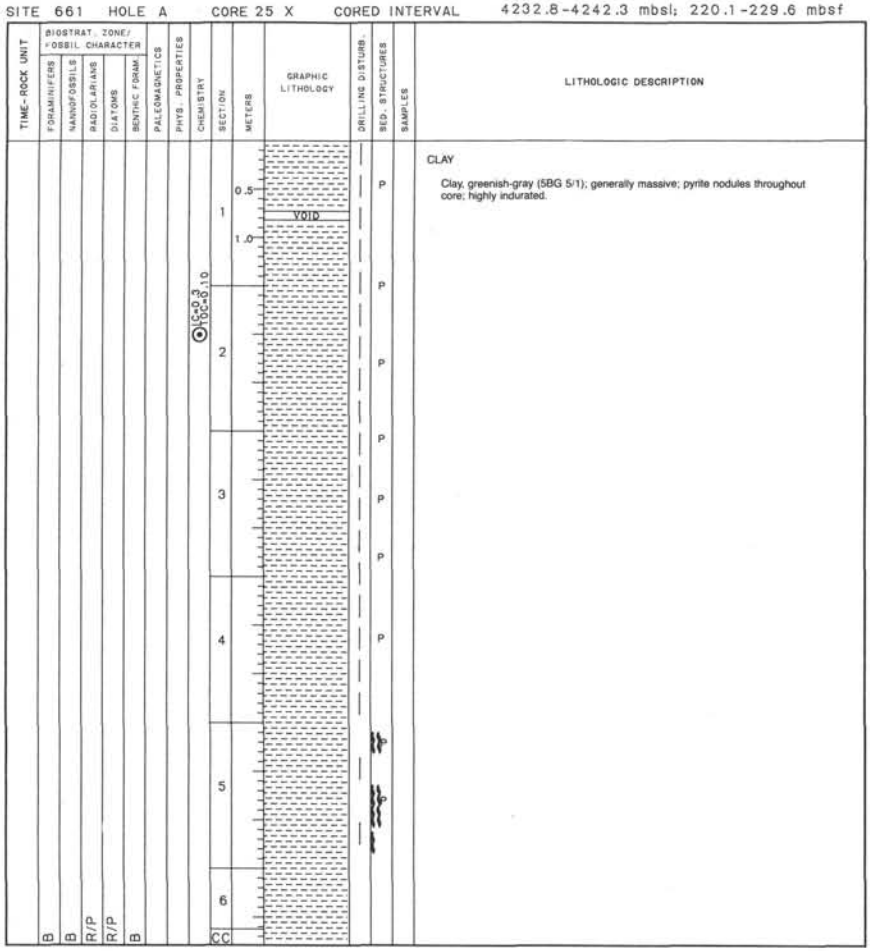

SITE 661 HOLE A CORE 26 X CORED INTERVAL 4242.3-4251.8 mbsl; 229.6-239.1 mbsf

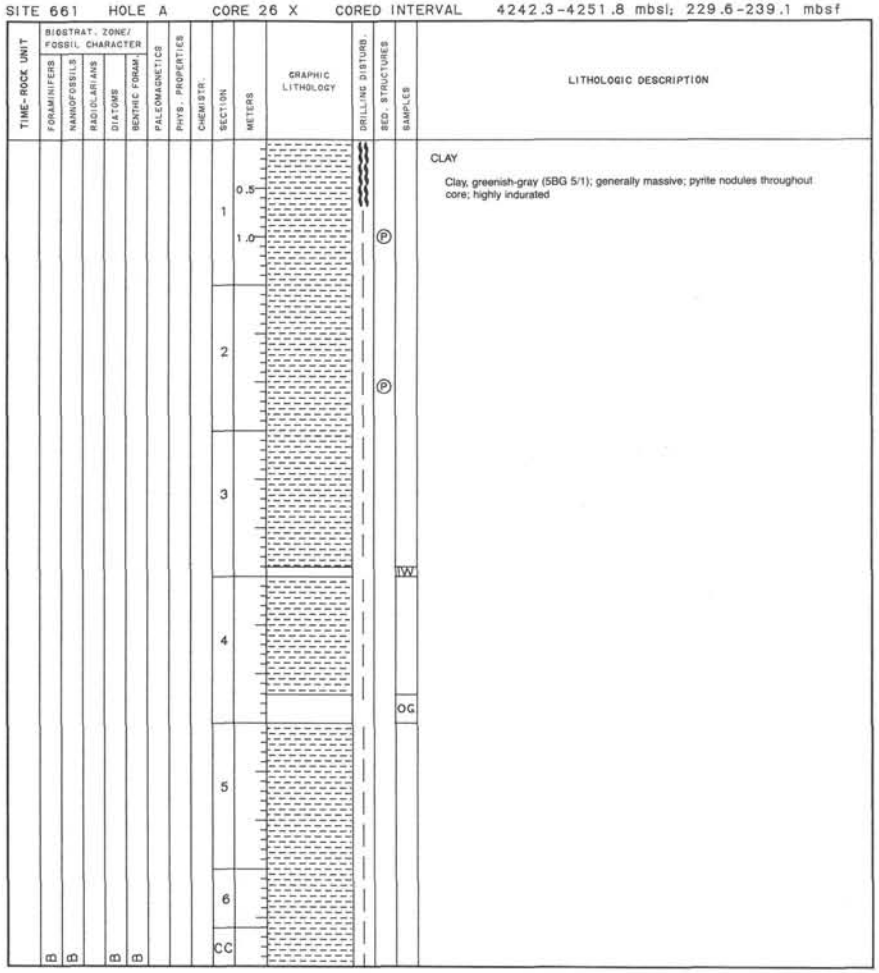

SITE 661 HOLE A CORE 27 X CORED INTERVAL 4251.8-4261.3 mbsl; 239.1-248.6 mbsf

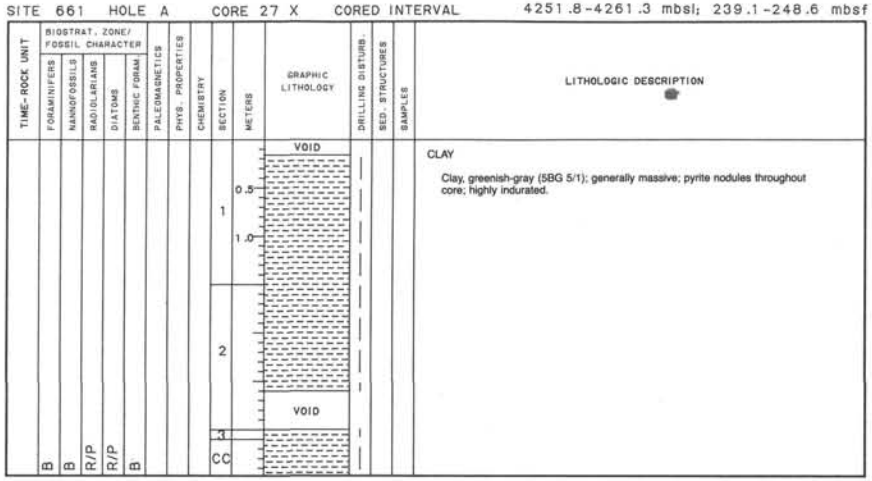

SITE 661 HOLE A CORE 28 X CORED INTERVAL 4261.3-4270.8 mbsl; 248.6-258.1 mbsf

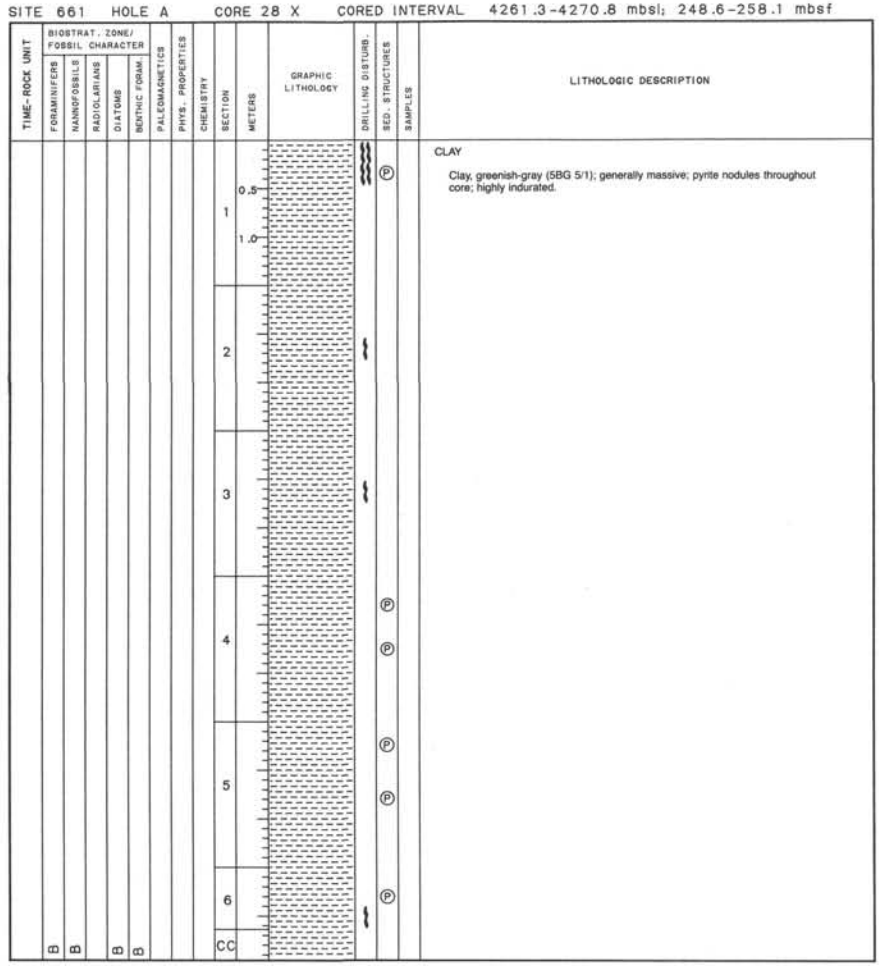

SITE 661 HOLE A CORE 29 X CORED INTERVAL 4270.8-4280.3 mbsl; 258.1-267.6 mbsf

TIME-ROCK UNIT	BIOSTRAT. ZONE/ FOSSIL CHARACTER: FORAMINIFERS	NANNOFOSSILS	RADIOLARIANS	DIATOMS	BENTHIC FORAM.	PALEOMAGNETICS	PHYS. PROPERTIES	CHEMISTRY	SECTION	METERS	GRAPHIC LITHOLOGY	DRILLING DISTURB.	SED. STRUCTURES	SAMPLES	LITHOLOGIC DESCRIPTION
	B	B		B	B				1	0.5			P		CLAY
										1.0			P		Clay, greenish-gray (5BG 5/1); generally massive; pyrite nodules throughout core; highly indurated.
									2				P		
													P		
									3				P		
														OG	
									4						
									CC						

SITE 661 HOLE A CORE 30 X CORED INTERVAL 4280.3-4289.8 mbsl; 267.6-277.1 mbsf

TIME-ROCK UNIT	BIOSTRAT. ZONE/ FOSSIL CHARACTER: FORAMINIFERS	NANNOFOSSILS	RADIOLARIANS	DIATOMS	BENTHIC FORAM.	PALEOMAGNETICS	PHYS. PROPERTIES	CHEMISTRY	SECTION	METERS	GRAPHIC LITHOLOGY	DRILLING DISTURB.	SED. STRUCTURES	SAMPLES	LITHOLOGIC DESCRIPTION
	B	B		B	B				1	0.5					CLAY
										1.0					Clay, greenish-gray (5BG 5/1); generally massive; pyrite nodules throughout core; highly indurated.
									2		VOID				
									CC						

SITE 661 HOLE A CORE 31X CORED INTERVAL 4289.8-4299.3 mbsl; 277.1-286.6 mbsf

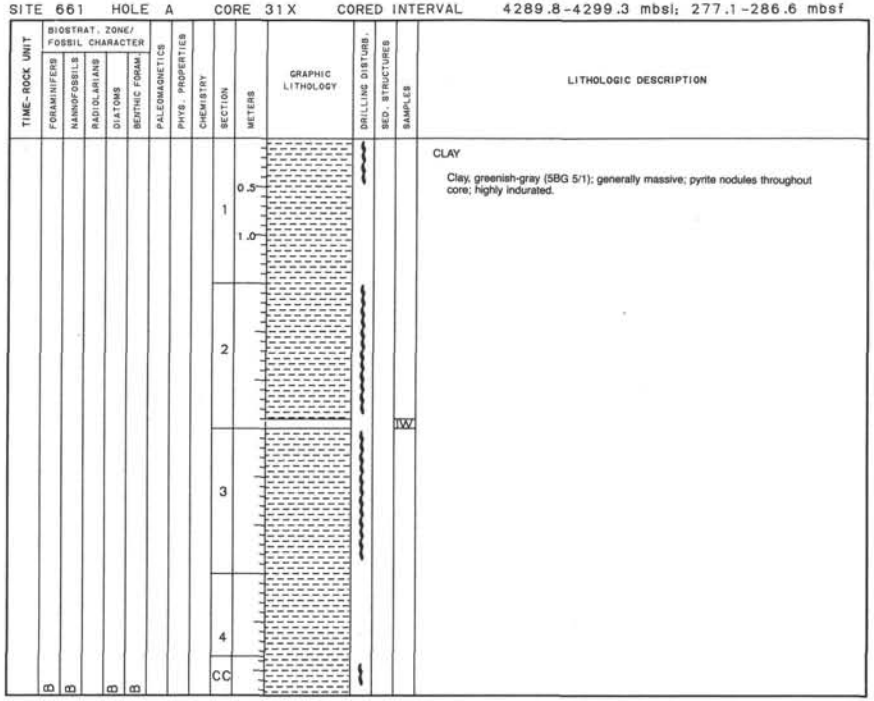

SITE 661 HOLE A CORE 32 X CORED INTERVAL 4299.3-4308.8 mbsl; 286.6-296.1 mbsf

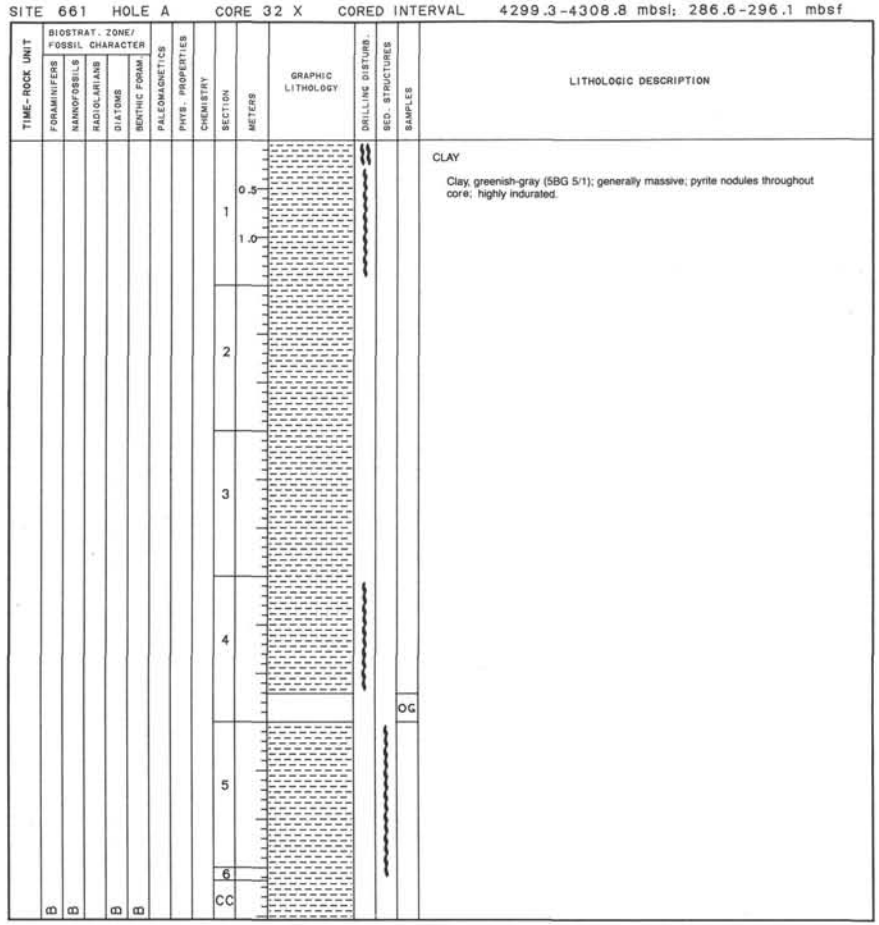

SITE 661 HOLE B CORE 1 H CORED INTERVAL 4013.1-4018.8 mbsl; 0-5.7 mbsf

TIME-ROCK UNIT: PLEISTOCENE TO HOLOCENE

BIOSTRAT. ZONE/FOSSIL CHARACTER: FORAMINIFERS: *G. truncatulinoides*; NANNOFOSSILS: NN20-21; RADIOLARIANS: —; DIATOMS: R/P

PALEOMAGNETICS: A/M; PHYS. PROPERTIES: A/G; CHEMISTRY: —

SECTION: 1, 2, 3, 4, CC; METERS: 0.5, 1.0

GRAPHIC LITHOLOGY; DRILLING DISTURB.; SED. STRUCTURES; SAMPLES

LITHOLOGIC DESCRIPTION

SILTY NANNOFOSSIL OOZE; CLAY-BEARING NANNOFOSSIL SILT; FORAMINIFER-BEARING, MUDDY NANNOFOSSIL OOZE

Silty nannofossil ooze, light yellowish-brown (10YR 6/4) in Section 1, 0-55 cm.

Clay-bearing nannofossil silt, dark gray (10YR 4/1), light olive-gray (5Y 6/2), dark gray (5Y 4/1) to very dark gray (5Y 3/1) in Section 1, 55 cm, through CC, alternating with foraminifer-bearing, muddy nannofossil ooze, olive-gray (5Y 5/2), light gray (10YR 7/2), or gray (10YR 6/1); moderately bioturbated with dark microlaminations at base of Sections 2 and 3.

SMEAR SLIDE SUMMARY (%):

	1, 40 D	2, 50 D	2, 100 D
TEXTURE:			
Sand	—	10	—
Silt	30	30	30
Clay	70	60	70
COMPOSITION:			
Quartz	25	10	20
Clay	—	10	20
Accessory Minerals	15	5	20
Foraminifers	Tr	15	—
Nannofossils	60	60	40

SITE 661 HOLE B CORE 2 H CORED INTERVAL 4018.8-4028.3 mbsl; 5.7-15.2 mbsf

TIME-ROCK UNIT: PLEISTOCENE

BIOSTRAT. ZONE/FOSSIL CHARACTER: FORAMINIFERS: *G. truncatulinoides*; NANNOFOSSILS: NN20; RADIOLARIANS: —; DIATOMS: B

PALEOMAGNETICS: A/M; PHYS. PROPERTIES: A/M; CHEMISTRY: NN19

SECTION: 1, 2, 3, 4, 5, 6, 7, CC; METERS: 0.5, 1.0

GRAPHIC LITHOLOGY; DRILLING DISTURB.; SED. STRUCTURES; SAMPLES

LITHOLOGIC DESCRIPTION

SILTY CLAY, FORAMINIFER-BEARING to FORAMINIFER NANNOFOSSIL OOZE

Silty clay, gray (5Y 6/1, 5/1), dark-gray (5Y 4/1), or very dark-gray (5Y 3/1), alternating with foraminifer-bearing to foraminifer-nannofossil ooze, light-gray (5Y 7/2, 7/1), light-olive-gray (5Y 6/2), or pale-olive-(5Y 6/3); moderate to strong bioturbation with dark microlaminations at top of Section 5.

SMEAR SLIDE SUMMARY (%):

	2, 80 D	5, 50 D
TEXTURE:		
Sand	5	15
Silt	30	35
Clay	65	50
COMPOSITION:		
Quartz	30	10
Rock Fragments	5	—
Clay	55	20
Accessory Minerals	5	5
Foraminifers	—	20
Nannofossils	5	40

SITE 661 HOLE B CORE 3 H CORED INTERVAL 4028.3-4037.8 mbsl; 15.2-24.7 mbsf

TIME-ROCK UNIT	BIOSTRAT. ZONE/ FOSSIL CHARACTER: FORAMINIFERS	NANNOFOSSILS	RADIOLARIANS	DIATOMS	PALEOMAGNETICS	PHYS. PROPERTIES	CHEMISTRY	SECTION	METERS	GRAPHIC LITHOLOGY	DRILLING DISTURB.	SED. STRUCTURES	SAMPLES
PLEISTOCENE / UPPER PLIOCENE	PL6 / *G. truncatulinoides*	NN19	A/G / A/M	B				1, 2, 3, 4, 5, 6, 7, CC	0.5, 1.0				

LITHOLOGIC DESCRIPTION

NANNOFOSSIL-BEARING CLAY; FORAMINIFER-BEARING to FORAMINIFER-NANNOFOSSIL OOZE

Nannofossil-bearing clay, gray (5Y 5/1) to olive-gray (5Y 5/2), alternating with foraminifer-bearing to foraminifer-nannofossil ooze, light-gray (5Y 7/1) to gray (5Y 6/1); moderate bioturbation in some intervals with dark microlaminations in Sections 2, 3, 5, and 6.

SITE 661 HOLE B CORE 4 H CORED INTERVAL 4037.8-4047.3 mbsl; 24.7-34.2 mbsf

TIME-ROCK UNIT	BIOSTRAT. ZONE/ FOSSIL CHARACTER: FORAMINIFERS	NANNOFOSSILS	RADIOLARIANS	DIATOMS	PALEOMAGNETICS	PHYS. PROPERTIES	CHEMISTRY	SECTION	METERS	GRAPHIC LITHOLOGY	DRILLING DISTURB.	SED. STRUCTURES	SAMPLES
UPPER PLIOCENE	PL6 / PL5	NN19 / NN18	R/P	C/P / A/M	B			1, 2, 3, 4, 5, 6, 7, CC	0.5, 1.0				* * *

LITHOLOGIC DESCRIPTION

NANNOFOSSIL-BEARING, SILT-BEARING CLAY; FORAMINIFER-BEARING to FORAMINIFER-NANNOFOSSIL OOZE

Nannofossil-bearing, silt-bearing clay, gray (5Y 5/1) to olive-gray (5Y 5/2), alternating with foraminifer-bearing to foraminifer-nannofossil ooze, light gray (5Y 7/1) to gray (5Y 6/1). Minor void in Section 1, 146–150 cm.

SMEAR SLIDE SUMMARY (%):

	3, 80 D	4, 80 D
TEXTURE:		
Sand	—	5
Silt	20	20
Clay	80	75
COMPOSITION:		
Quartz	15	5
Clay	65	20
Accessory Minerals	5	—
Foraminifers	—	20
Nannofossils	15	55

SITE 661 HOLE B CORE 5 H CORED INTERVAL 4047.3-4056.89 mbsl; 34.4-43.7 mbsf

TIME-ROCK UNIT: UPPER PLIOCENE

BIOSTRAT. ZONE/FOSSIL CHARACTER
- FORAMINIFERS: A/M, PL3, A/G, PL4, A/M, PL5
- NANNOFOSSILS: A/M, NN16, NN17
- RADIOLARIANS
- DIATOMS: B

PALEOMAGNETICS
PHYS. PROPERTIES
CHEMISTRY
SECTION: 1, 2, 3, 4, 5, 6, 7, CC
METERS: 0.5, 1.0
GRAPHIC LITHOLOGY
DRILLING DISTURB.
SED. STRUCTURES
SAMPLES: *

LITHOLOGIC DESCRIPTION

FORAMINIFER-BEARING to FORAMINIFER-NANNOFOSSIL OOZE; MUDDY NANNOFOSSIL OOZE

Foraminifer-bearing to foraminifer-nannofossil ooze, light-gray (5Y 7/1), alternating with muddy nannofossil ooze, light-olive-gray (5Y 6/2); moderate bioturbation.

SMEAR SLIDE SUMMARY (%):

	6, 10 D
TEXTURE:	
Sand	I
Silt	25
Clay	75
COMPOSITION:	
Quartz	15
Clay	25
Accessory Minerals	10
Nannofossils	50

SITE 661 HOLE B CORE 6 H CORED INTERVAL 4056.8-4066.3 mbsl; 43.7-53.2 mbsf

TIME-ROCK UNIT: UPPER PLIOCENE

BIOSTRAT. ZONE/FOSSIL CHARACTER
- FORAMINIFERS: A/M, PL3, A/G
- NANNOFOSSILS: A/M, NN16
- RADIOLARIANS
- DIATOMS: B

PALEOMAGNETICS
PHYS. PROPERTIES
CHEMISTRY
SECTION: 1, 2, 3, 4, 5, 6, CC
METERS: 0.5, 1.0
GRAPHIC LITHOLOGY: VOID
DRILLING DISTURB.
SED. STRUCTURES
SAMPLES

LITHOLOGIC DESCRIPTION

FORAMINIFER-BEARING NANNOFOSSIL OOZE; NANNOFOSSIL-BEARING, SILTY CLAY

Foraminifer-bearing nannofossil ooze, light-gray (5Y 7/1), alternating with nannofossil-bearing silty clay, light-olive-gray (5Y 6/2); moderate bioturbation.

SITE 661 HOLE B CORE 7 H CORED INTERVAL 4066.3-4075.8 mbsl; 53.2-62.7 mbsf

TIME-ROCK UNIT	BIOSTRAT. ZONE/ FOSSIL CHARACTER: FORAMINIFERS	NANNOFOSSILS	RADIOLARIANS	DIATOMS	PALEOMAGNETICS	PHYS. PROPERTIES	CHEMISTRY	SECTION	METERS	GRAPHIC LITHOLOGY	DRILLING DISTURB.	SED. STRUCTURES	SAMPLES	LITHOLOGIC DESCRIPTION
UPPER PLIOCENE / LOWER PLIOCENE	A/M PL1 / A/M NN13	PL3 / NN15 / NN16	B					1, 2, 3, 4, 5, 6, 7, CC	0.5, 1.0					FORAMINIFER-BEARING NANNOFOSSIL OOZE; NANNOFOSSIL-BEARING, SILTY CLAY Foraminifer-bearing nannofossil ooze, light gray (5Y 7/1), alternating with nannofossil-bearing, silty clay, light olive-gray (5Y 6/2); moderate bioturbation.

SITE 661 HOLE B CORE 8 H CORED INTERVAL 4075.8-4085.3 mbsl; 62.7-72.2 mbsf

TIME-ROCK UNIT	BIOSTRAT. ZONE/ FOSSIL CHARACTER: FORAMINIFERS	NANNOFOSSILS	RADIOLARIANS	DIATOMS	PALEOMAGNETICS	PHYS. PROPERTIES	CHEMISTRY	SECTION	METERS	GRAPHIC LITHOLOGY	DRILLING DISTURB.	SED. STRUCTURES	SAMPLES	LITHOLOGIC DESCRIPTION
LOWER PLIOCENE / UPPER MIOCENE	B A/M NN11	NN12	B					1, 2, 3, 4, 5, 6, 7, CC	0.5, 1.0					FORAMINIFER-BEARING to FORAMINIFER-NANNOFOSSIL OOZE; CLAY-BEARING NANNOFOSSIL OOZE Foraminifer-bearing to foraminifer-nannnofossil ooze, pale-yellow (5Y 7/3) to light gray (5Y 7/2) alternating with clay-bearing nannofossil ooze, yellowish-brown (10YR 5/4) to olive-yellow (5Y 6/4); moderate bioturbation; drilling breccia in Section 1, 0–40 cm.

SITE 661 HOLE B CORE 9 H CORED INTERVAL 4085.3-4094.8 mbsl; 72.2- mbsf

TIME-ROCK UNIT	BIOSTRAT. ZONE/ FOSSIL CHARACTER: FORAMINIFERS	NANNOFOSSILS	RADIOLARIANS	DIATOMS	PALEOMAGNETICS	PHYS. PROPERTIES	CHEMISTRY	SECTION	METERS	GRAPHIC LITHOLOGY	DRILLING DISTURB.	SED. STRUCTURES	SAMPLES	LITHOLOGIC DESCRIPTION
UPPER MIOCENE	R/P	NN11		B				1	0.5 1.0					FORAMINIFER-BEARING to FORAMINIFER-NANNOFOSSIL OOZE; CLAY-BEARING NANNOFOSSIL OOZE Foraminifer-bearing to foraminifer-nannofossil ooze, pale-yellow (5Y 7/3) to light gray (5Y 7/2), alternating with clay-bearing nannofossil ooze, yellowish-brown (10YR 5/4) to olive-yellow (5Y 6/4); moderate bioturbation; drilling breccia in Section 1, 0–90 cm.
	F/P	NN10						2						
								3						
								4						
								5						
								6						
								CC						

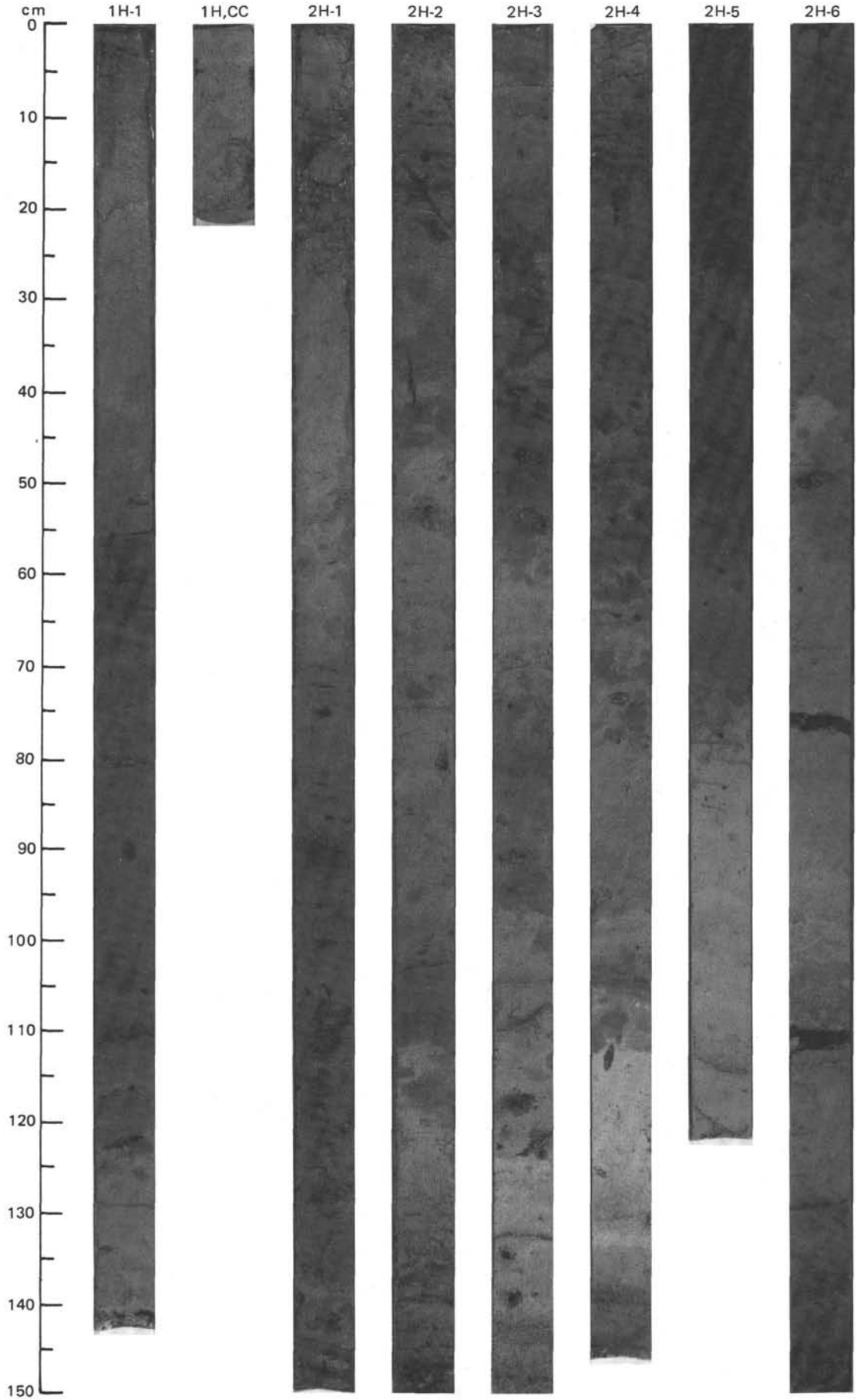
cm
1H-1
1H,CC
2H-1
2H-2
2H-3
2H-4
2H-5
2H-6
0
10
20
30
40
50
60
70
80
90
100
110
120
130
140
150

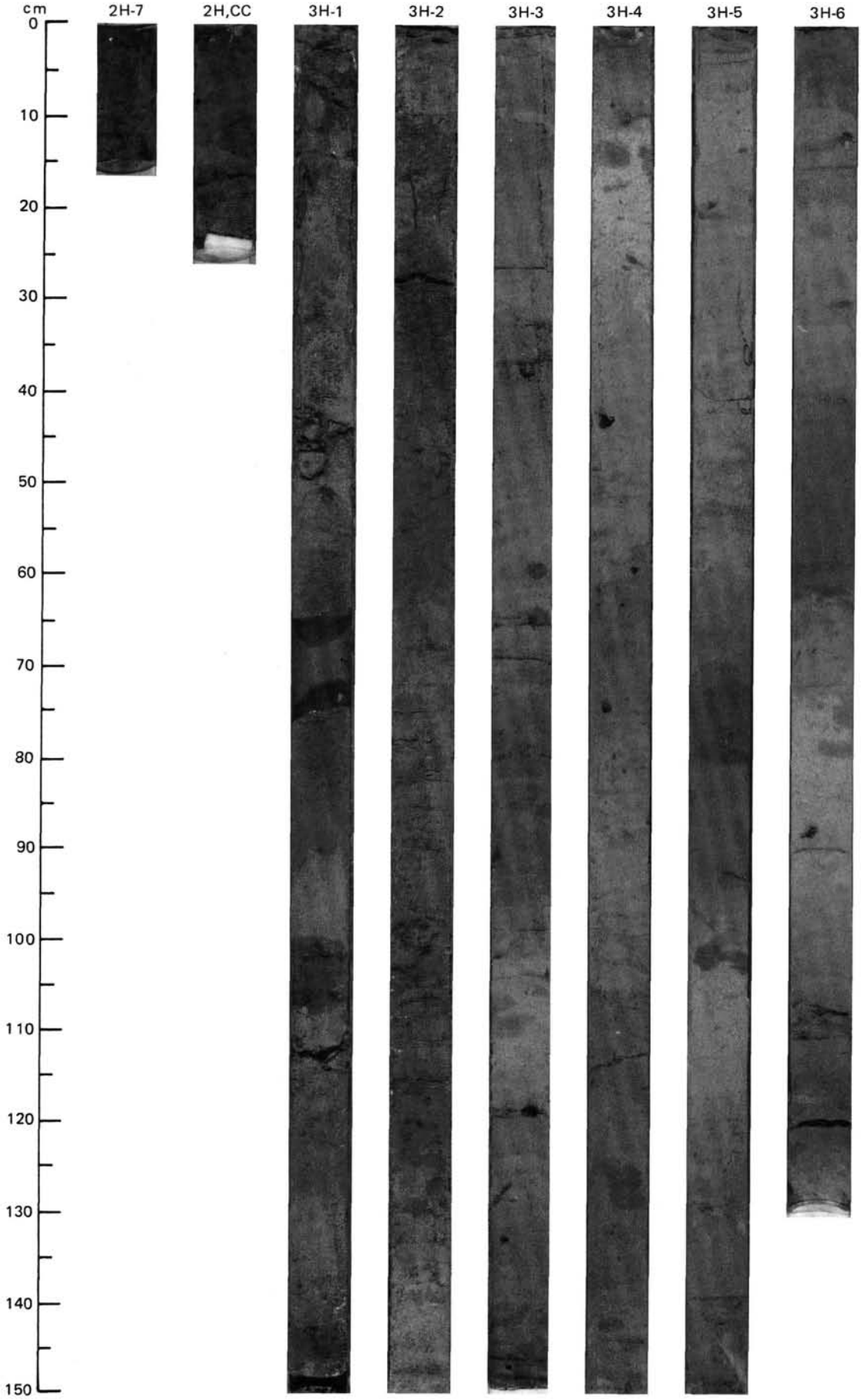
cm
2H-7
2H,CC
3H-1
3H-2
3H-3
3H-4
3H-5
3H-6
0
10
20
30
40
50
60
70
80
90
100
110
120
130
140
150

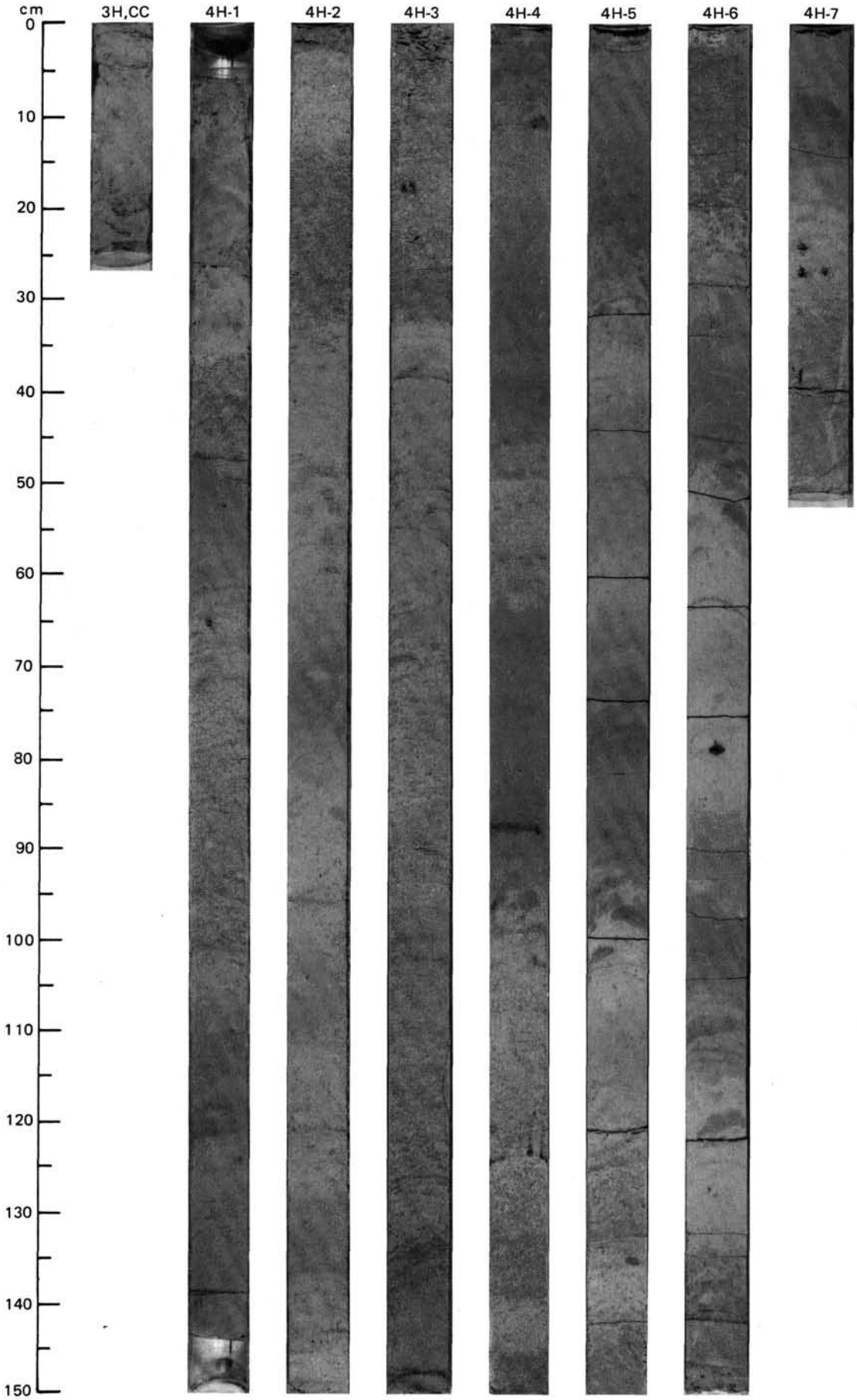
cm
0
10
20
30
40
50
60
70
80
90
100
110
120
130
140
150
3H,CC
4H-1
4H-2
4H-3
4H-4
4H-5
4H-6
4H-7

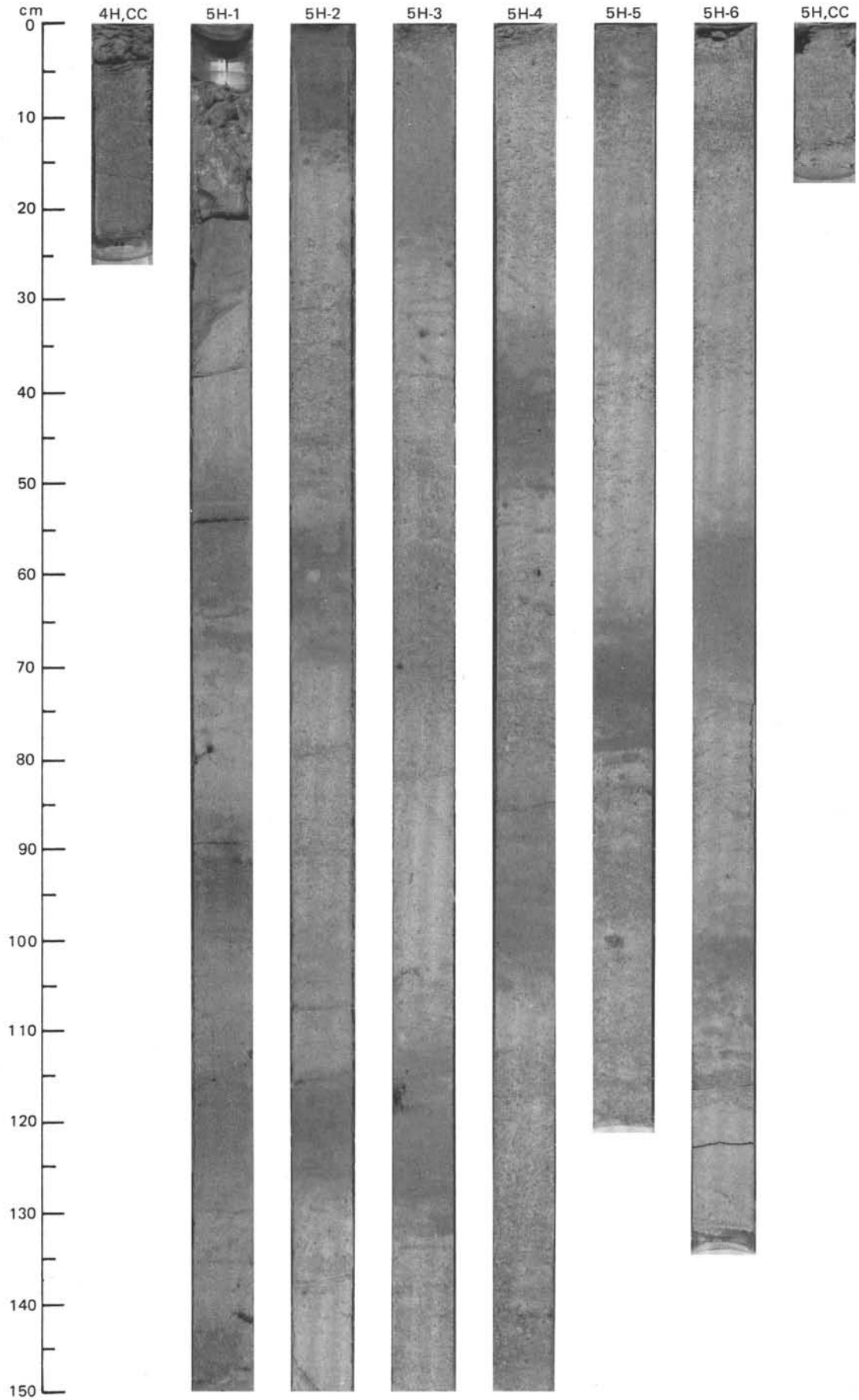
cm
0
10
20
30
40
50
60
70
80
90
100
110
120
130
140
150
4H,CC
5H-1
5H-2
5H-3
5H-4
5H-5
5H-6
5H,CC

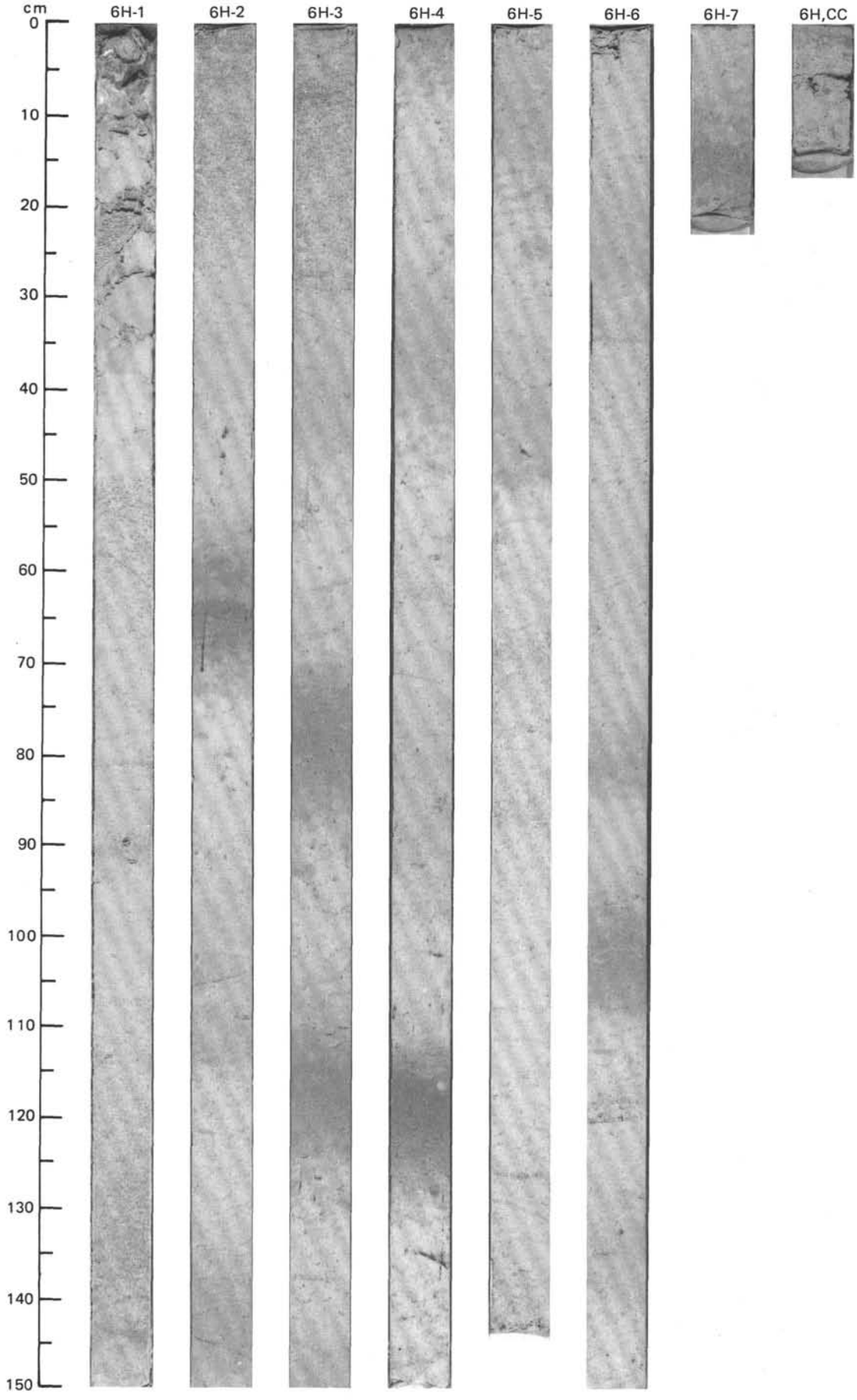
cm
0
10
20
30
40
50
60
70
80
90
100
110
120
130
140
150
6H-1
6H-2
6H-3
6H-4
6H-5
6H-6
6H-7
6H,CC

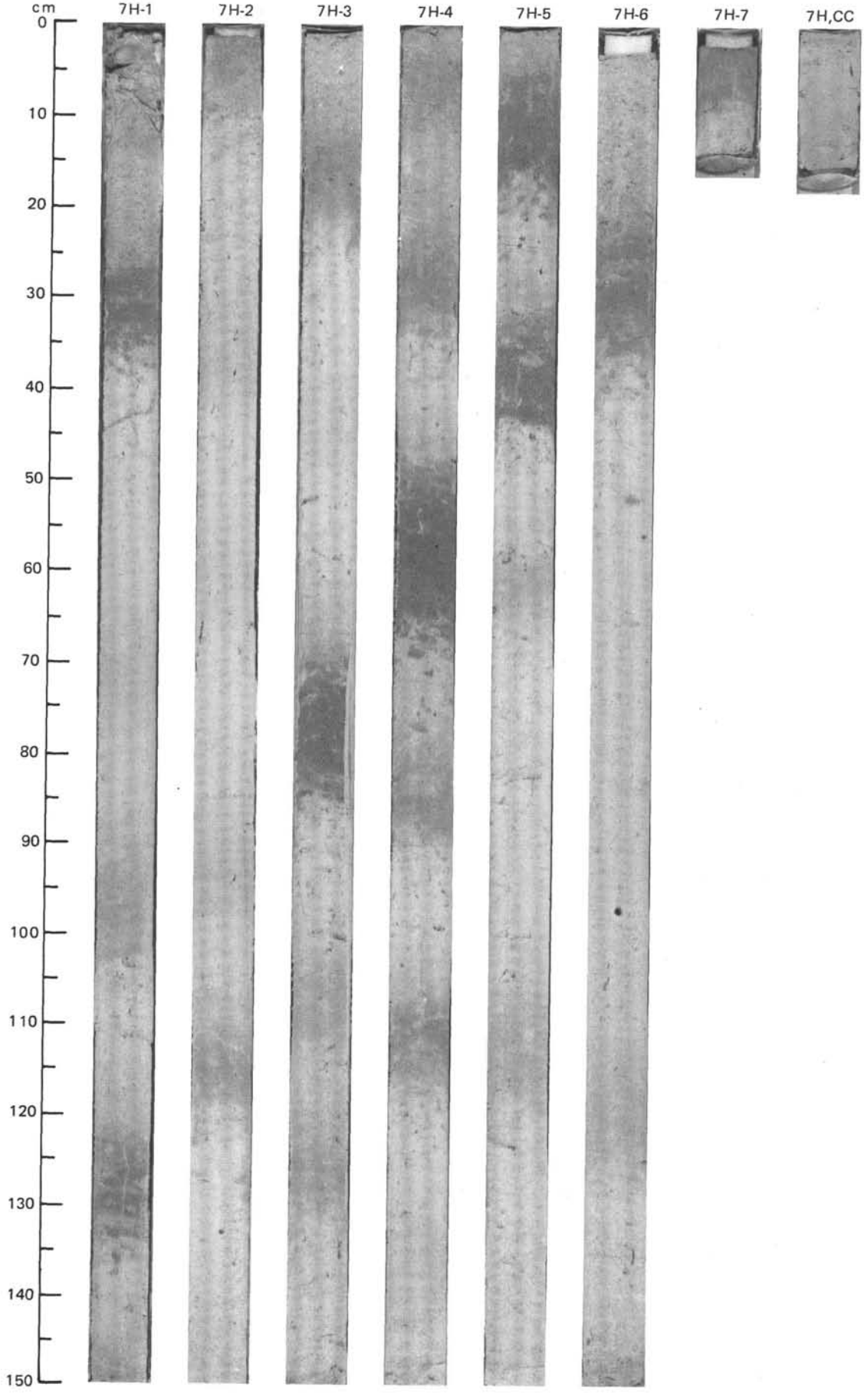
cm
0
10
20
30
40
50
60
70
80
90
100
110
120
130
140
150
7H-1
7H-2
7H-3
7H-4
7H-5
7H-6
7H-7
7H,CC

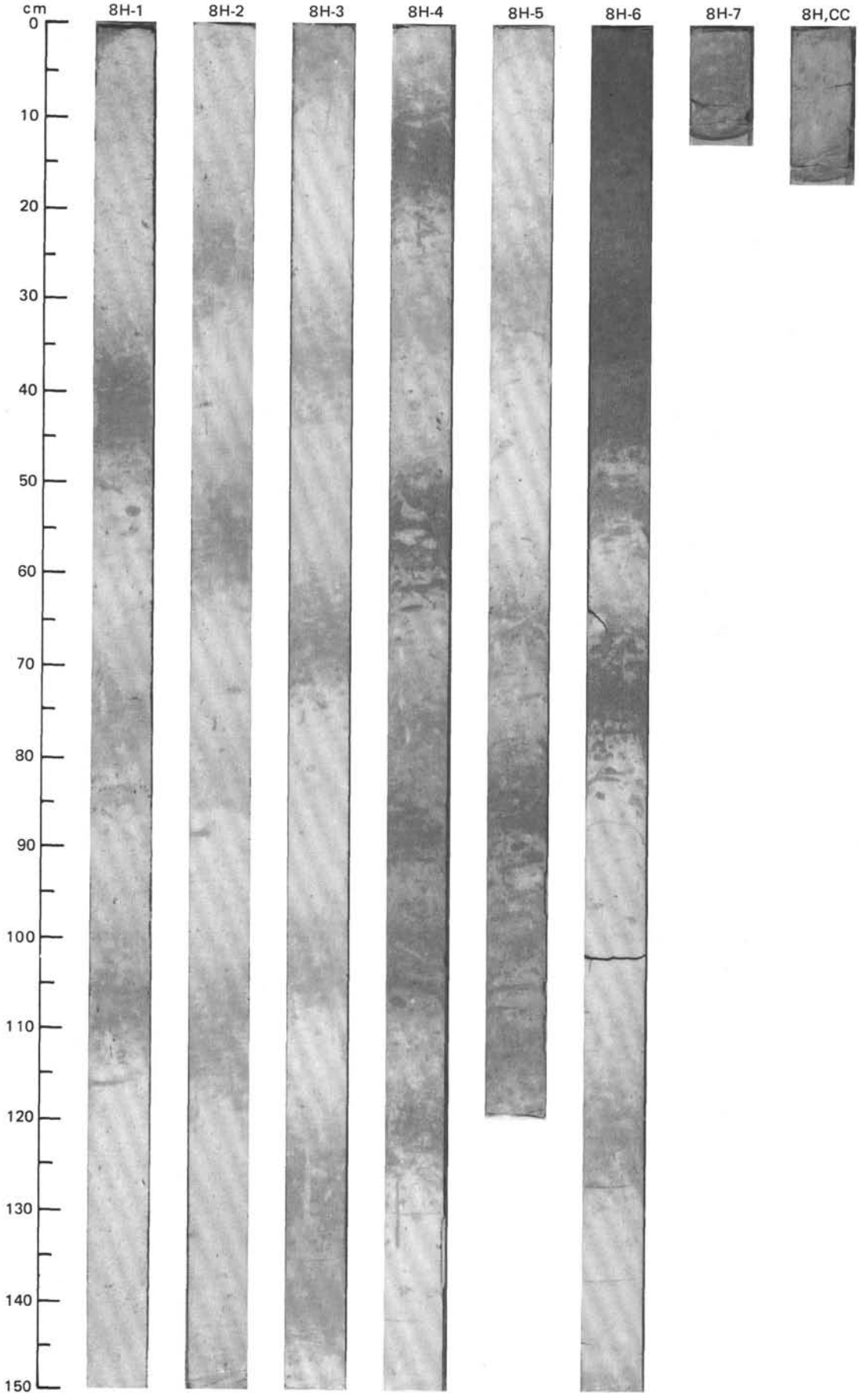
cm
0
10
20
30
40
50
60
70
80
90
100
110
120
130
140
150
8H-1
8H-2
8H-3
8H-4
8H-5
8H-6
8H-7
8H,CC

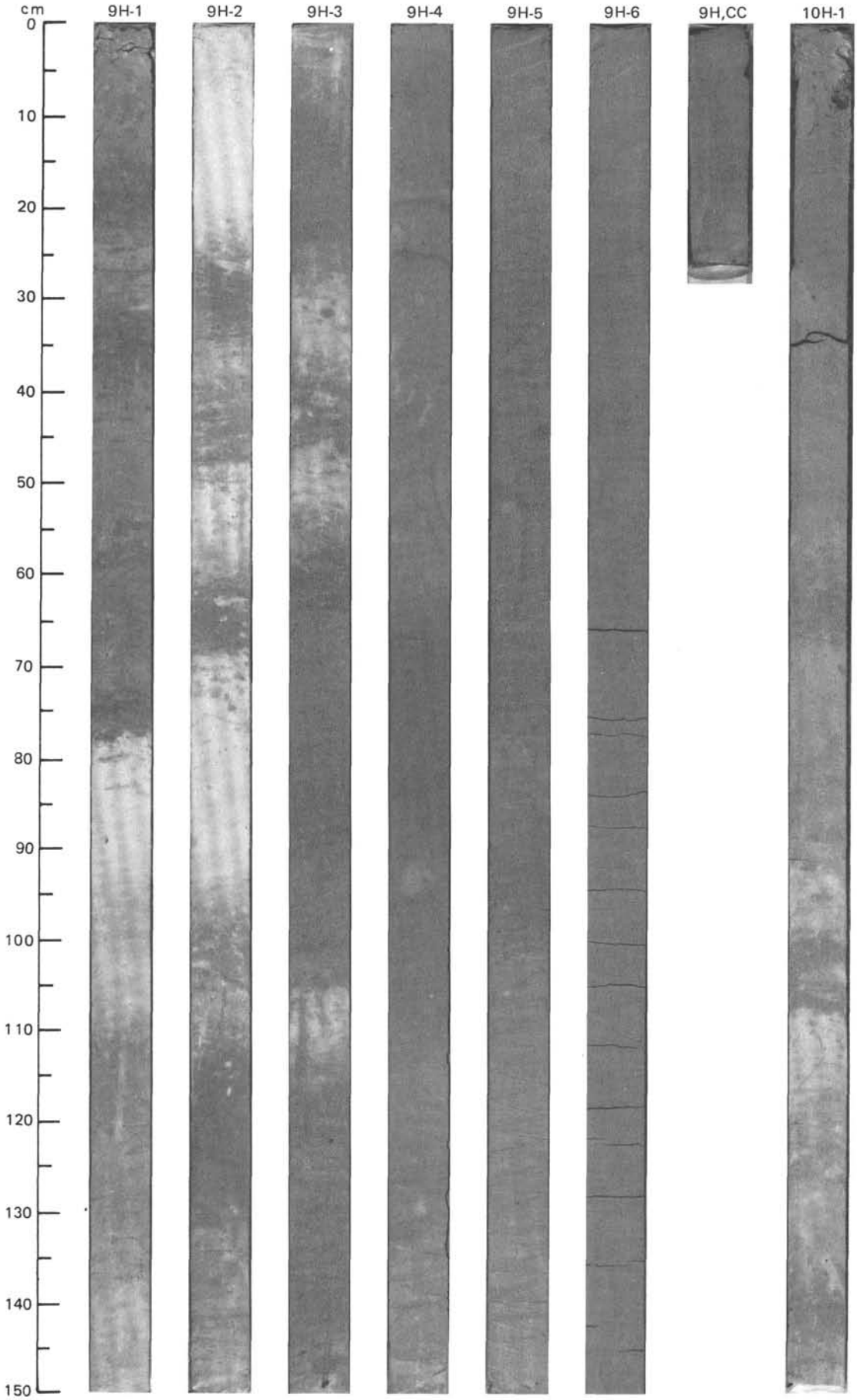
cm
9H-1
9H-2
9H-3
9H-4
9H-5
9H-6
9H,CC
10H-1
0
10
20
30
40
50
60
70
80
90
100
110
120
130
140
150

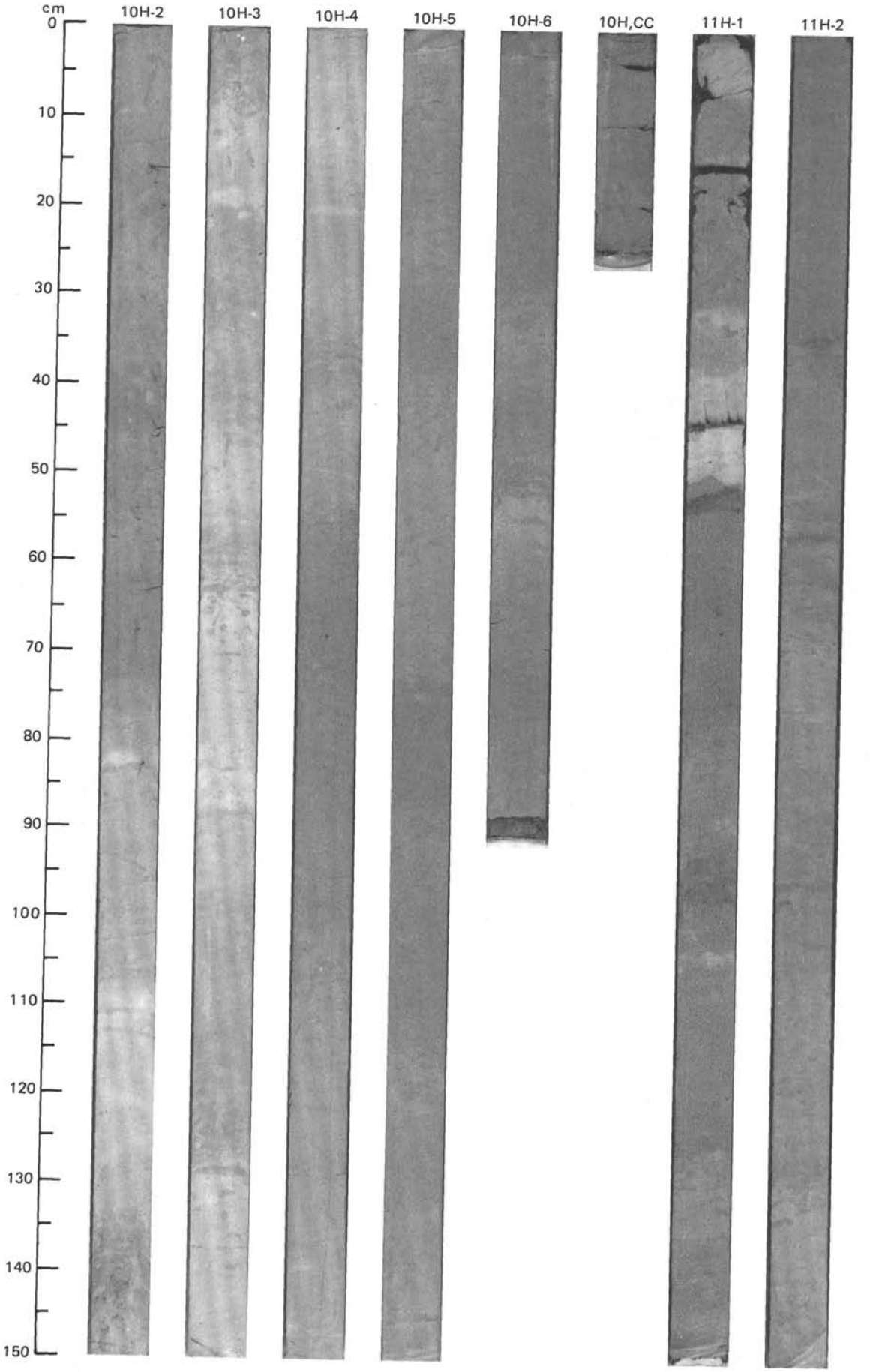
cm
0
10
20
30
40
50
60
70
80
90
100
110
120
130
140
150
10H-2
10H-3
10H-4
10H-5
10H-6
10H,CC
11H-1
11H-2

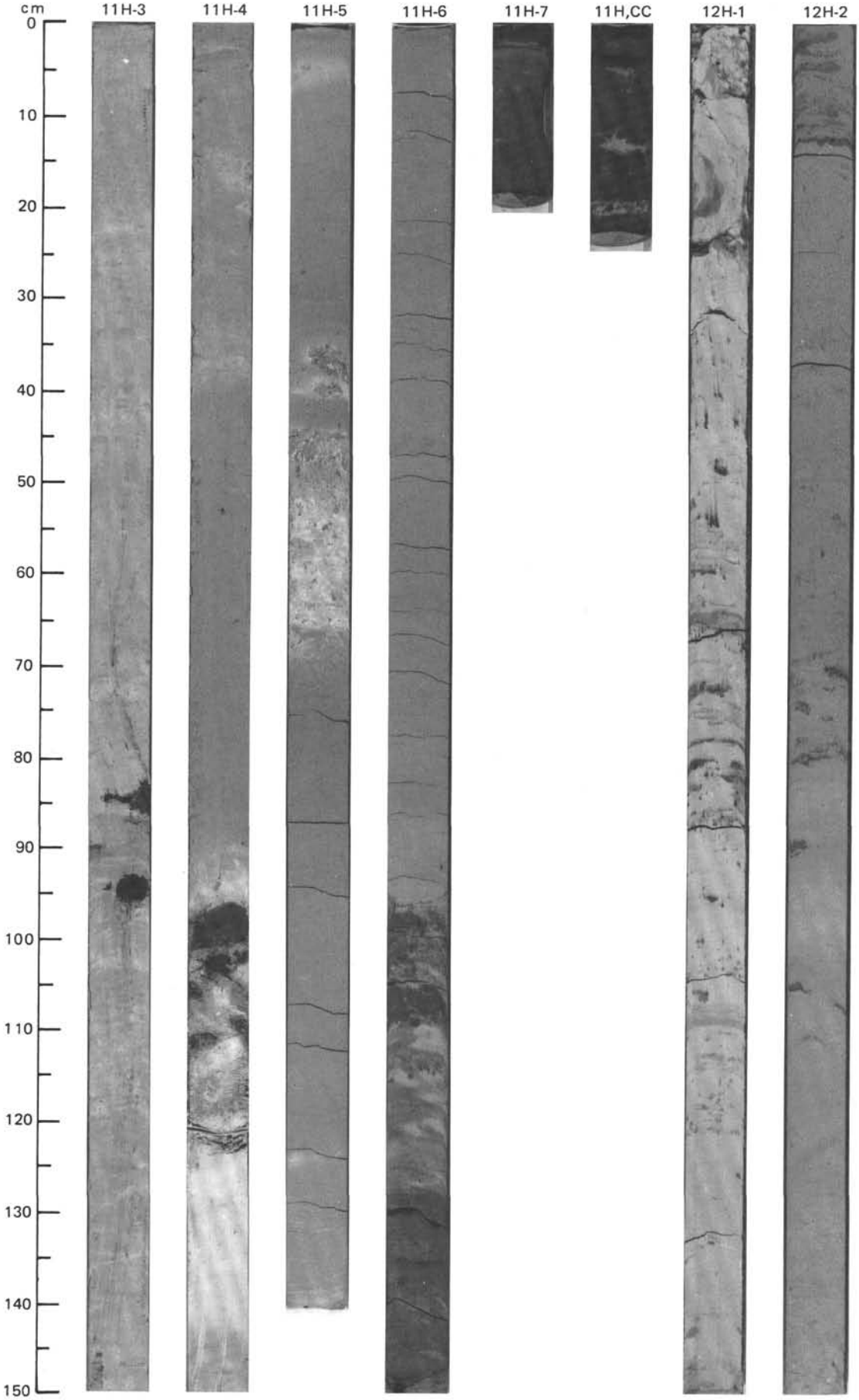
cm
11H-3
11H-4
11H-5
11H-6
11H-7
11H,CC
12H-1
12H-2
0
10
20
30
40
50
60
70
80
90
100
110
120
130
140
150

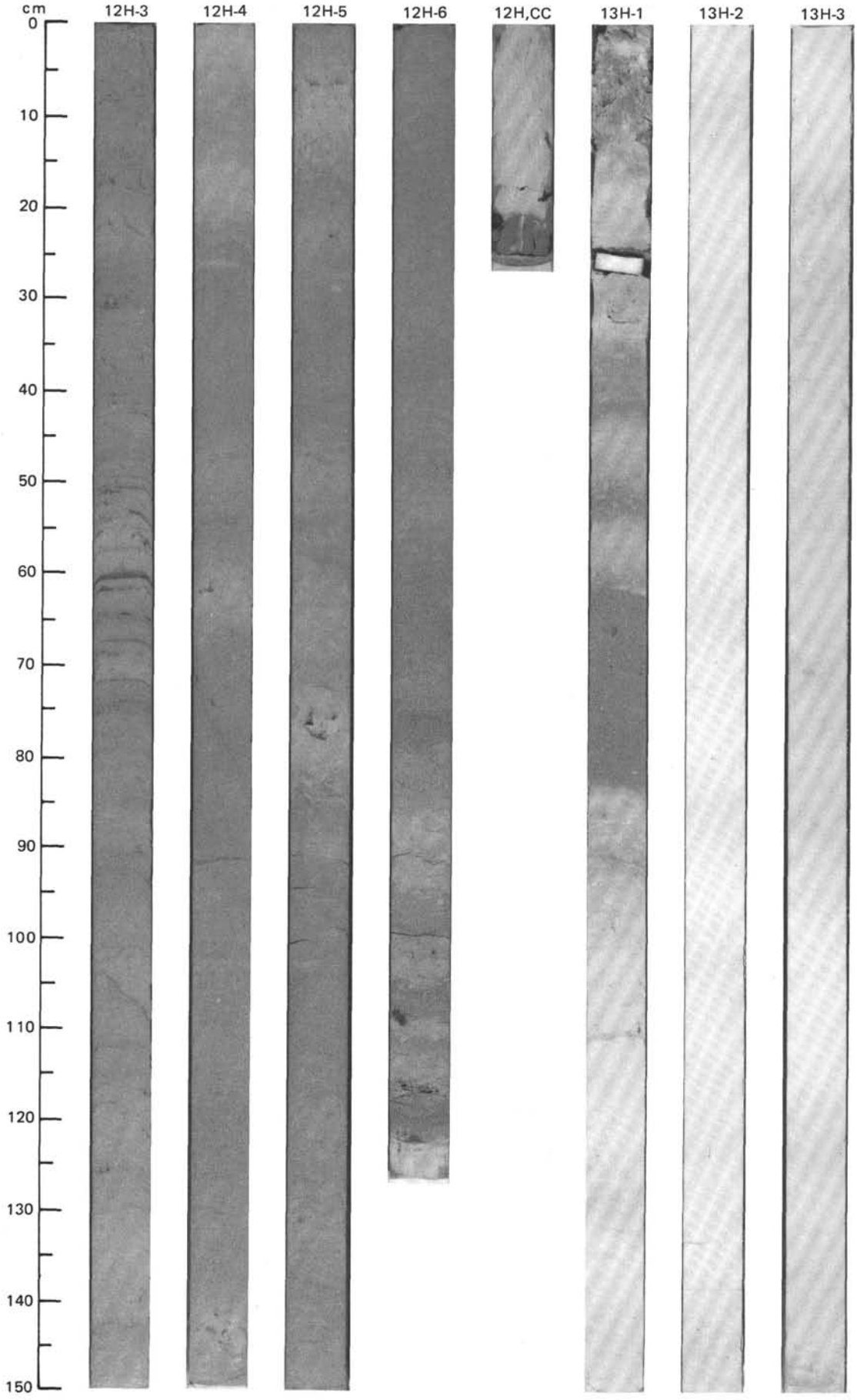
cm
0
10
20
30
40
50
60
70
80
90
100
110
120
130
140
150
12H-3
12H-4
12H-5
12H-6
12H,CC
13H-1
13H-2
13H-3

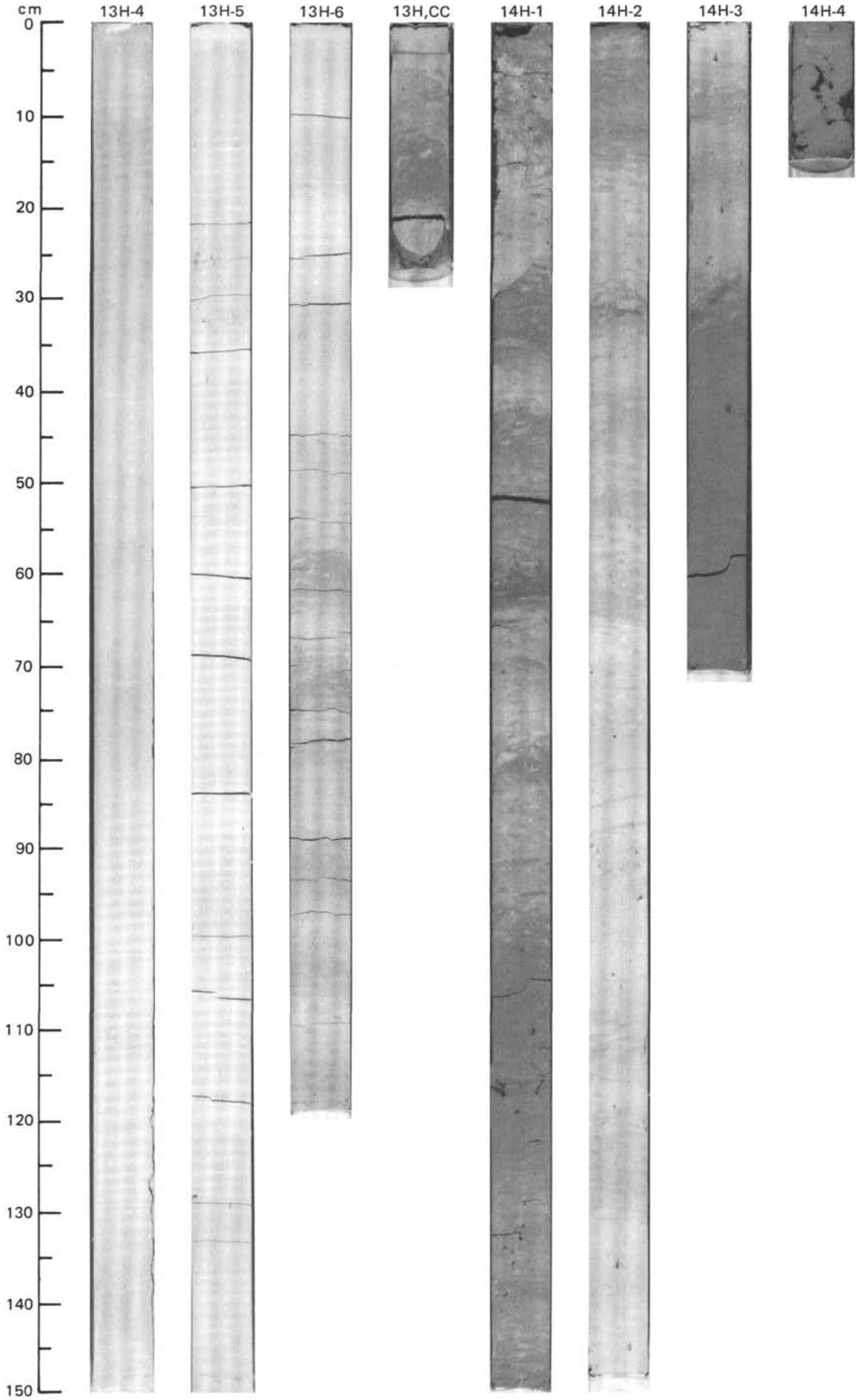
cm
13H-4
13H-5
13H-6
13H,CC
14H-1
14H-2
14H-3
14H-4
0
10
20
30
40
50
60
70
80
90
100
110
120
130
140
150

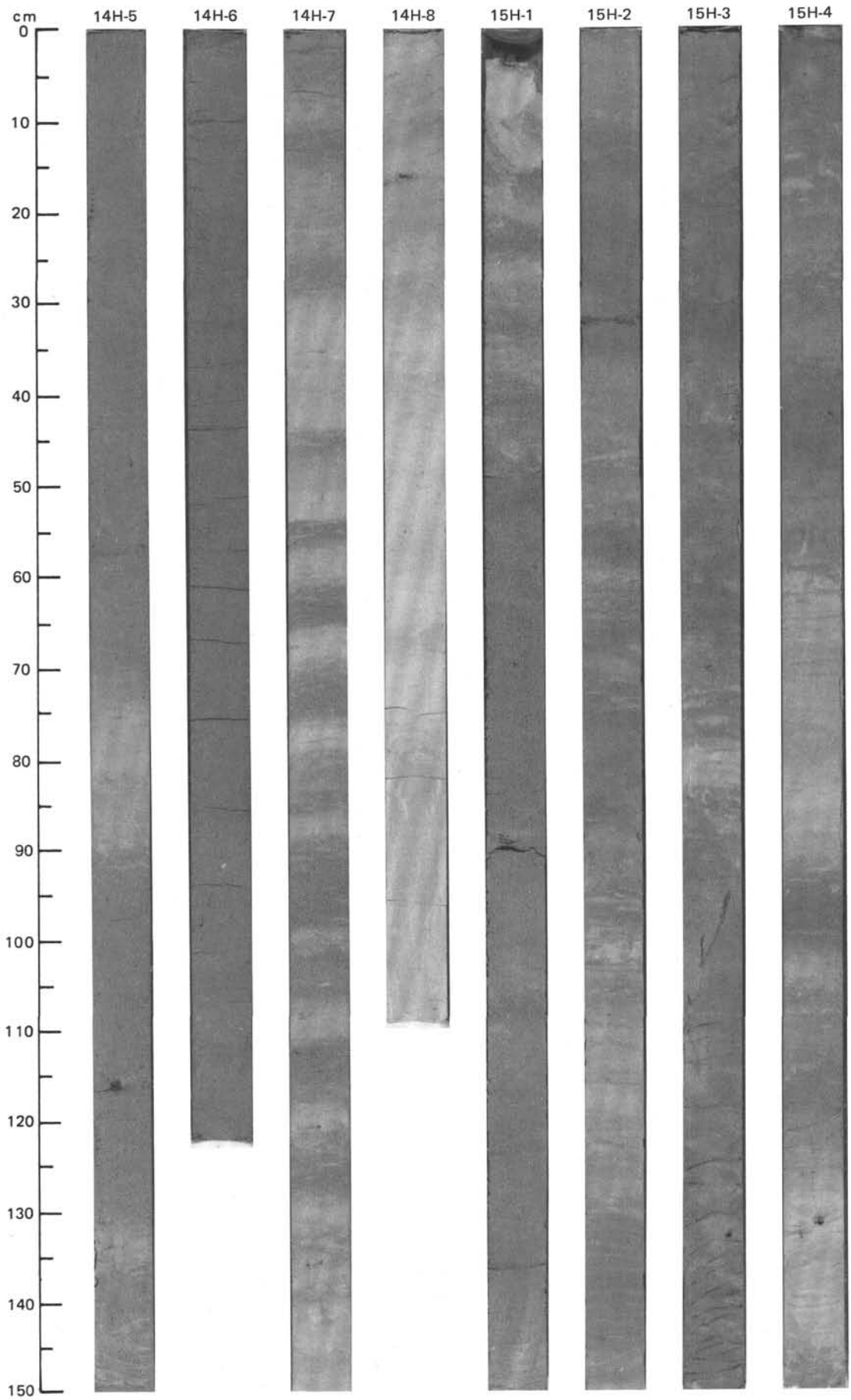
cm
14H-5
14H-6
14H-7
14H-8
15H-1
15H-2
15H-3
15H-4
0
10
20
30
40
50
60
70
80
90
100
110
120
130
140
150

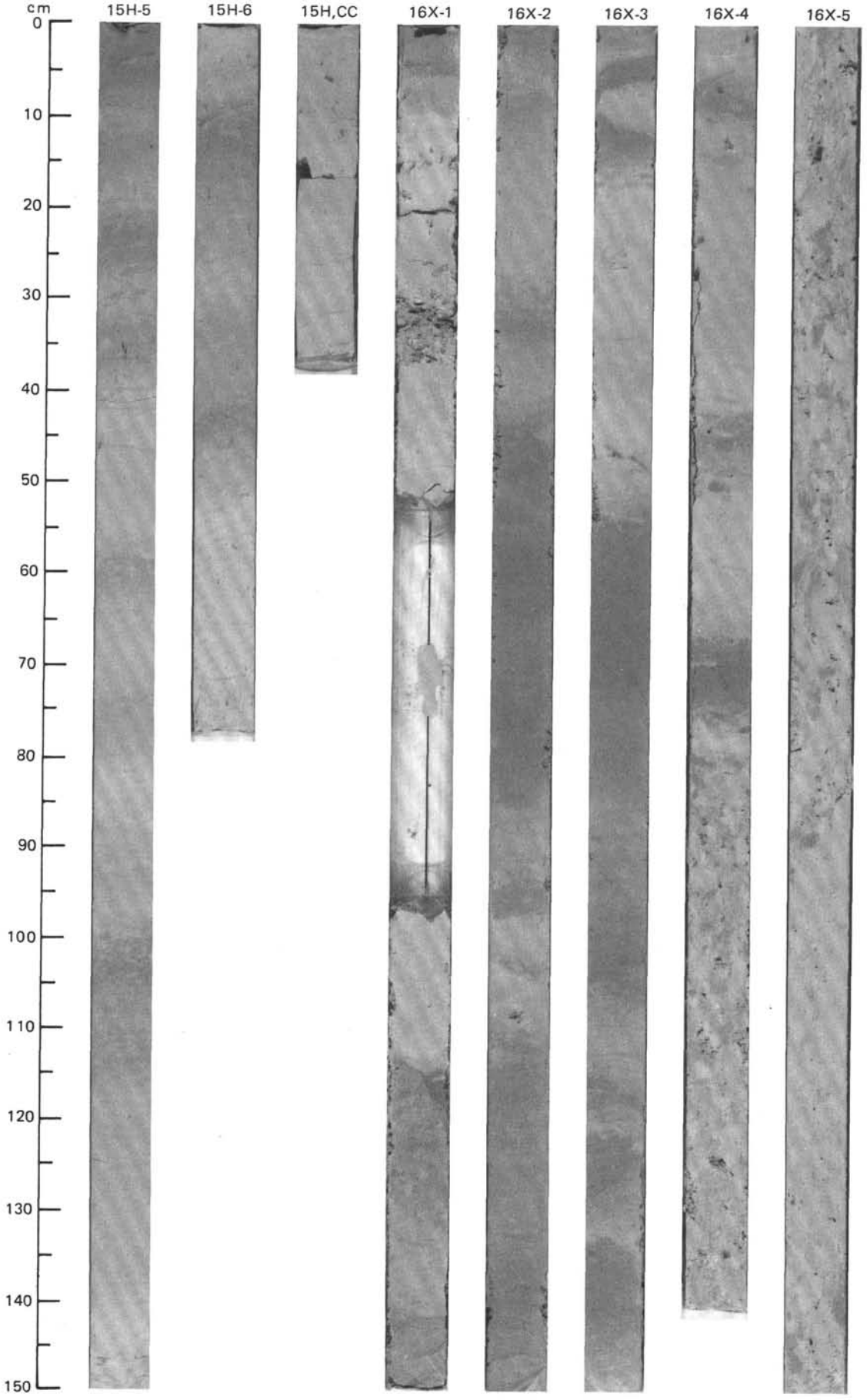
cm
0
10
20
30
40
50
60
70
80
90
100
110
120
130
140
150
15H-5
15H-6
15H,CC
16X-1
16X-2
16X-3
16X-4
16X-5

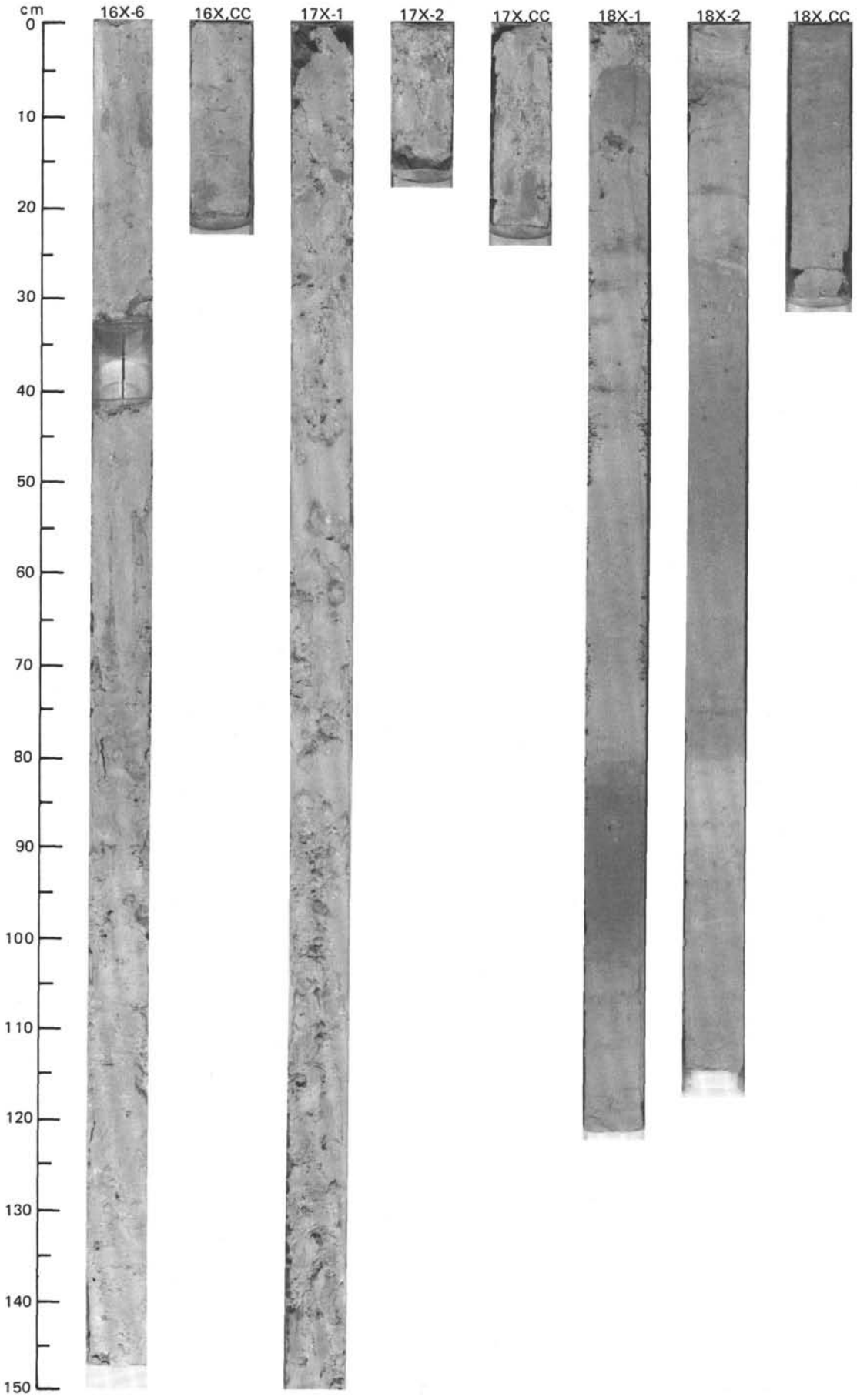
cm
0
10
20
30
40
50
60
70
80
90
100
110
120
130
140
150
16X-6
16X,CC
17X-1
17X-2
17X,CC
18X-1
18X-2
18X,CC

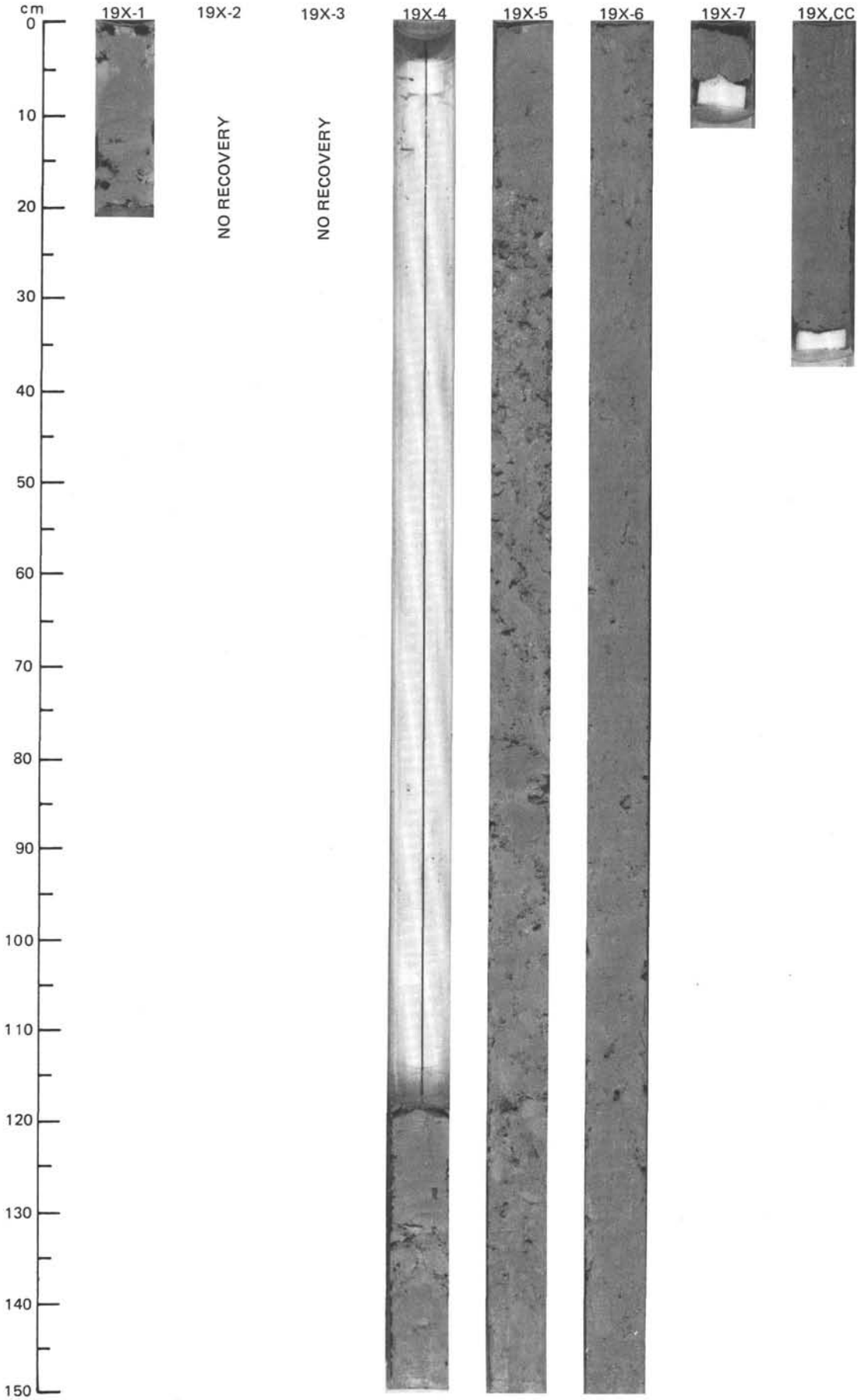
cm
0
10
20
30
40
50
60
70
80
90
100
110
120
130
140
150
19X-1
19X-2
NO RECOVERY
19X-3
NO RECOVERY
19X-4
19X-5
19X-6
19X-7
19X,CC

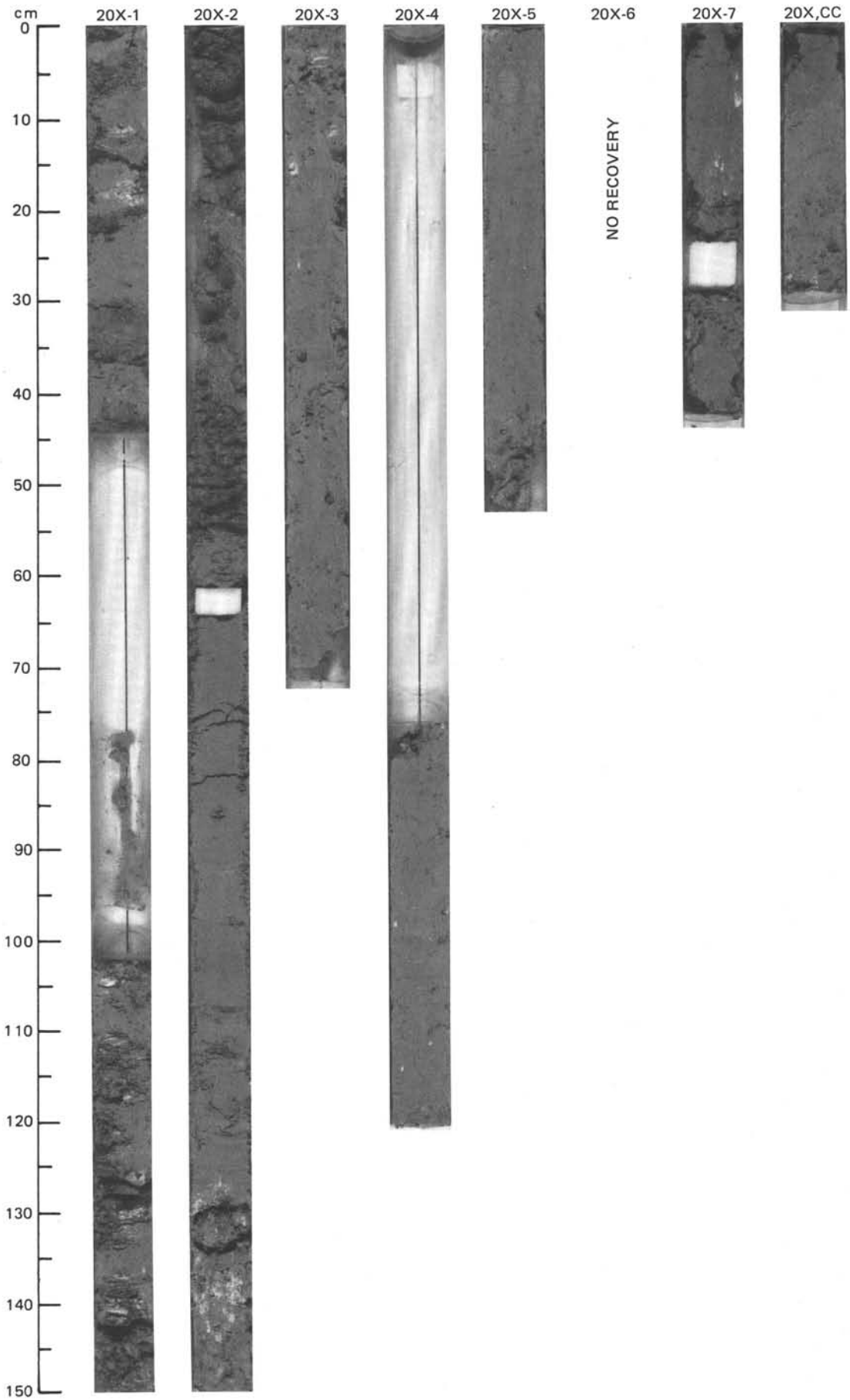
cm
0
10
20
30
40
50
60
70
80
90
100
110
120
130
140
150
20X-1
20X-2
20X-3
20X-4
20X-5
20X-6
NO RECOVERY
20X-7
20X,CC

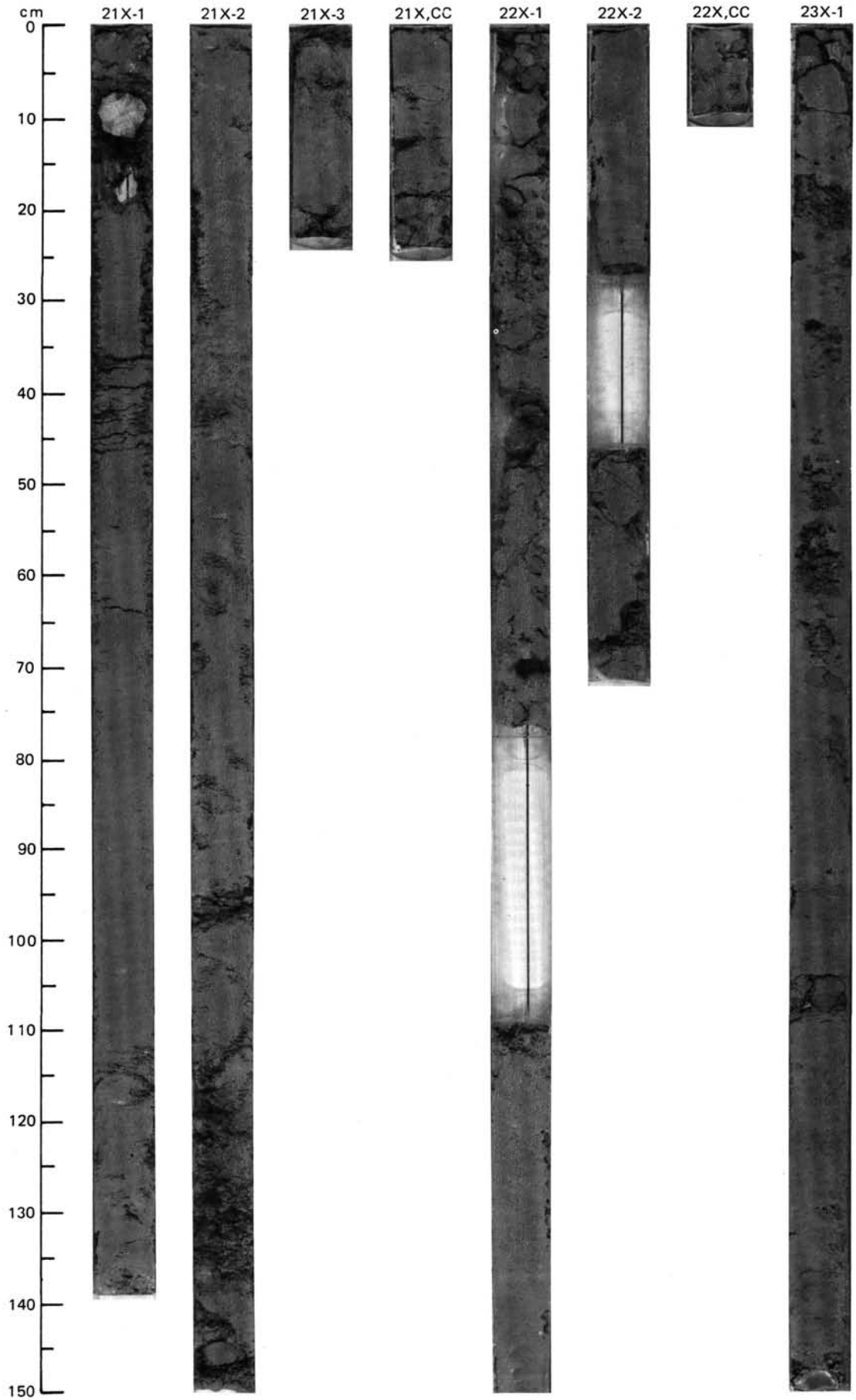
cm
21X-1
21X-2
21X-3
21X,CC
22X-1
22X-2
22X,CC
23X-1
0
10
20
30
40
50
60
70
80
90
100
110
120
130
140
150

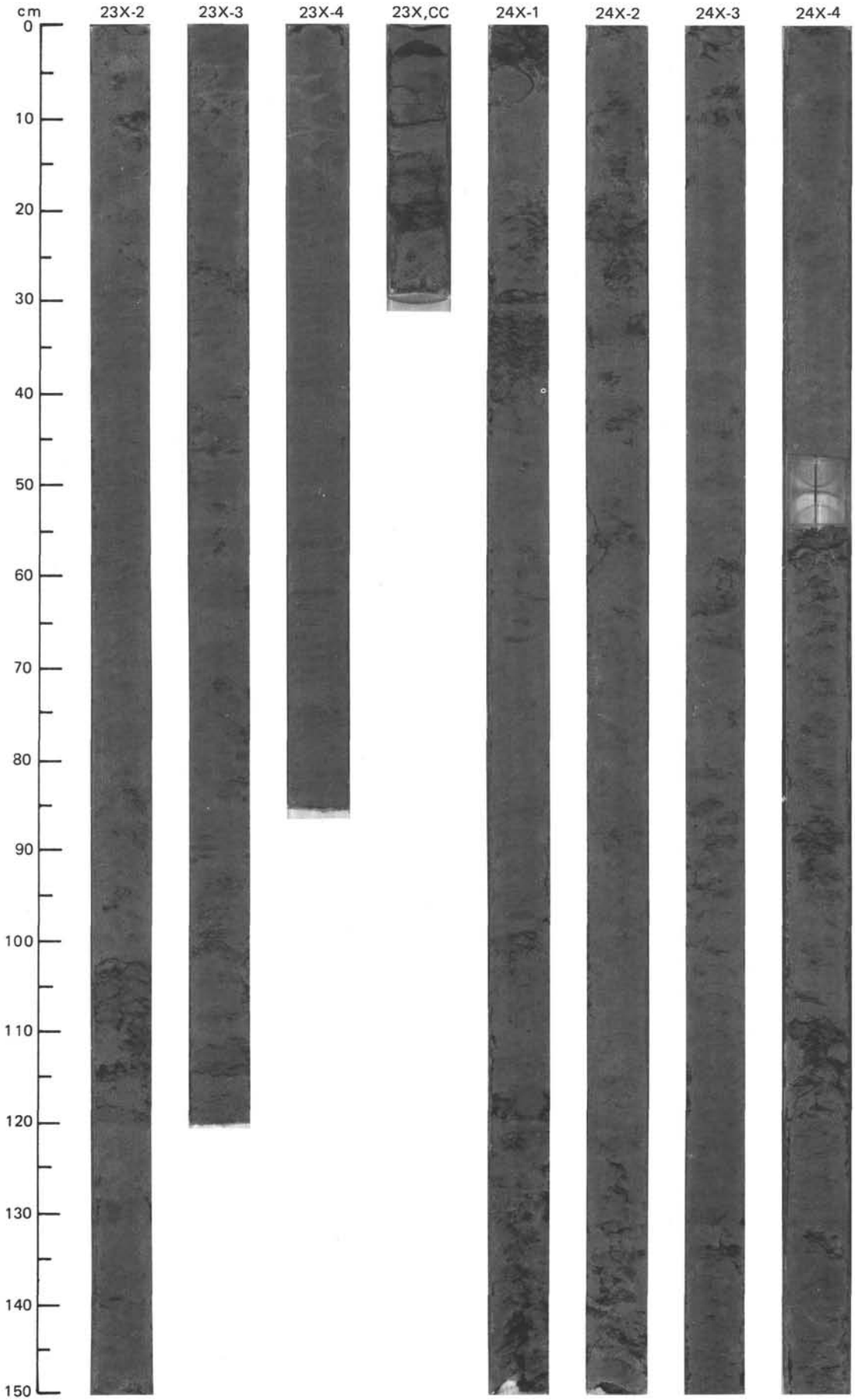
cm
23X-2
23X-3
23X-4
23X,CC
24X-1
24X-2
24X-3
24X-4
0
10
20
30
40
50
60
70
80
90
100
110
120
130
140
150

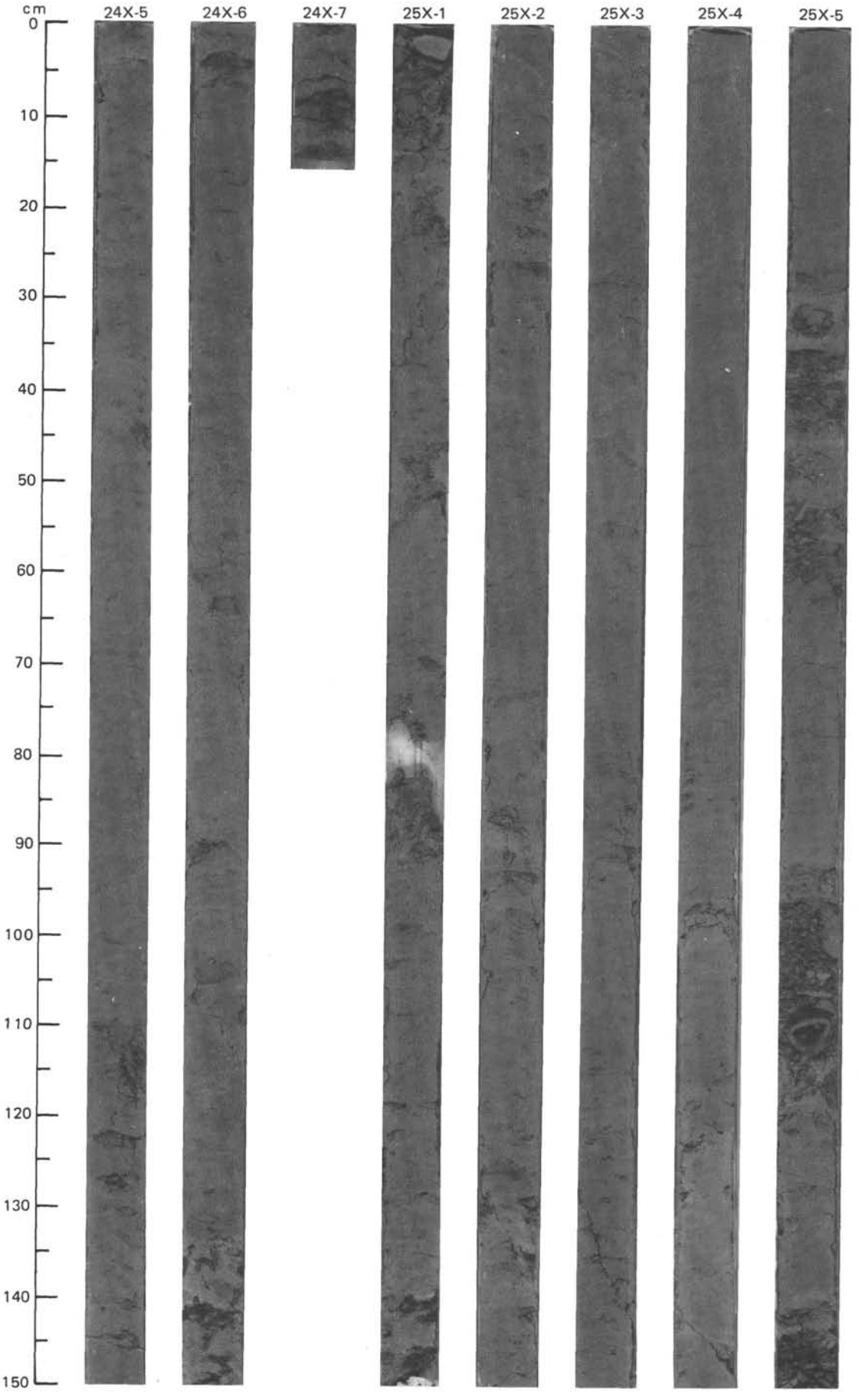
cm
0
10
20
30
40
50
60
70
80
90
100
110
120
130
140
150
24X-5
24X-6
24X-7
25X-1
25X-2
25X-3
25X-4
25X-5

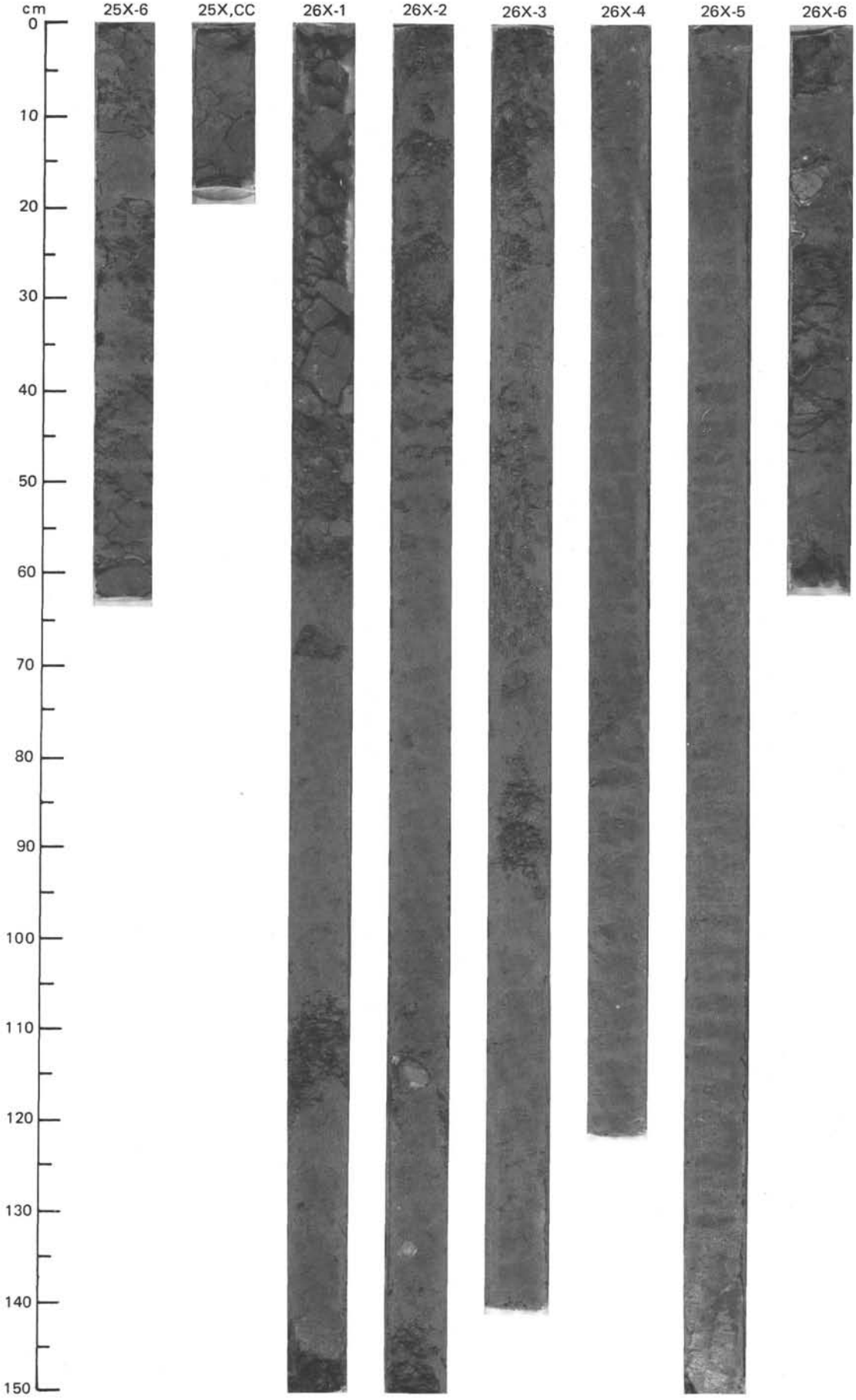
cm
25X-6
25X,CC
26X-1
26X-2
26X-3
26X-4
26X-5
26X-6
0
10
20
30
40
50
60
70
80
90
100
110
120
130
140
150

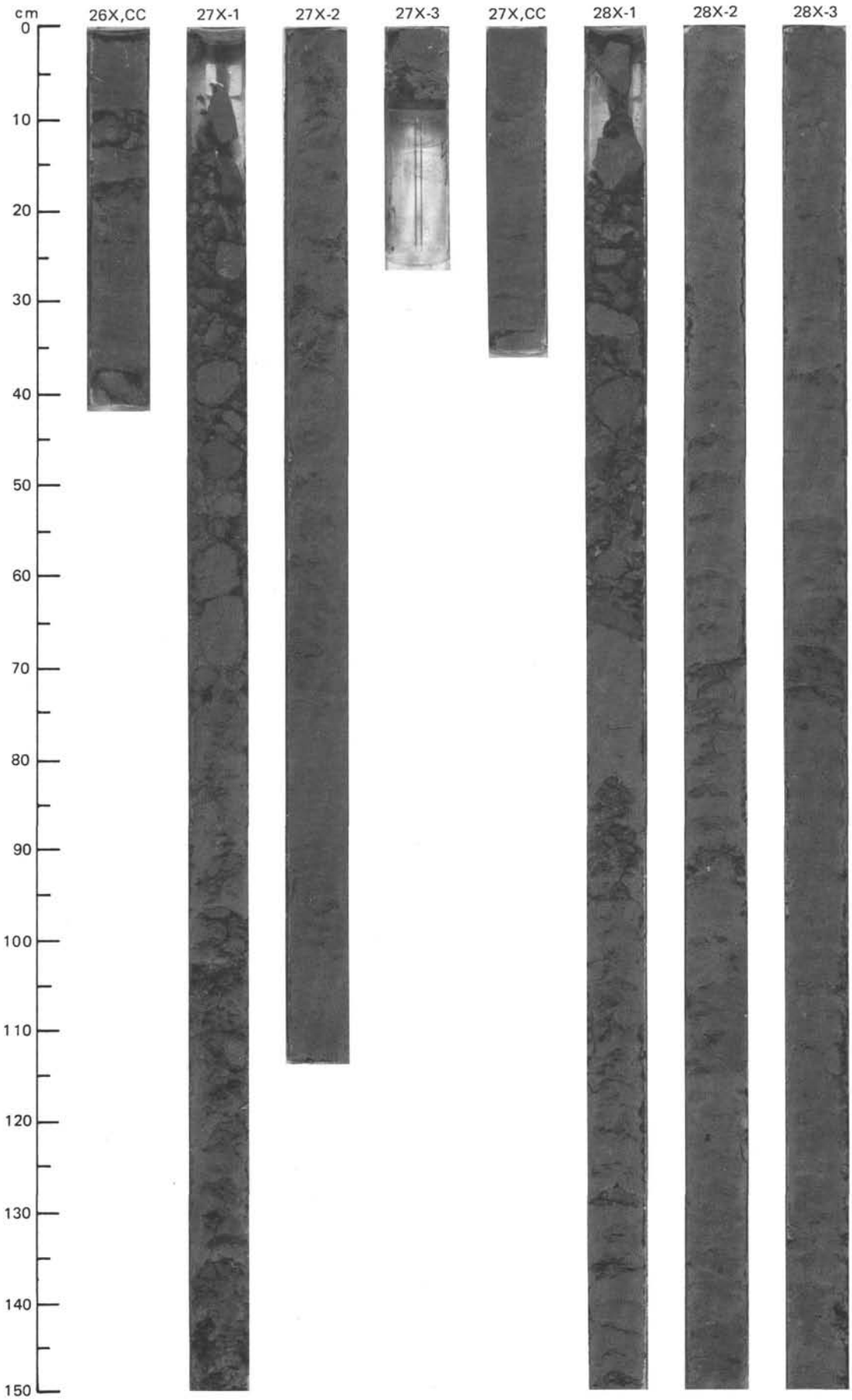
cm
0
10
20
30
40
50
60
70
80
90
100
110
120
130
140
150
26X,CC
27X-1
27X-2
27X-3
27X,CC
28X-1
28X-2
28X-3

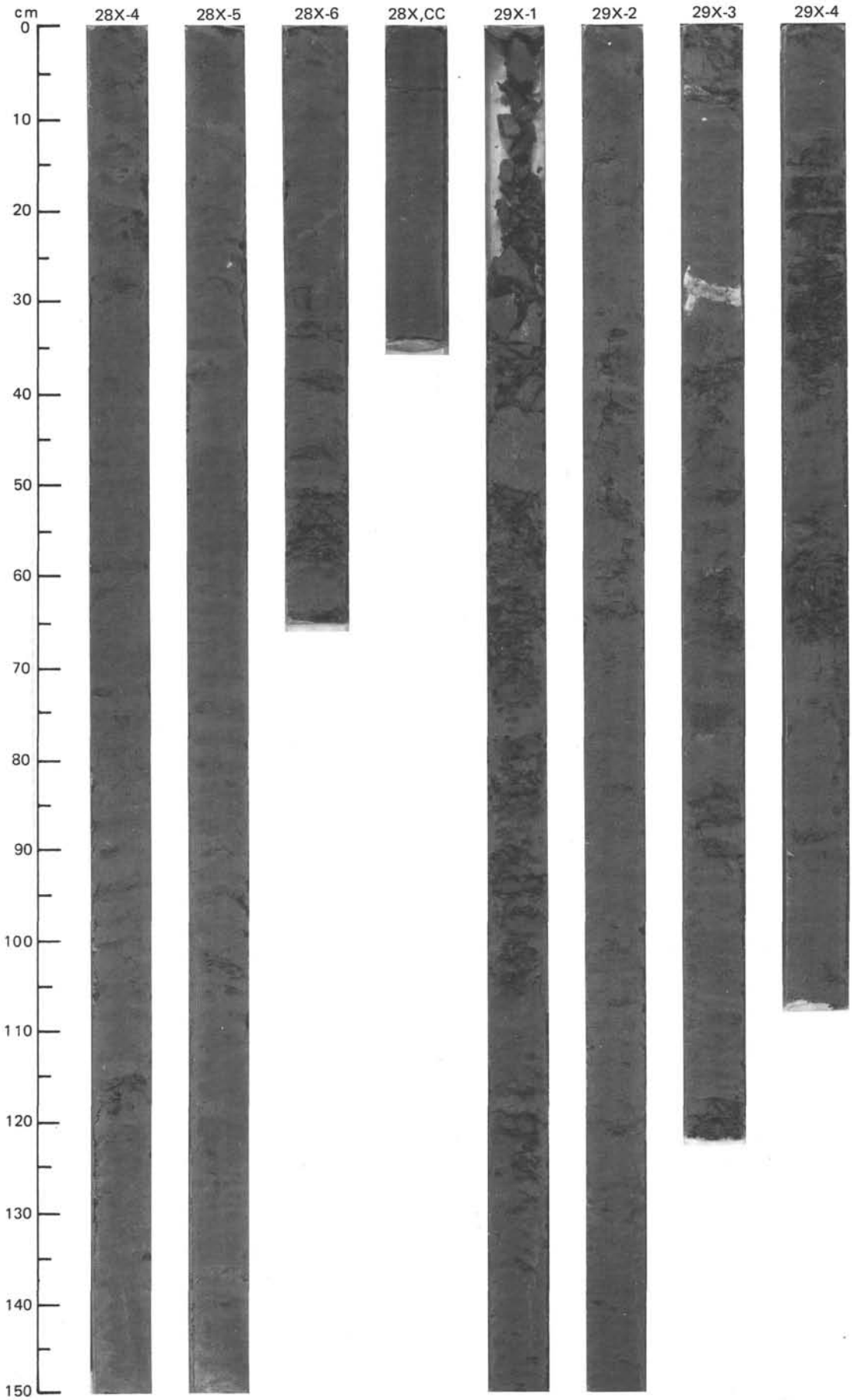
cm
28X-4
28X-5
28X-6
28X,CC
29X-1
29X-2
29X-3
29X-4
0
10
20
30
40
50
60
70
80
90
100
110
120
130
140
150

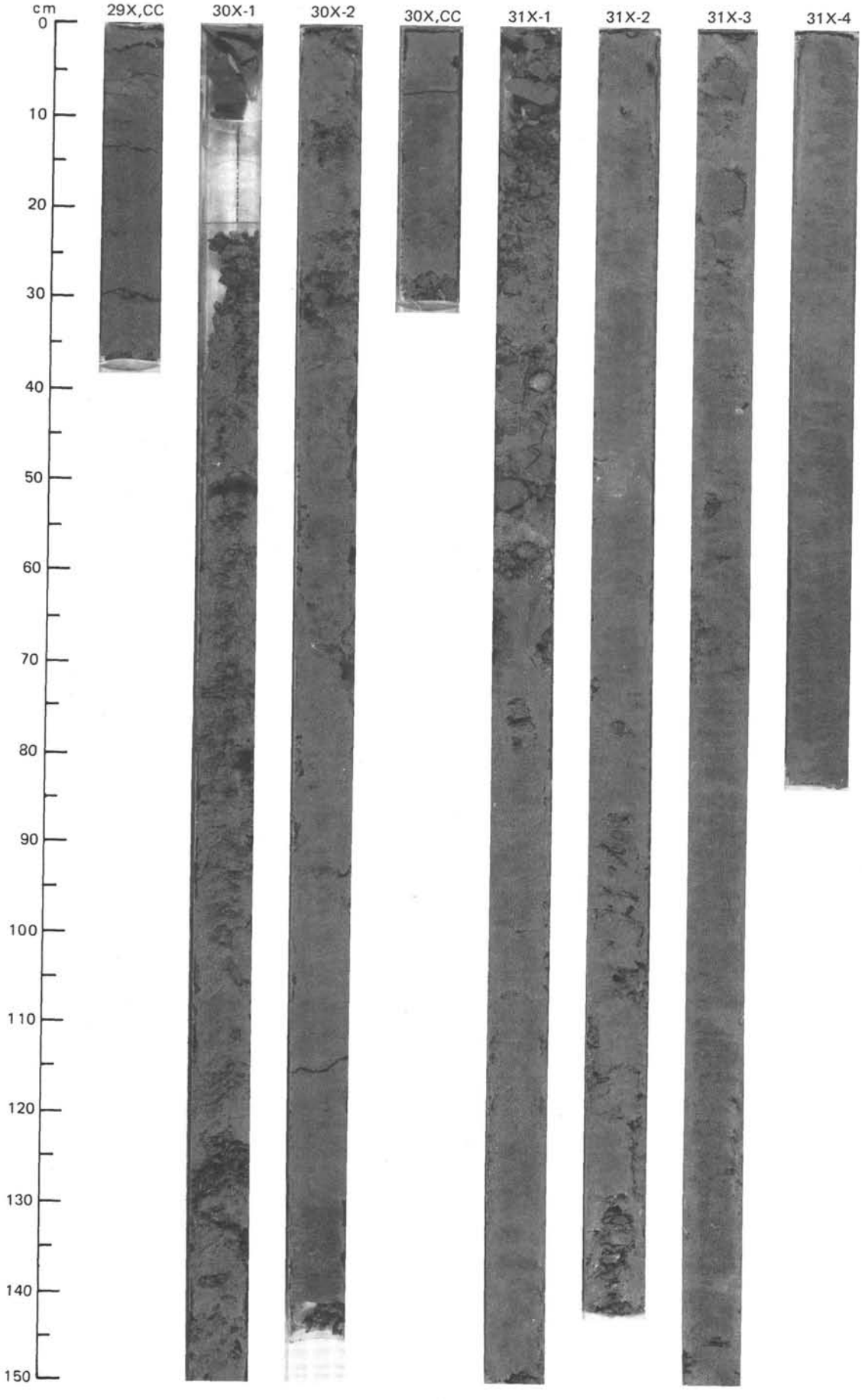
cm
0
10
20
30
40
50
60
70
80
90
100
110
120
130
140
150
29X,CC
30X-1
30X-2
30X,CC
31X-1
31X-2
31X-3
31X-4

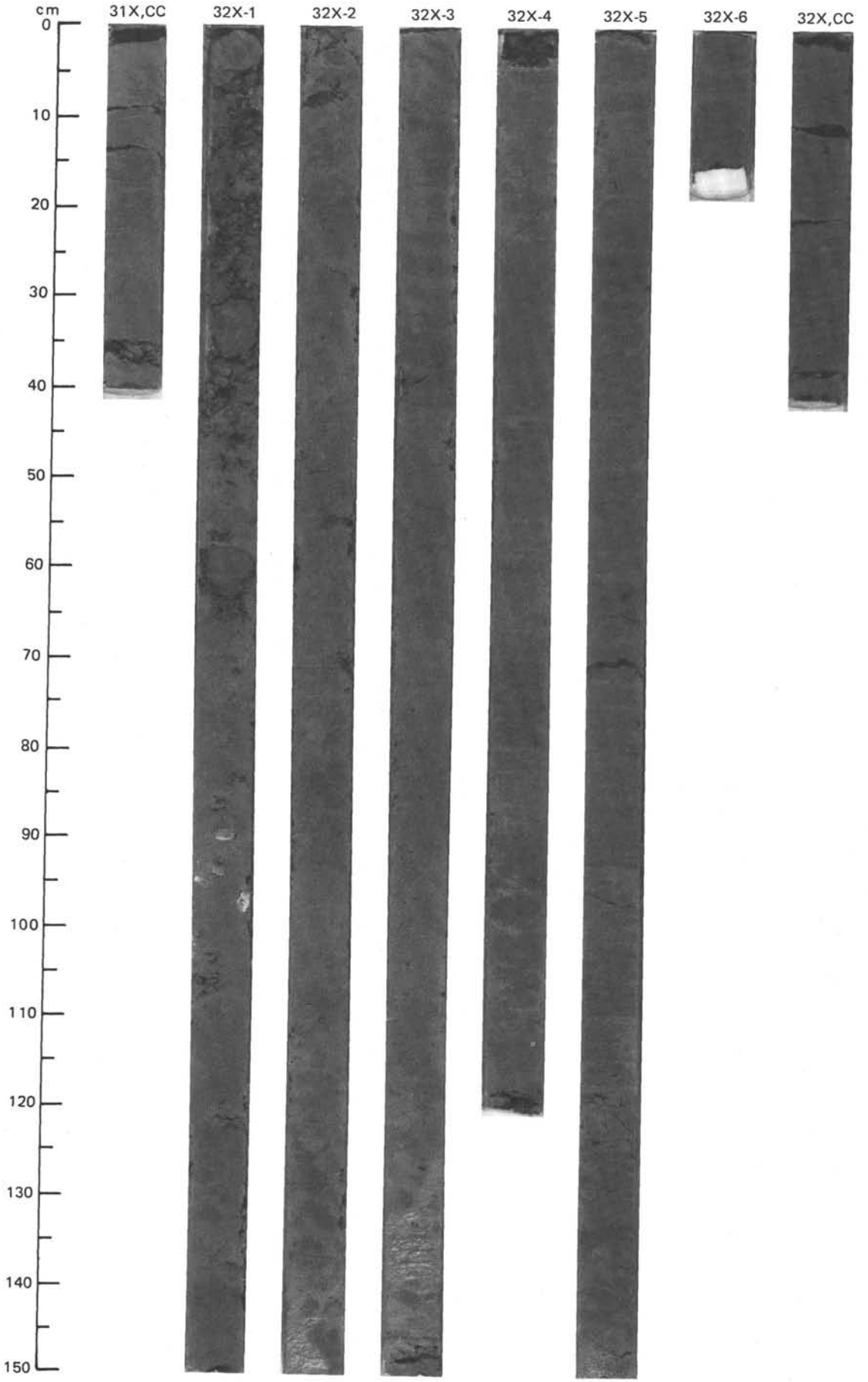
cm
0
10
20
30
40
50
60
70
80
90
100
110
120
130
140
150
31X,CC
32X-1
32X-2
32X-3
32X-4
32X-5
32X-6
32X,CC

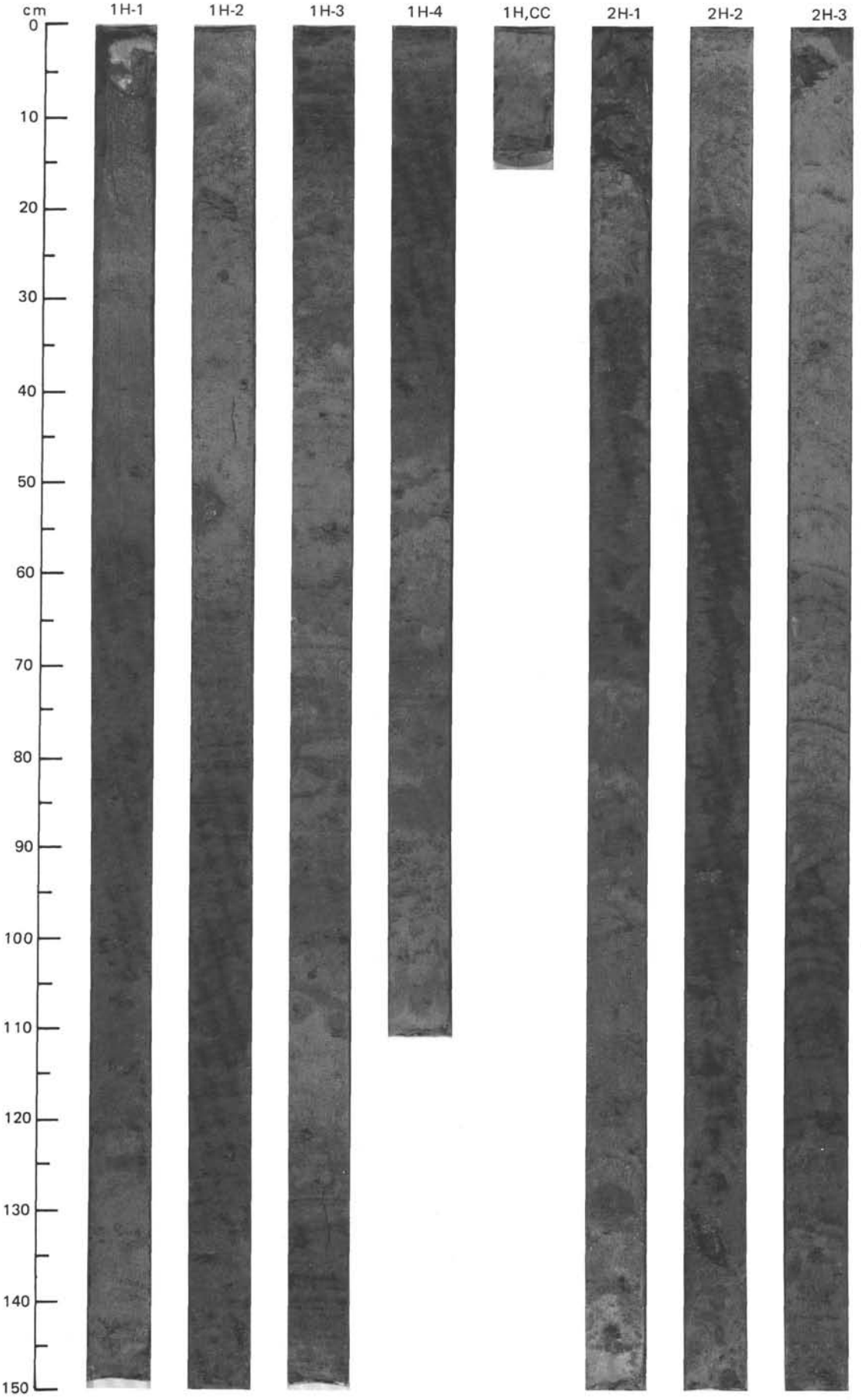
cm
1H-1
1H-2
1H-3
1H-4
1H,CC
2H-1
2H-2
2H-3
0
10
20
30
40
50
60
70
80
90
100
110
120
130
140
150

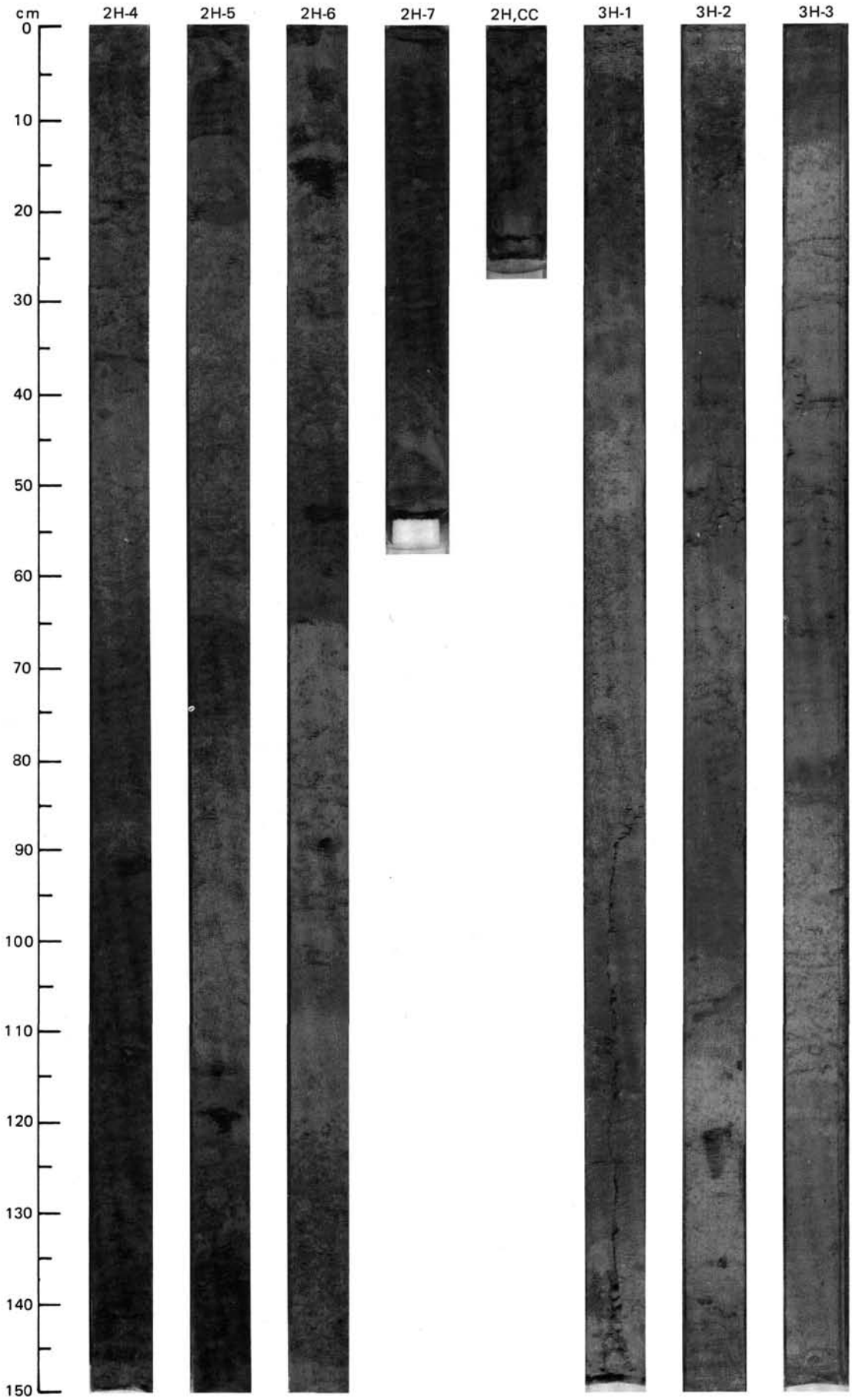
cm
2H-4
2H-5
2H-6
2H-7
2H,CC
3H-1
3H-2
3H-3
0
10
20
30
40
50
60
70
80
90
100
110
120
130
140
150

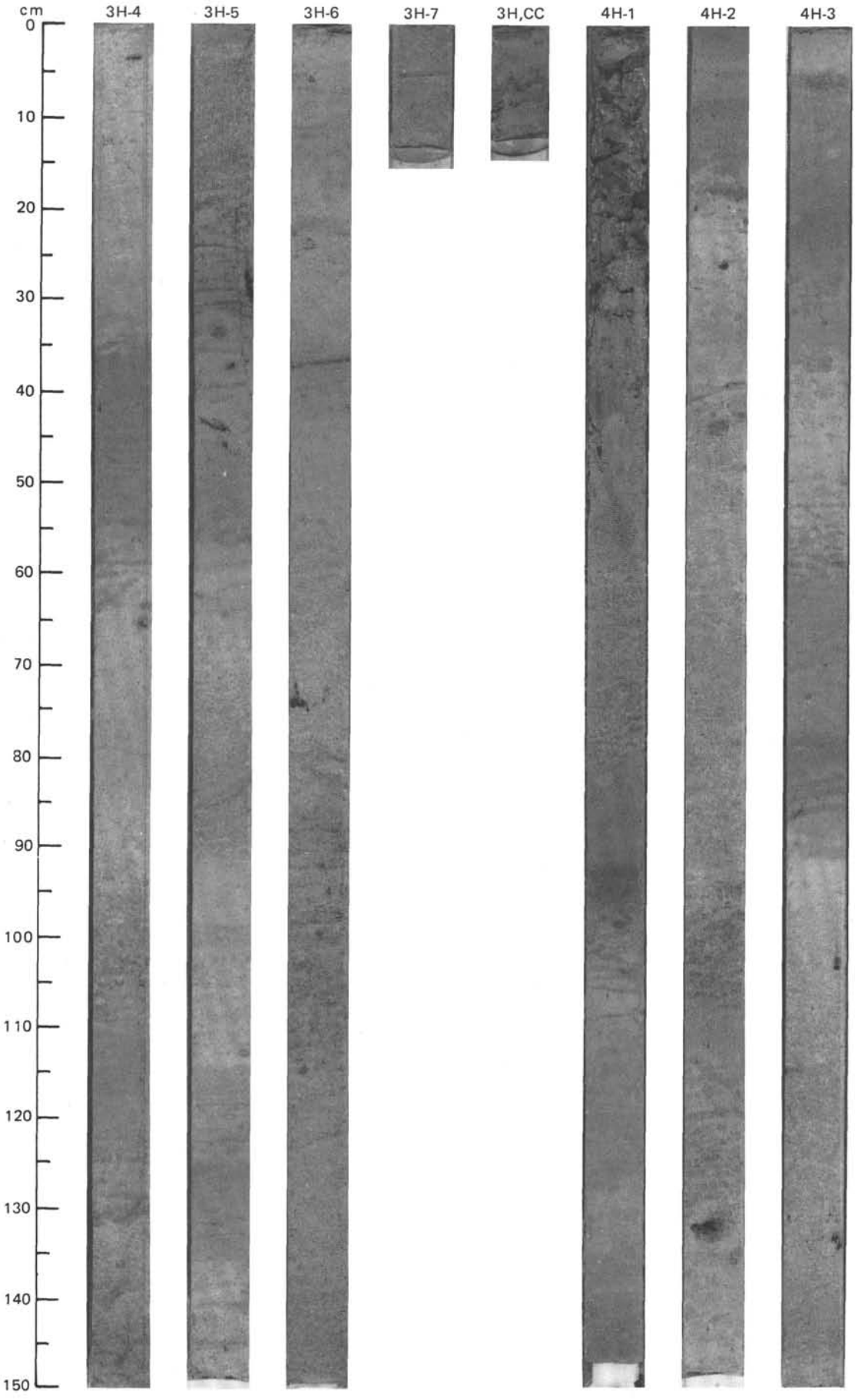
cm
3H-4
3H-5
3H-6
3H-7
3H,CC
4H-1
4H-2
4H-3
0
10
20
30
40
50
60
70
80
90
100
110
120
130
140
150

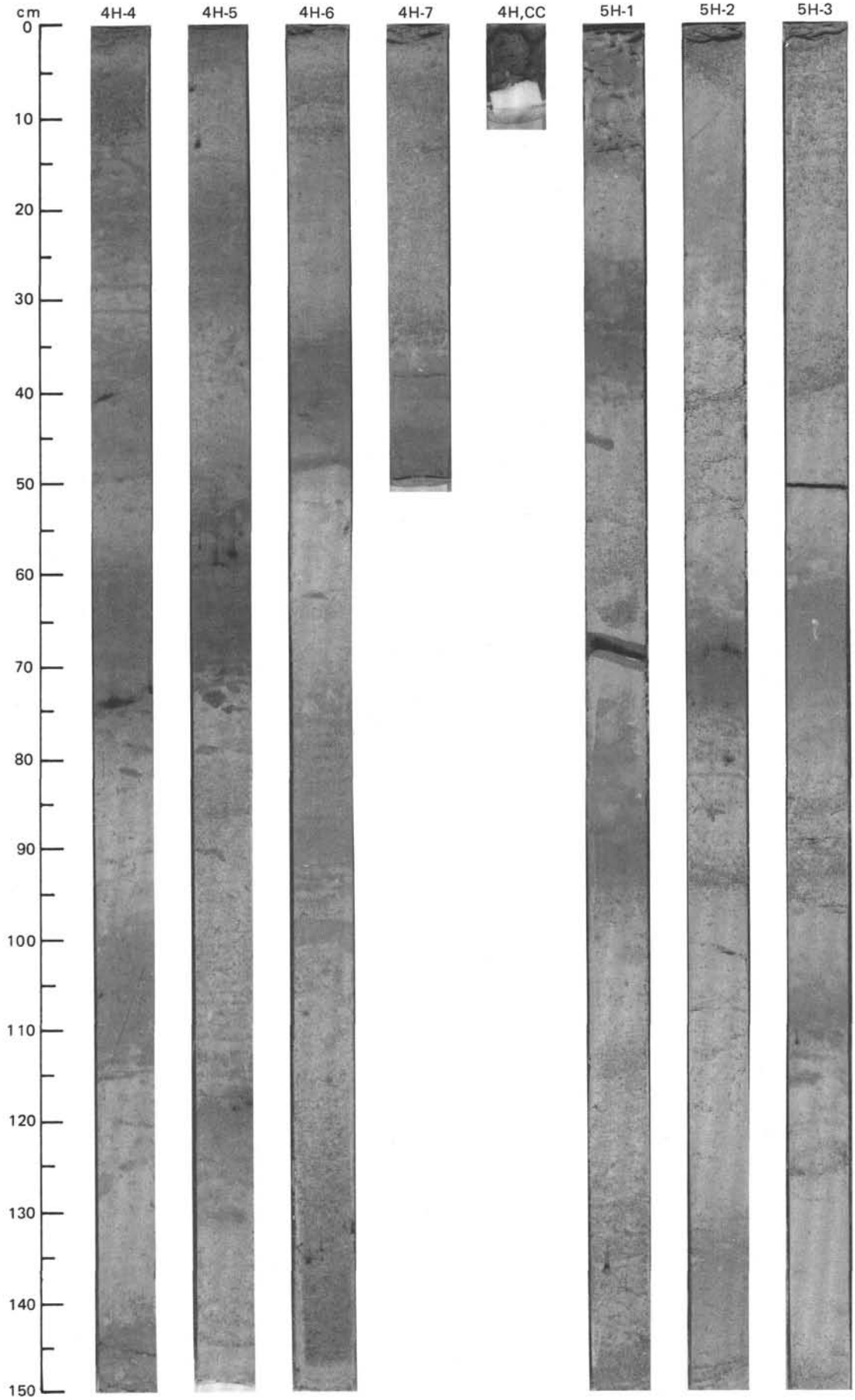
cm
4H-4
4H-5
4H-6
4H-7
4H,CC
5H-1
5H-2
5H-3
0
10
20
30
40
50
60
70
80
90
100
110
120
130
140
150

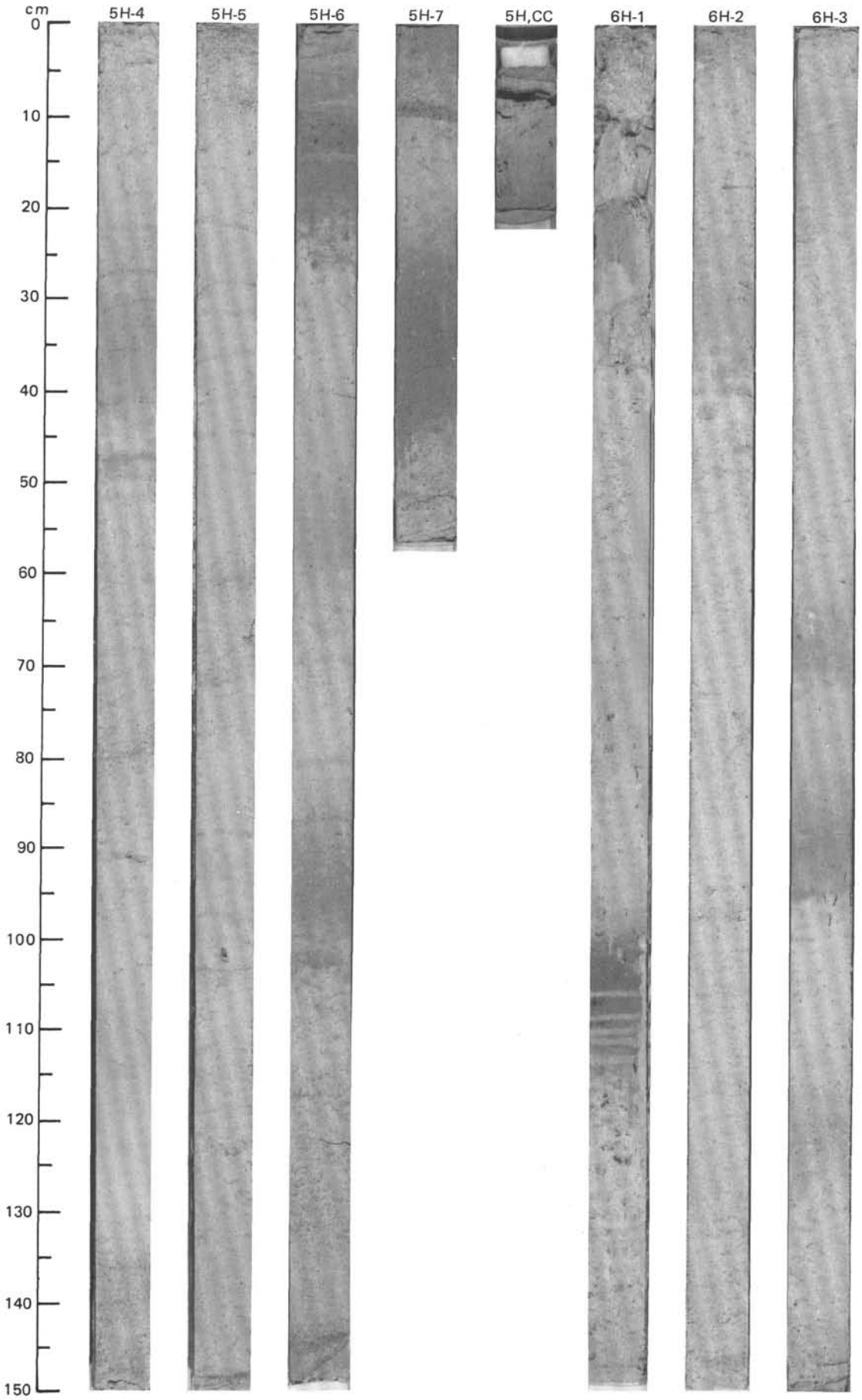
cm
0
10
20
30
40
50
60
70
80
90
100
110
120
130
140
150
5H-4
5H-5
5H-6
5H-7
5H,CC
6H-1
6H-2
6H-3

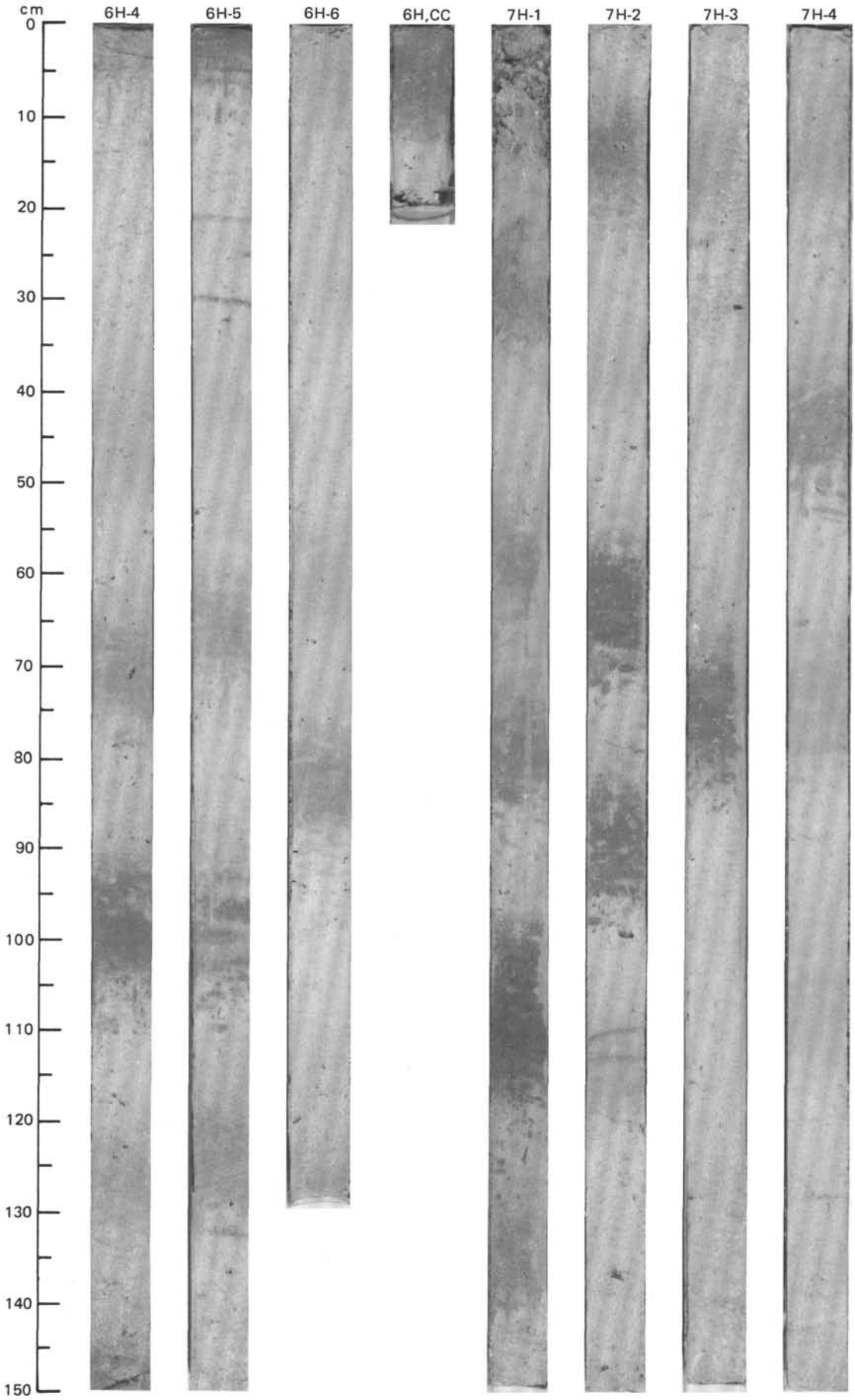
cm
0
10
20
30
40
50
60
70
80
90
100
110
120
130
140
150
6H-4
6H-5
6H-6
6H,CC
7H-1
7H-2
7H-3
7H-4

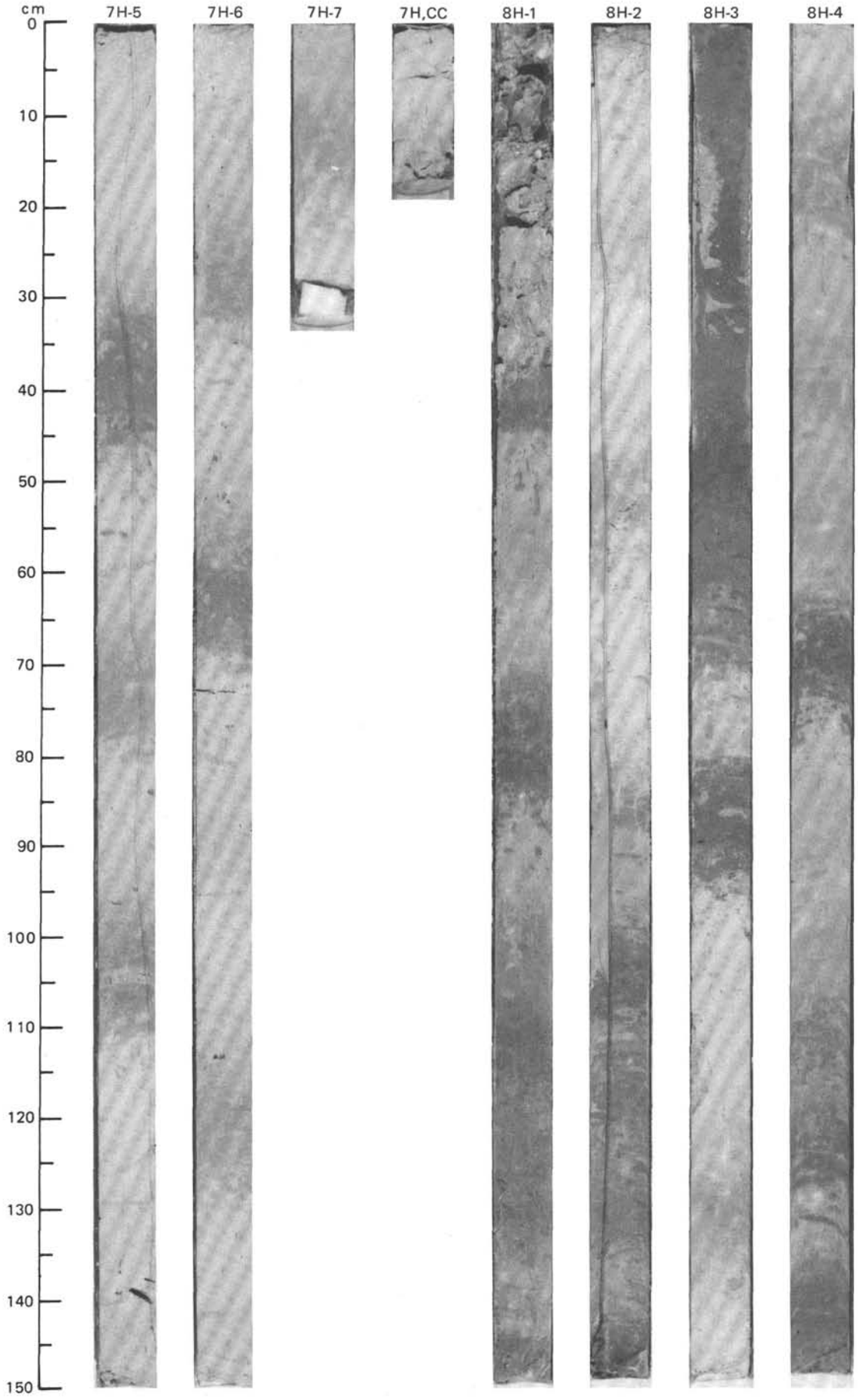
cm
0
10
20
30
40
50
60
70
80
90
100
110
120
130
140
150
7H-5
7H-6
7H-7
7H,CC
8H-1
8H-2
8H-3
8H-4

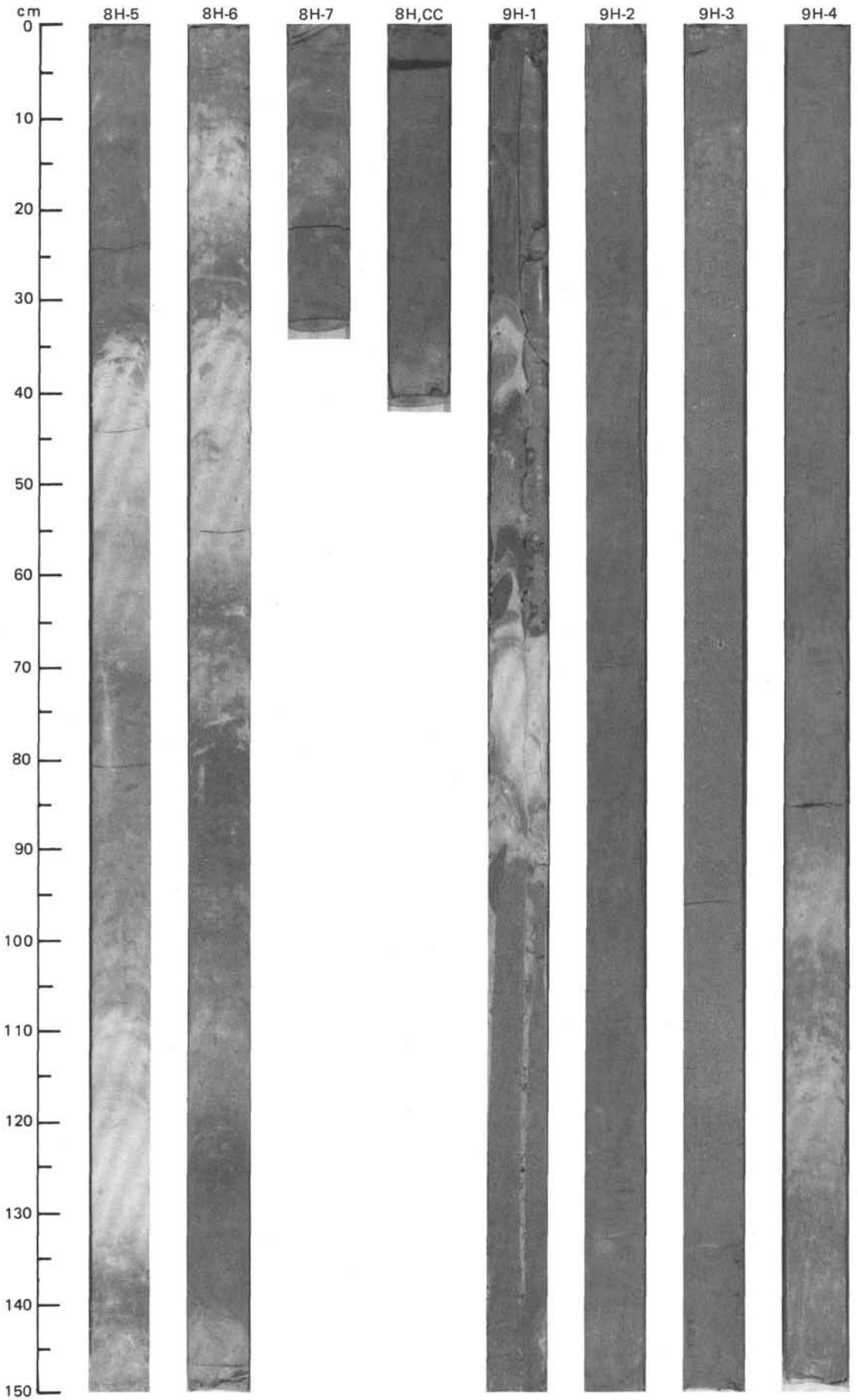
cm
0
10
20
30
40
50
60
70
80
90
100
110
120
130
140
150
8H-5
8H-6
8H-7
8H,CC
9H-1
9H-2
9H-3
9H-4

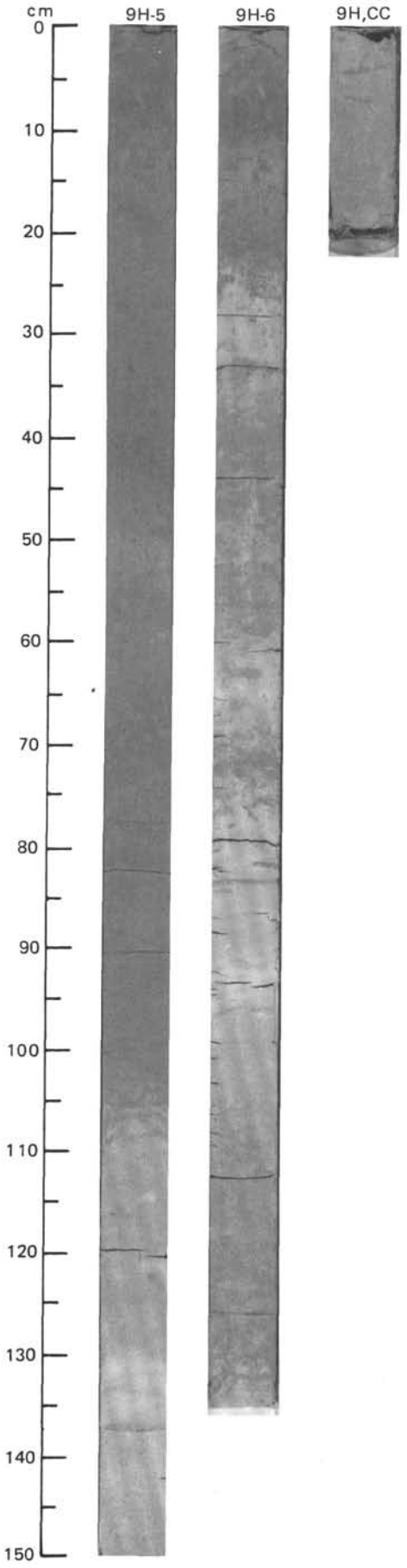
cm
9H-5
9H-6
9H,CC
0
10
20
30
40
50
60
70
80
90
100
110
120
130
140
150